VITAMIN D RECEPTOR ACTIVITY IS DIFFERENTIALLY AFFECTED BY THE CO-REGULATOR HIC-5 IN PROSTATE CANCER AND STROMAL CELLS

by

Joshua David Solomon

BS, Duke University, 2005

Submitted to the Graduate Faculty of

the School of Medicine in partial fulfillment

of the requirements for the degree of

Doctor of Philosophy

University of Pittsburgh

2013

UNIVERSITY OF PITTSBURGH

SCHOOL OF MEDICINE

This dissertation was presented

by

Joshua David Solomon

It was defended on

August 5, 2013

and approved by

Dr. Donald B. DeFranco
Committee Chair and Dissertation Advisor
Department of Pharmacology and Chemical Biology

Dr. Thomas E. Smithgall
Department of Microbiology and Molecular Genetics

Dr. William Walker
Department of Cell Biology and Physiology

Dr. Martin C. Schmidt
Department of Microbiology and Molecular Genetics

Dr. Shivendra Singh
Department of Pharmacology and Chemical Biology

VITAMIN D RECEPTOR ACTIVITY IS DIFFERENTIALLY AFFECTED BY THE CO-REGULATOR HIC-5 IN PROSTATE CANCER AND STROMAL CELLS

Joshua David Solomon, PhD

University of Pittsburgh, 2013

Prostate cancer patients treated with androgen deprivation therapy (ADT) eventually develop castrate-resistant prostate cancer (CRPC). 1,25-dihydroxyvitamin D_3 ($1,25D_3$), is a potential adjuvant therapy that confers anti-proliferative and pro-differentiation effects *in vitro*, but has had mixed results in clinical trials. The impact of the tumor microenvironment on $1,25D_3$ therapy in CRPC patients has not been assessed. Transforming growth factor-β (TGF-β), which is associated with the development of tumorigenic "reactive stroma" in prostate cancer, induced VDR expression in the human WPMY-1 prostate stromal cell line. Similarly, TGF-β enhanced $1,25D_3$-induced upregulation of *CYP24A1*, which metabolizes of $1,25D_3$ and thereby limits VDR activity. Ablation of Hic-5, a TGF-β-inducible nuclear receptor co-regulator, inhibited basal VDR expression, $1,25D_3$-induced *CYP24A1* expression and metabolism of $1,25D_3$ and TGF-β-enhanced *CYP24A1* expression. Luciferase reporter mapping of the *CYP24A1* promoter identified a Hic-5-responsive sequence 392-451 bp upstream of the transcription start site (TSS). Ectopic expression of Hic-5 sensitized LNCaP prostate tumor cells to growth-inhibitory effects of $1,25D_3$ at a lower concentration by a pathway independent of CYP24A1. The sensitivity of Hic-5-expressing LNCaP cells to $1,25D_3$-induced growth inhibition was accentuated in co-culture with Hic-5-ablated WPMY-1 cells. Therefore, my findings suggest that the search for mechanisms to sensitize prostate cancer cells to the anti-proliferative effects of VDR ligands needs to account for the impact of VDR activity in the tumor microenvironment. By acting as a co-regulator with distinct effects on VDR transactivation in prostate cancer and stromal cells, Hic-5 could exert diverse effects on adjuvant therapy designed to exploit VDR activity in prostate cancer.

TABLE OF CONTENTS

LIST OF TABLES

LIST OF FIGURES

DEDICATION

This dissertation is dedicated to the memory of my grandparents, Frederick Philip Germaine (Ephraim ben Shmuel, z”l) and Laura Diana Germaine (Leah Devorah bat Chaim Hirsh, z”l). May their memories be a blessing and their spirits be bound in the bond of eternal life.

ACKNOWLEDGMENTS

I would first like to thank H-shem for bestowing patience and strength of resolve upon me as well as many other people whose words and advise were valuable to the production of this dissertation.

I would like to thank my advisor Donald B. DeFranco for his guidance and patience with me as I adjusted to his laboratory. Though I joined his laboratory late in my graduate career, he has taught me much about designing experiments, interpreting data, and scientific writing. I would also like to thank my dissertation committee members, Drs. Martin C. Schmidt, Thomas E. Smithgall, William Walker, and Shivendra Singh, as well as former committee members Drs. Stefan Duensing (University of Heidelberg) and Jack Yalowich (Ohio State University). They provided many valuable ideas and suggestions that were useful to the completion of this dissertation. I want to thank Neil Bhowmick (Cedars Sinai Medical Center), Pamela Hershberger (Roswell Park Cancer Institute), and David Callen (University of Adelaide) for providing materials necessary for the development of this dissertation. I also want to thank Jan H. Beumer, Robert A. Parise, and Grant Buchanan (University of Adelaide) for assistance in experiments important to the development of the thesis. Much thanks go to Daniel P. Normolle for assistance with advanced statistics.

I would also like to thank lab members, both past and present, in the DeFranco lab for their assistance and friendships. In particular, I would like to thank Marjet D. Heitzer, Melanie J.

Grubisha, and Teresa T. Liu for their assistance and critiques as well as their friendship. Within the DeFranco lab. Also within the DeFranco lab, I would like to thank Marcia Lewis, Ranmal A. Samasinghe, Maria A. Tsiarli, and Melanie E. Peffer for their friendships and companionship within the lab, especially during March Madness.

In addition, I would like to thank my friends and family for their immense support. My parents, Randi C. Solomon and Sanford E. Solomon, taught me how to persevere and never back down in the face of adversity. My departed grandparents, Frederick P. Germaine (z"l) and Laura D. Germaine (z"l), taught me the value of patience. My siblings Elicia I. Solomon and Joel A. Solomon have continued to encourage me, and I hope to be there for only future simchas, keyn aynhora. My immense family in Pittsburgh, including Rochelle S. Solomon, Jack E. Solomon and his wife Susan, Mildred Solomon Belkin and her husband Arnold, and Joshua R. Tepper, have been a source of support and drive. I also acknowledge the friendships I have made as member of the Chabad House of Pittsburgh, including Rabbi Shmuel Weinstein and his family, Rivka Rosenthal, Zalman Poller, and Mordechai Markel, who has been a wonderful housemate for the past year. I thank my wonderful girlfriend Alexandra R. Levine for her loving patience and companionship, being just a phone call away. I hope we can spend more time together in closer proximity.

Throughout the years, I have had had many struggles and many doubters, especially among professionals who did not quite understand high-functioning autism. Rather than break me down, they have only made me stronger and more resilient in the face of adversity. I hope to be that shining beacon for other children with high-functioning autism and Asperger's syndrome, for in the words of Theodor Herzl, "If you will it, it is no dream."

1.0 INTRODUCTION

Prostate cancer is one of the leading causes of cancer among men in the United States. It was the most diagnosed cancer among men in 2011, affecting 241,740 new patients, and directly leading to 28,170 deaths, second only to lung cancer (1). Approximately 1 in 6 males in the US can expect to develop prostate cancer in their lifetimes. Increased screening for prostate-specific antigen (PSA) in the blood, which is elevated in prostate cancer, attributes to the precipitous reduction in the mortality rate and increase of 5-year survival rates by allowing for early detection at a phase when the cancer is localized (2). Between 1999 and 2006, 80% of diagnoses were at the localized stage, compared to 12% with regional metastases and 4% with distant metastases (3). Patients with cancers diagnosed at the localized and regional stages had a 5-year survival rate of 100%, whereas those diagnosed with distant metastases had a poor survival rate of 27.8% (4). Despite the increased detection, PSA screening has become controversial due to the number of false positives and indolent tumors that it detects (5). New guidelines established by the American Urology Association in April 2013 recommend screening tailored to the individual, with high-risk individuals given the option of screening after age 40 and shared decision-making on a regimen between ages 55 and 69 to increase quality of life (6).

The poor survival rate of those diagnosed with and who progress to metastatic prostate cancer is due to the lack of effective therapy options to the patient. Androgen-

deprivation therapy (which will be discussed later) is only effective for 2-3 years, but eventually the cancer becomes castrate-resistant. Abiraterone acetate, a novel therapeutic to be discussed in detail below, increases median progression-free survival time to 27.2 months with prednisone adjuvant, delaying chemotherapy (7). Chemotherapy with paclitaxel, a microtubule stabilizer, only increases the median survival time to 14 months from 9 months, while therapy with docetaxel and estramustine, a genotoxic alkylating agent, is only slightly better at 20 months (8). However, palliative care ultimately becomes the only course of treatment after all other therapies fail. Thus, a novel form of treatment needs to be developed to supplement chemotherapy and the novel abiraterone acetate therapy. In this project, I sought to understand the molecular pathways of one such potential treatment: 1,25-dihydroxycholecalciferol ($1,25D_3$), the active metabolite of Vitamin D, and the conditions that sensitize the cancer to it.

1.1 THE PROSTATE GLAND: STRUCTURE, FUNCTION, AND PATHOLOGY

1.1.1 Normal development of the gland

Most male accessory glands, such as the epididymis, vas deferens, and seminal vesicles, develop during embryogenesis from the Wolffian ducts, which is a mesodermal structure (9). However, the prostate gland develops from the urogenital sinus (UGS), which has endodermal heritage (10). At 9 weeks in fetal human development, the fetal testes initiate production of testosterone (T), which can bind to the androgen receptor (AR) in the UGS mesenchyme either intact or converted to a more potent form, dihydrotestosterone (DHT), by 5α-reductase (11). Secretion of

paracrine factors induces epithelial budding from the UGS that penetrates into the mesenchyme in directions dorsal, ventral, and lateral to the bladder (10). As the epithelial buds mature and express AR, paracrine signals to the mesenchyme induce differentiation into the smooth muscle cells that compose the mature stroma (11). Upon maturation, AR expression retreats into the muscular sheath immediately surrounding the epithelium and the epithelium itself (12, 13). In adulthood, testosterone secreted from the testes is required to maintain viability of the epithelium.(14)

In the model proposed by McNeal, the human prostate contains four main zones: the peripheral zone, the central zone, the transition zone, and the periurethral gland region. 95% of the glandular mass is contained within the peripheral and central zones (15). Differences between the central and peripheral zones are indicated in the differing composition of stroma and glandular architecture between the two zones, with the central zone having larger ducts in higher concentration of ductal arborization of acini and stroma composed of compact smooth muscle fibers. In the peripheral zone, the normal stroma is more loosely woven, with higher abundance than in the central zone. Whereas the central zone has been relegated in clinical circles to a “nonclinical curiosity”, the peripheral zone is more susceptible to prostatitis and prostate cancer (16).

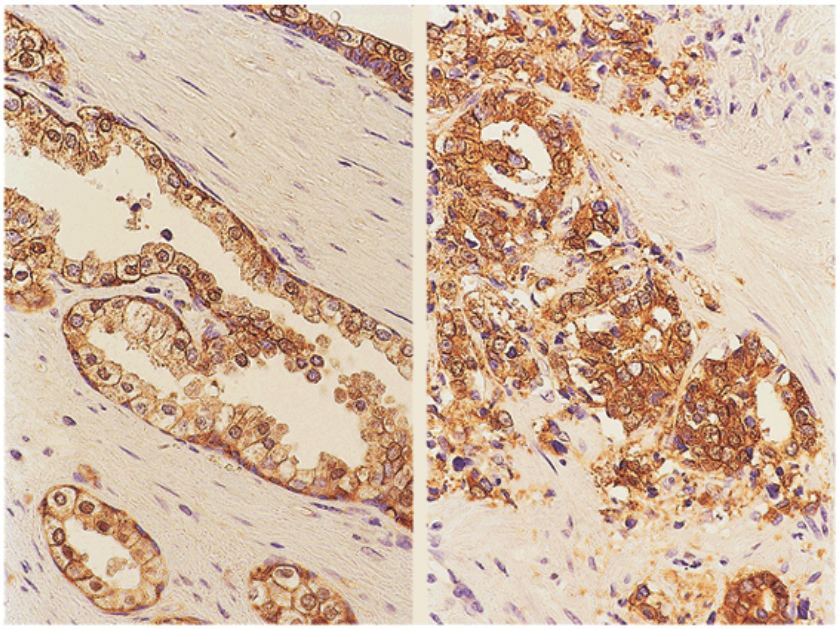

Figure 1: Tumorigenesis in prostate cancer.

The normal prostate contains well-defined epithelial ducts within a fibromuscular stroma. As the tumor progresses, the epithelium gradually loses its glandular structure until it become completely de-differentiated and diffused among the stroma.

1.1.2 Neoplasia and carcinogenesis

The causes of prostate cancer are poorly understood. Attempts to understand precursors of the disease center on proliferative inflammatory atrophy (PIA) and prostatic intraepithelial neoplasia (PIN). Like prostate cancer, PIA arises primarily from the peripheral zone, where it retains glandular structure while undergoing proliferation (18). PIA has the potential to transition to and merge with PIN, with 40% of PIN lesions merging with PIA (19). High-grade PIN is recognized

as a precursor to prostate cancer, which loses the delineated glandular structure clearly separated by a basement membrane as it transitions to an invasive state (Figure 1) (20).

Because most prostate cancers are multi-focal, physicians take 8 to 12 core samples from the prostate for biopsies, typically from the peripheral zone (21). The samples are analyzed for glandular differentiation and invasion using the Gleason grading system. Each sample is graded on a scale of 1 to 5, by which a Gleason grade 1 indicates well-defined glandular architecture and 5 a diffuse, de-differentiated tumor. Two grades are given to each sample for a primary (most predominant) grade and a secondary (second most predominant) grade. The two grades are added to give a total Gleason score, which is notated, for example, as 4 + 3 = 7. Under the modifications made to the scale in 2005, the predictive power of the system regarding recurrence after radical prostatectomy improved, with a total Gleason score >7 indicating a high risk for recurrence (22).

Not all cancers will necessarily lead to a metastatic state and may remain indolent for the lifespan of the patient (23). For most patients, prostate cancer that is detected at a localized or regional stage via PSA screening and biopsy and for whom treatment is indicated can be cured at high rates using curative therapies, such as prostatectomy and radiation therapy (3, 4). However, a tumor with a high Gleason score and recurrence of PSA levels post-surgery has a high potential to become metastatic, with cells entering the bloodstream via the neovasculature (24). Primary targets of metastasis include the lymph nodes and bone, which provides a fertile “soil” of growth factors stored in the bone matrix to the metastatic “seed” (25). Cross-communication between the “seed” and “soil” stimulates the osteoclastic resorption of bone matrix to release more soluble growth factors, increasing metastatic growth, and irregular osteoblastic growth. The

clinical result of these processes is a presentation of pain, increased bone fractures, and spinal-cord compression (26).

Currently, therapies for metastatic prostate cancer are limited. Androgen-deprivation therapy and hormone therapies are currently the standard at this stage, but the cancer eventually becomes castrate-resistant, and chemotherapy has limited success beyond palliative care (27). The problem of castrate resistance and a novel therapy for castrate-resistant prostate cancer (CRPC) will be discussed in the subsequent sections.

1.2 ROLE OF NUCLEAR RECEPTORS IN PROSTATE CANCER

1.2.1 Nuclear receptor structure and function

Nuclear receptors are a superfamily of receptor proteins that have descended from a common ancestor. The human genome contains genes coding for 48 known nuclear receptors (28). These receptors directly bind to DNA in the presence of their specific ligand, such as T, estrogen, glucocorticoids, and thyroid hormones, although some “orphan receptors” currently have no known ligand (29). A typical nuclear receptor is composed of at least four distinct domains. The highly variable N-terminal domain is responsible for modulation of receptor function, typically involving phosphorylation and other modifications like SUMOylation (30). The DNA-binding domain (DBD), the most conserved domain among nuclear receptors, comprises 66-68 amino acids that form two zinc fingers, which bind to specific DNA motifs (31, 32). The hinge domain assists in maintaining the structural integrity of the nuclear receptor and, in some cases, contains residues whose phosphorylation enhances transactivation of target promoters (33, 34). The

ligand-binding domain (LBD), another structurally conserved domain, comprises 12 conserved α-helical regions whose size differs between different ligand types and conformational state upon ligand binding (Figure 2) (35).

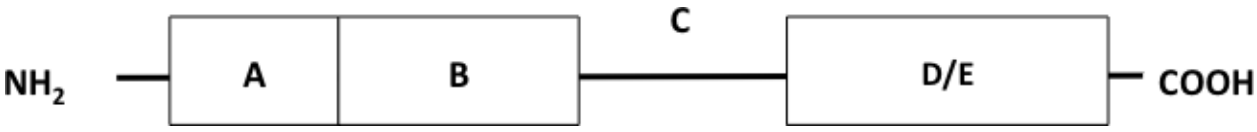

Figure 2: General structure of a nuclear receptor.

The N-terminal A domain is variable and confers modulation by covalent modification. The DNA-binding domain (B) is the most conserved domain of the nuclear receptor superfamily. The ligand-binding domain (D/E), which is connected to B by the hinge domain (C), changes conformation upon ligand binding, facilitating binding to co-regulators.

In the absence of ligand, steroid hormone receptors are associated with a complex of chaperone proteins predominantly in the cytoplasm. The primary component of this complex, HSP90, binds to the LBD (36). HSP90 is required for proper steroid binding to the hydrophobic cleft of the LBD, as it creates a stable complex in the LBD at physiological temperatures to facilitate binding of the hydrophobic steroid (37). Other members of the chaperone complex include HSP70, p23, and the immunophilin FKBP52 (38). Ligand binding induces an exposure of the nuclear localization sequence and a dynamic state of interaction with the chaperone complex that facilitates movement along microtubules by dynein (39). Nuclear receptors residing in the cytoplasm, such as the glucocorticoid receptor (GR), interact with importin-β and the nuclear pore glycoprotein Nup62 to facilitate import into the nucleus (38). However, many other nuclear receptors, such as retinoid A receptor (RAR), estrogen receptor (ER), and thyroid receptor (TR) constitutively reside within the nucleus (40).

Nuclear receptors are classified according to how they bind to their respective ligand response elements within the promoter of the target gene, at intergenic sites, or within introns (35, 41-44). Type I receptors, which contain the steroid hormone receptors, bind as homodimers at palindromic inverted repeats (45). Type II receptors, which include TR, RAR, and Vitamin D receptor (VDR), bind as heterodimers with retinoid X receptor α (RXRα) at direct repeats (35). Most orphan receptors tend to be classified as Type III receptors, which bind as homodimers at direct repeats, and Type IV receptors, which bind as monomers at extended core sites (46).

Co-activators that bind to the AF-2 domain, contained in the most C-terminal part of the LBD, confer tissue-specific activation of nuclear receptors. Additional co-activators may also bind at the AF-1 domain close to the N-terminal domain and indirectly through complexes (47). Some of these co-activators have acetyltransferase activity (e.g.: SRC-1, CBP/p300) and ATPase chromatin remodeling activity (e.g.: TIF1α), opening the chromatin for transcription. Other co-activators that do not have any intrinsic acetyltransferase or remodeling activity, such as the VDR-interacting protein (DRIP) and Hic-5, recruit the transcription initiation complex and serve as scaffolding to bridge nuclear receptors to various co-activators (48, 49).

The most prominent receptor in the prostate is AR. Its preferential ligand, T, is synthesized under the positive control of luteinizing hormone in the Leydig cells of the testes, upon which it diffuses to the prostate (50). However, DHT exhibits 5-fold greater specificity for AR, indicating a preference for DHT *in situ* (51). In the adult prostate, AR is mainly expressed in the secretory cells of the epithelium, with minimal stromal expression (52). Normal serum amounts of T induce a proliferation rate that balances the normal rate of cell death of 1-2% per day, maintaining prostate health (53). Additionally, T supplementation to castrated rats induces angiogenesis and vascular survival in the prostate (54). Withdrawal of androgens or inhibition of

their signaling through AR can induce prostatic apoptosis (55). The following section will discuss the biochemical and clinical implications of this process in prostate cancer as well as the consequences of failure of treatment.

1.2.2 Androgen deprivation therapy and castrate-resistant prostate cancer

While the AR is associated with maintenance of prostate epithelial growth, its aberrant activation is also associated with disease development. Typically, such induction can occur due to presence of gene translocations, increased levels of growth factors, deregulated growth pathways, and activating mutations with AR itself (56-59). Androgen-deprivation therapy (ADT) is usually indicated as a treatment for patients who have locally advanced or metastatic disease and has recently been suggested as an adjuvant with radiation therapy and surgery for patients with medium to high risk, according to Gleason score (60, 61). Anti-androgens, such as bicalutamide, compete with androgen for access to AR and inhibit its function (62). Often, this therapy may be given together with a gonadotropin releasing hormone agonist (GnRHa), which induces a high release of LH, interrupting its pulsatile secretion and inducing GnRH receptor internalization and desensitization (63-65). While this induces an initial flare, over time LH release decreases, thus reducing T synthesis (66).

The net effect of this therapy is to decrease available T from binding to AR from the supply (receptor) and demand (synthesis) sides, thus reducing overall AR signaling. Reduced AR signaling indirectly induces expression of the pro-apoptotic protein Bax to thirteen times its normal expression 2 to 3 days after administration, inducing the intrinsic pathway of apoptosis (67). ADT may also induce the extrinsic apoptotic pathway by inhibiting IκB kinase and inducing RelA/p65 expression, sensitizing cancer cells to apoptosis-inducing signaling molecules

TNF-α, TRAIL, and FasL (68-70). The principle behind this is the "saturation model", by which a level of T at or near near-castrate levels results in significant reductions in PSA levels (71).

However, an additional effect of ADT is the upregulation of the anti-apoptotic protein Bcl-2. Unlike the relatively rapid increase of Bax, Bcl-2 increases steadily reaching a peak at 10 days (72). Repeated treatment, however, may induce a more permanent induction of Bcl-2 in the tumor. As opposed to 30% of androgen-dependent prostate cancers, almost all CRPCs express elevated levels of Bcl-2, suggesting that ADT will eventually contribute to a castrate-resistant phenotype, by which the tumor becomes hypersensitive to androgens or loses androgen dependence for growth, via this pathway (73). Additionally, effectiveness of ADT directly on AR may be reduced by gene amplification, mutations to a more promiscuous phenotype, and a change in balance between AR co-activators and co-repressors (74-76). Mutations independent of AR, such as those in growth pathways, also contribute to CRPC (77). Patients undergoing ADT typically become castrate-resistant at 18-24 months after commencing the therapy (78).

At this point, treatment options for CRPC are limited. Recent advances that delay the use of chemotherapy, as seen with abiraterone acetate, an inhibitor of androgen synthesis through 17 α-hydroxylase, have lengthened median progression-free survival time to 27.2 months (7). Docetaxel, the current first-line therapy for CRPC, only extends survival to a median of 19 months (79). Other treatments do not yet show this length of survival (80). Thus, there is an unmet need to develop additional primary and adjuvant therapies that may be used in androgen-dependent and castrate-resistant prostate cancer. One such promising therapy involves Vitamin D and its derivatives, which will be discussed in the next section.

1.3 THE VITAMIN D RECEPTOR AND ITS IMPACT ON THE PROSTATE

1.3.1 Synthesis of 1,25-dihydroxycholecalciferol

In 1919, Kurt Huldschinsky found that exposure of children to radiation from sunlight or a mercury-vapor quartz lamp either cured or prevented rickets, a disease that involves softening of the bones (81). A traditional treatment for the disease, cod-liver oil, had been known from the folklore of northern Europe. In 1922, Mellanby and McCollum found that when cod-liver oil was heated, it lost its protectiveness against Vitamin A deficiency, but not against rickets. They termed this new substance Vitamin D, as it was the fourth in sequence of vitamins discovered (82). Adolf Windaus later discovered that the precursor to Vitamin D is 7-dehydrocholesterol (7-DHC), found in cod-liver oil by J. Waddell, and that it is activated upon exposure to UV-B radiation (82). In 1980, Michael Holick and Hector DeLuca found that ultraviolet radiation penetrates into the stratum spinosum and the stratum basale of the epidermis, inducing the photoconversion of 7-DHC to Previtamin D_3 by breaking the B-ring of the sterol (83). Then, driven by temperature, Previtamin D_3 isomerizes over three days to a more stable form, Vitamin D_3, also known as cholecalciferol (83). Production eventually plateaus to 10 to 15 percent of original 7-DHC content, at which point the biologically inactive lumisterol accumulates through photoisomerization of Previtamin D_3, which is then sloughed off with the skin or converted back to Previtamin D_3 as its stores decrease (84).

Vitamin D-binding protein (DBP), which prefers Vitamin D_3 to lumisterol, facilitates transport of Vitamin D_3 in the blood to the liver (83, 84). Within the mitochondrial inner membrane and microsomes of hepatocytes, the cytochrome P450 enzyme CYP27A1 hydroxylates Vitamin D_3 at C-25, forming 25-hydroxycholecalciferol ($25D_3$) (85-87). This is

the major circulating form of Vitamin D_3 in the serum (88). A major site of conversion of $25D_3$ is the kidney, where another cytochrome P450 enzyme, CYP27B1, hydroxylates it at the 1α position on the A-ring to produce the active form of the vitamin, 1α,25-dihydroxycholecalciferol ($1,25D_3$) (Figure 3) (89). However, CYP27B1 is also expressed in numerous other tissues, including the skin, pancreas, brain, lymph nodes, and prostate, where local conversion permits autocrine and paracrine signaling (90, 91).

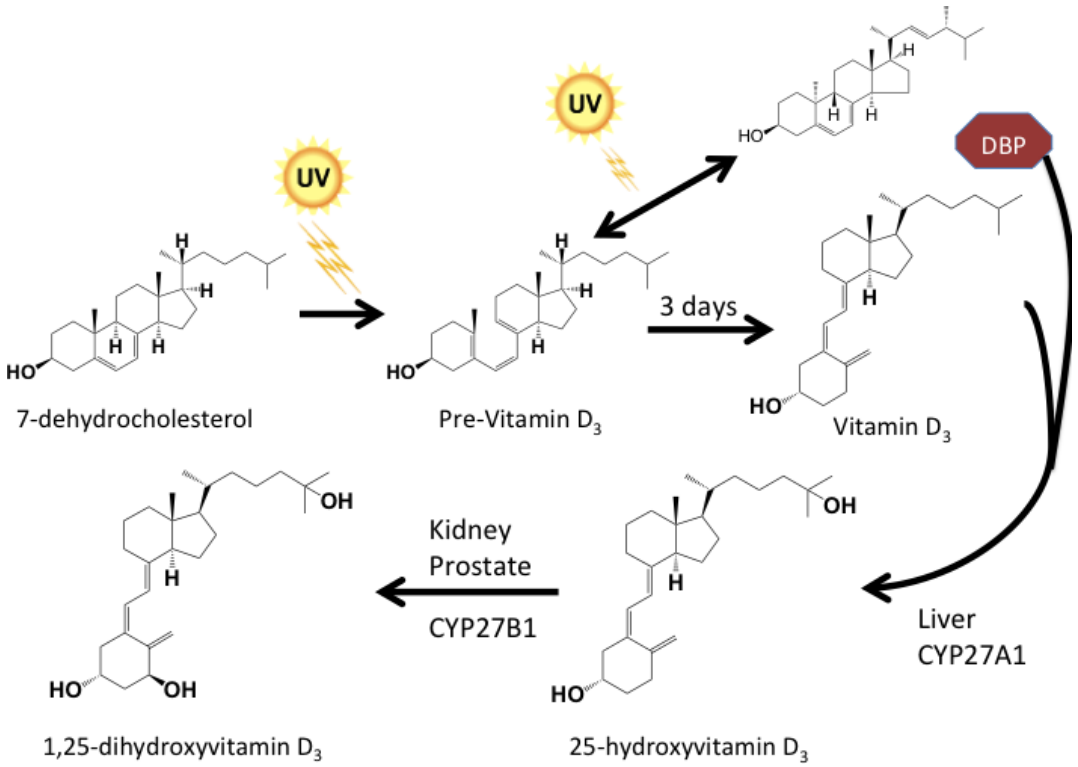

Figure 3: Photosynthesis of $1,25D_3$.

7-DHC is converted to Previtamin D_3 upon UV irradiation, which isomerizes to Vitamin D_3 over 3 days. Excess Vitamin D_3 is converted to inactive lumisterol upon UV irradiation. DBP binding stabilizes Vitamin D_3 for transport in the bloodstream to the liver, where CYP27A1 converts it to $25D_3$, and the kidney and other target organs (ie.: the prostate), where CYP27B1 converts it to active $1,25D_3$.

1.3.2 Structure and activation of the Vitamin D receptor

The intracellular receptor for $1,25D_3$ is the Vitamin D receptor (VDR), which is a Class II (thyroid receptor-like) nuclear receptor (92, 93). VDR is distributed between the cytoplasm and the nucleus, but shifts its localization to be predominantly nuclear upon binding $1,25D_3$ (94). $1,25D_3$ docks into VDR in its 6-S-*trans* form, oriented equatorially (95). The C-1α hydroxyl group on the A ring coordinates with helices H3 and H5 in the ligand-binding pocket, and the C-25 hydroxyl group in the aliphatic chain coordinates with helix H12 to activate the AF-2 domain, which forms a closed cleft for binding cofactors (96, 97). Unlike other steroid receptors, VDR requires heterodimerization with a second receptor, the retinoid X receptor (RXR), in order to fully transactivate target genes (98). In the absence of ligand, a stable VDR/RXR complex, which is formed through interactions between H7 on VDR and H7, H10, and H11 in RXR, binds weakly to a target Vitamin D response element (VDRE) and recruits a repressive SMRT/nuclear co-repressor (NCoR) complex (97, 99). The SMRT/NCoR complex recruits histone deacetylases, impeding transcriptional access to the chromatin. Binding of $1,25D_3$ induces allosteric changes in the H3 helix of RXR, distant from the heterodimer interface (97). This "phantom ligand effect" allows RXR to recruit cofactors of its own to the VDR/RXR complex (98). The hinge domain between the LBD and DBD facilitates recognition of the VDRE, which is a DR3 element consisting of two half-sites of the consensus sequence 5'-AGGTCA-3' (33). VDR binds to the VDRE through two C4 zinc-finger moieties, located at residues 24-44 and 60-79 (100).

Ligand activation of the VDR induces changes in the state of the chromatin that are dependent on the effect on transcription that VDR has on the target gene. For genes being upregulated, ligand activation of the AF-2 domain and binding to DNA facilitate dissociation of

the repressive complex and associations with LXXLL-containing cofactors such as the p160 co-activators, CBP/p300, and DRIP205 (101, 102). Formation of the ternary VDR/SRC-1/NCoA620-SKIP complex facilitates acetylation of histones and de-repression of the chromatin (Figure 4) (103). In turn, Vitamin D receptor interacting proteins (DRIPs) form complexes on the AF-2 domain and interact with the transcriptional machinery through TFIIB (104). Alternately, liganded VDR may also facilitate transcriptional repression of a promoter. In this case, liganded VDR instead recruits SMRT and NCoR complexes, which in turn recruit histone deacetylases (105, 106).

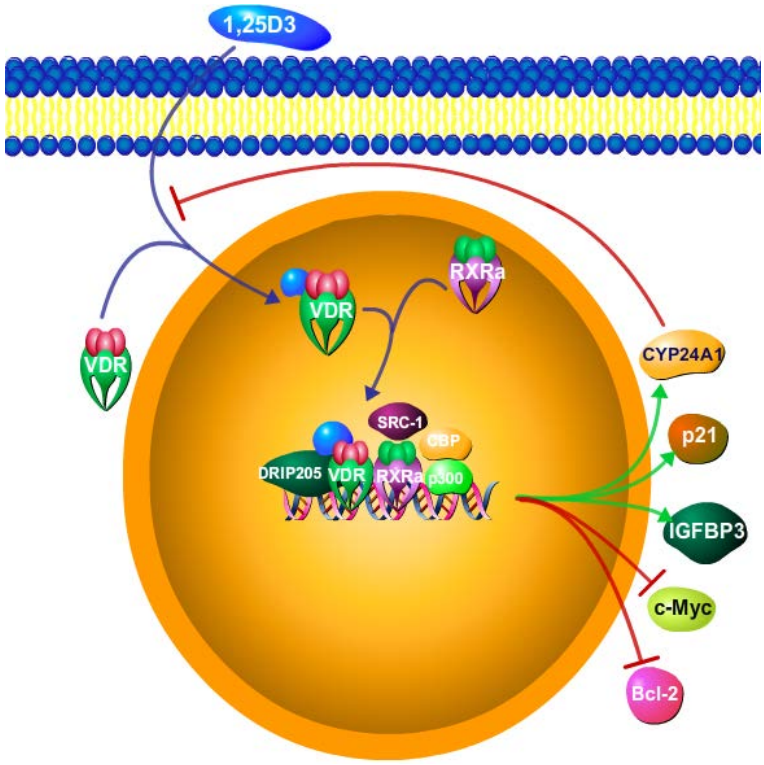

Figure 4: VDR activation pathway.

$1,25D_3$ diffuses across the plasma membrane and binds with VDR to trigger nuclear localization. Liganded VDR forms a heterodimer with RXRα and binds to a VDRE. The VDR/RXRα recruits co-activators to activate transcription. For negatively regulated genes, VDR/RXRα inhibits transcription.

One VDR target that is induced, the gene encoding for the cytochrome P450 enzyme CYP24A1 acts as a negative feedback on VDR activation. CYP24A1 catalyzes the hydroxylation of the C-24 carbon of $1,25D_3$, rendering it unable to bind to VDR and vulnerable to six-step monooxygenation (107). The final product, calcitroic acid, is water-soluble and excreted in the urine (107).

1.3.3 Molecular effects of Vitamin D in cancer

Treatment with $1,25D_3$ in the Dunning rat prostate tumor model resulted in a reduction of tumor volume as well as the number and size of lung metastases (108). Additionally, a prostate-specific VDR knockout showed reduced cell death and greater proliferation of the prostate than their wild-type counterparts, solidifying the roles of VDR and its ligand in controlling cancer growth (109). These preclinical findings have been supported in human clinical trials, which exhibited an inverse correlation between prostate levels of $1,25D_3$ and Ki67, a marker for proliferation (110).

Several pathways have been identified that could contribute to $1,25D_3$'s effects on reducing tumor growth and volume. One such pathway is cell-cycle inhibition, within which a direct target of VDR is the oncogene c-Myc. For example, in the C4-2 prostate cancer cell line, ligand-activated VDR inhibits expression of c-Myc through direct binding to its promoter. This in turn leads to reduced expression of downstream targets of c-Myc such as E2F1, a pro-proliferative transcription factor, and Bcl-2, an anti-apoptotic protein. These effects are Rb-independent (111). However, knockdown of Rb in LNCaP, the parental cell line of C4-2 cells, leads to induction of cyclin E and thus progression of the cell cycle to S phase, indicating dependence on Rb in other contexts (112). Expression of cyclins and cyclin-dependent kinases

are also impacted by VDR activation. For example, *CDKN1A*, which encodes p21, an inhibitor of CDK1 and CDK2, is a VDR target gene. VDR binding to the *CDKN1A* promoter in G_1 and S phases induces acetylation at H3K9, activating *CDKN1A* transcription and enhancing transcriptional activation with p53 (113). However, this activation is modulated by VDR-induced transcription of *MCM7*, which later induces the *CDKN1A* target miRNA miR-106b (113). Additionally, VDR stabilizes expression of p27, which inhibits CDK2, the kinase activated by cyclin E, and retains it in the cytoplasm (114).

In addition to regulating the cell cycle directly, $1,25D_3$ and VDR also impact other growth signaling pathways through crosstalk. In the Hedgehog (Hh) pathway, $1,25D_3$ acts in a VDR-independent fashion at the level of the transmembrane G-coupled protein receptor Smo, inhibiting transduction of the Hh growth signal and thus preventing Gli-dependent transcription of pro-proliferative factors in basal cell carcinoma (115, 116). Additionally, 1,25D3 treatment of primary prostate epithelial and cancer cells demonstrated an early induction of DUSP10, a non-receptor tyrosine kinase that inactivates the stress-activated protein kinases p38 and JNK (117). The canonical MAPK pathway is itself affected when VDR displaces Sp1 from the *EGFR* promoter, downregulating its expression and thus attenuating EGF-mediated cell growth in breast cancer cells (118).

In some contexts, $1,25D_3$ not only mediates control over growth, but also of apoptosis. $1,25D_3$-mediated downregulation of Bcl-2 appears to be the major mediator of apoptosis in LNCaP prostate cancer cells, as overexpression of this anti-apoptotic protein inhibits induction of apoptosis (119). In K562 chronic myelogenous leukemia cells, not only is Bcl-2 downregulated, but Bax, the pro-apoptotic protein it inhibits, is itself induced upon $1,25D_3$ treatment, and leading to release of cytochrome *c* (120). This ultimately leads to activation of

the intrinsic apoptosis pathway through caspase-9 and caspase-3 (121). However, this is not the only apoptotic pathway through which $1,25D_3$ functions. Co-treatment of PC-3 prostate cancer cells of $1,25D_3$ with the general cytochrome P450 inhibitor ketoconazole does not induce the intrinsic apoptotic pathway, but rather the caspase-8-mediated apoptotic pathway (122). Also implicated in this co-treatment is a caspase-independent pathway through translocation of apoptosis-inducing factor (AIF) from the mitochondria to the nucleus, where it binds to DNA and induces chromosomal condensation and fragmentation (122-124).

Not all growth inhibition induced by $1,25D_3$ treatment is necessarily apoptosis-related, but may instead be due to cancer cells adopting a quiescent state. In conjunction with T treatment, $1,25D_3$ induces greater differentiation of normal rat prostate cells to epithelial tissue in correlation with an increase in expression of five nuclear matrix proteins (125). A direct target of VDR, E-cadherin, adheres cells together in junctions, preventing independent movement typical of metastasis in colon carcinoma (126). Accordingly, this also induces translocation of β-catenin to the plasma membrane, where it is sequestered from the Wnt pathway in conjunction with rapid VDR signaling to the RhoA/ROCK stress fiber-signaling pathway (126, 127). VDR also induces expression of IGFBP3 as a direct target, confirmed by the identification of a VDRE in the promoter (128, 129). In turn, IGFBP3 inhibits angiogenesis and induces p21 expression (130, 131). IGFBP3 expression is correlated to differentiated state of the prostate, with lower expression due to hypermethylation of the promoter correlating with aggressiveness of the tumor (132, 133). $1,25D_3$ also upregulates intracellular interleukin-1α (IL-1α), which pleiotropically suppresses growth of prostate progenitor/stem cells (PrP/SCs) (134).

Similarly, a VDR agonist can also inhibit progression to pathogenic states, such as cancer and fibrosis. Knockout of VDR in mice rendered their livers susceptible to fibrosis, inducing upregulation of transforming growth factor-β (TGF-β), an important mediator of epithelial-to-mesenchymal transition (EMT) and promoter of fibrosis, upon exposure to CCl_4 (135). Liganded VDR inhibits the ability of TGF-β to induce fibrosis and EMT upon being recruited by Smad3 to TGF-β-target genes that have been epigenetically modified, whereupon it displaces the Smad3/Smad4 dimer from the Smad binding element (SBE) (135). However, this relationship between VDR and Smad3 is not universal. In the context of cutaneous injury, TGF-β signaling requires liganded VDR in order to have full phosphorylation of Smad3 and normal inflammatory response (136). In a mammalian reporter assay, Smad3 can potentiate VDR-induced transactivation (137). Additionally, an osteocalcin promoter with modifications in spacing between the SBE and VDRE exhibited synergistic activation upon co-treatment of TGF-β and $1,25D_3$, indicating a VDR/pSmad3 interaction (138). Thus, the relation of VDR to TGF-β signaling is context-dependent.

In addition to interactions with TGF-β, liganded VDR reduces inflammatory signaling, a tumorigenic promoter. For example, interleukin-8 (IL-8) stimulates membrane translocation of RhoA, activating the RhoA/ROCK pathway, which then activates NF-κB (139, 140). In turn, NF-κB induces transcription of IL-8, completing the autocrine feed-forward loop (141). Ultimately, IL-8 stimulates growth, invasive activity, and metastasis (142). Activated VDR inhibits IL-8-induced cell proliferation and NF-κB p65 translocation into the nucleus, in turn repressing NF-κB-mediated transcription of IL-8 (139, 141). Another downstream target of NF-κB, the prostaglandin synthesis rate-limiting enzyme cyclooxygenase-2 (COX-2), is also downregulated upon $1,25D_3$ treatment (143, 144). In conjunction with $1,25D_3$-induced

upregulation of the negative prostaglandin regulator 15-hydroxyprostaglandin dehydrogenase (15-PGDH), levels of prostaglandin E_2 (PGE_2), which stimulates migration and invasion, are significantly reduced (145, 146). In a third measure of control on prostaglandins, $1,25D_3$ also represses transcription of the PGE_2 target receptor EP_2 (145).

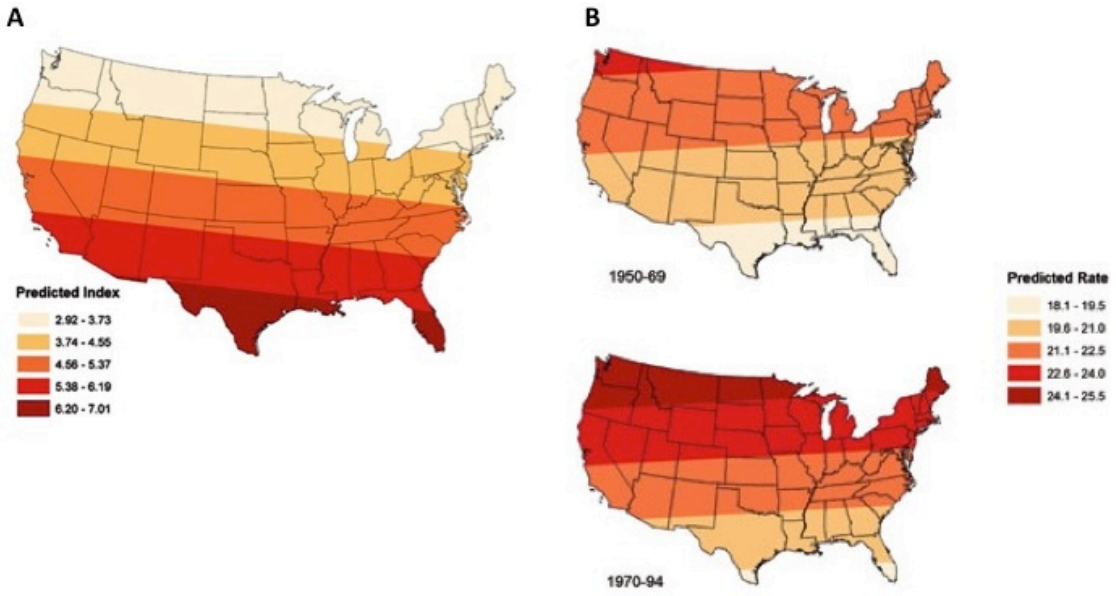

Figure 5: UV radiation correlates with incidence of lethal prostate cancer.

A. First-order trend surface map of UV radiation in the US. B. First-order trend surface maps of prostate cancer mortality by county among white males in the periods 1950-1969 and 1970-1994. Springer and *Cancer Causes & Control* (17(8), 2006, 1091-1101, "UV, latitude, and spatial trends in prostate cancer mortality: all sunlight is not the same (United States)", Schwartz GG, Hanchette CL, Figures 1-2) have given permission to reprint figures from the publication in which the material was originally published, with kind permission from Srpinger Science and Business Media. License number 3203830438030 (147).

1.3.4 Epidemiology and clinical significance of Vitamin D in prostate cancer

The ability of the prostate to synthesize its own active Vitamin D metabolite has implications regarding the relationship between sunlight exposure and development of prostate cancer. Geographic epidemiological studies via trend surface analysis with respect to UV exposure in the United States between 1950 and 1994 demonstrated a strong correlation between latitude and prostate cancer mortality rates, especially north of 40˚N (Figure 5) (147). This line of demarcation is important, because the necessary radiation for Vitamin D_3 synthesis is 18 mJ/cm^2, a daily level that is not reached between the months of November to February at this latitude (148). Indeed, diagnosis of skin cancers in the Netherlands correlated with decrease in risk of advanced prostate cancer (149). However, a study in New South Wales, Australia observed an increased risk in men who were exposed to high amounts of sunlight in their mid-adult years, suggesting a potential U-shaped curve at which an optimal level of sunlight protects against lethal prostate cancer (150). While multiple studies have concluded that there is no correlation between serum $25D_3$ levels and overall risk of prostate cancer, recent studies have implicated low serum $25D_3$ levels as a risk factor for aggressive prostate cancer and higher mortality (151-155). At the genetic level, polymorphisms of VDR such as FokI and BsmI, which define the restriction sites cut by the respective endonucleases, have also been associated with higher mortality (154, 156).

From the epidemiological studies, it should follow that treatment with high-dose $1,25D_3$ (DN-101) could improve prognosis (157). The Phase II Androgen-Insensitive Prostate Cancer (AIPC) Study of Calcitriol Enhancing Taxotere (ASCENT) trial suggested that such treatment would be effective as an adjuvant to docetaxel treatment (158). However, the following Phase III ASCENT II trial was disappointing, with the study being halted because the $1,25D_3$ adjuvant

therapy arm had significantly shorter survival than the control group (159). Two major factors affect response to $1,25D_3$ treatment. Basal and induced expression of CYP24A1 significantly reduces the bioavailability of $1,25D_3$ (160). In fact, increased expression of CYP24A1 is correlated with poor prognosis in esophageal and lung cancer (161, 162). In order to compensate for this metabolism, higher doses of $1,25D_3$ may be required in order to induce a pharmacological response. However, high dosage of intravenous $1,25D_3$ can lead to the condition of hypercalcemia. This increase in serum calcium concentration can cause bone pain, nausea, abdominal pain, development of kidney stones, and neuromuscular weakness (163, 164). Pre-clinically, ketoconazole, a general cytochrome P450 inhibitor that can inhibit CYP24A1, enhances $1,25D_3$-induced apoptosis in PC3 prostate carcinoma cells (122). Other levels of control may be important. There have been very few studies on the effects of the tumor microenvironment, namely the stroma, on $1,25D_3$ treatment in prostate cancer. The importance of the microenvironment will be discussed in the following section.

1.4 MICROENVIRONMENT EFFECTS ON TUMOR GROWTH

1.4.1 Normal and reactive stroma in prostate cancer

The Knudson multi-hit hypothesis has traditionally ascribed the major causes of carcinogenesis to multiple mutations of proto-oncogenes and tumor-suppressor genes in epithelial cells, leading to uncontrolled proliferation (165). However, mutations within these cells are not sufficient to generate tumors. In a study by Olumi et al., initiated prostate epithelial cells xenografted with normal human prostate fibroblasts into mice were unable to form tumors, whereas xenografts

containing carcinoma-associated fibroblasts (CAFs) were able to form tumors. Furthermore, CAFs grown with normal human prostate epithelial cells were unable to form tumors (166). Similarly, LNCaP cells grafted with normal prostate stroma into mice were rarely tumorigenic, and grafts with normal lung stroma did not produce any tumor growth (167). This correlated with the previous finding that rat fetal urogenital sinus mesenchyme (UGM) can induce a bladder transitional-cell carcinoma line to accelerate its proliferation in an androgen-inducible manner (168). Together, these results demonstrated the importance of the supporting stromal tissue for epithelial growth and development.

Fetal action of the prostate stroma is derived from the UGM, which directs differentiation of the urogenital sinus epithelium (UGE) and prostate development upon androgen stimulation (169). Reciprocally, prostate epithelium induces UGM to differentiate into smooth muscle (170). In the adult human, the stroma comprises a heterogeneous mixture of fibromuscular tissue, including fibroblasts, smooth muscle cells, and a collagen-rich extracellular matrix (171). The normal stroma produced paracrine factors, such as keratinocyte growth factor (KGF), upon T stimulation that promote epithelial development (172, 173). Paradoxically, high circulating levels of T can maintain the adult stroma in a quiescent state (174). This homeostasis is regulated by stromal targets, in which stromal fibroblasts stimulate epithelial proliferation and stroma smooth muscle cells inhibit it in response to T (175).

A disruption in the homeostasis is symptomatic of prostate cancer. Exposure of prostate stroma to PIN, primary, or metastatic tumor epithelium induces a desmoplastic phenotype, in which proliferation of stromal cells and deposition of extracellular matrix (ECM) is increased, precipitating a “fertile soil” for tumor development (176-178). The tumor secretes TGF-β to the stroma, where it activates stromal fibroblasts from their resting state (179, 180). The process of

transdifferentiation is similar to how fibroblasts are activated in wound healing, in that the fibroblasts are transdifferentiated to a myofibroblastic phenotype, expressing smooth muscle alpha-actin (SMAA), vimentin, and pro-collagen I (181, 182). This "reactive stroma", which resembles an overhealing wound, confers a fertile environment for the tumor by paracrine expression of factors such as vascular endothelial growth factor (VEGF), fibroblast growth factor-2 (FGF2), tumor necrosis factor-α (TNF-α), platelet-derived growth factor (PDGF), and KGF (183-185). These factors improve blood supply to the tumor, increase proliferation, and promote migration. TGF-β also induces its own stroma expression that feeds back onto the tumor and promotes EMT (186, 187). TGF-β also induces a pro-oxidant environment through induction of Cox-2, which produces hydrogen peroxide, inhibiting epithelial E-cadherin expression and increasing tumor mutagenesis (188). The reactive stroma further alters the microenvironment by remodeling the extracellular matrix, inducing expression of matrix metalloproteinase-1 (MMP1), MMP2, MMP3, MMP9, tenascin C, and versican (189-192). Together, they break down the basement membrane and inhibit adhesion of tumor cells, allowing them to migrate and eventually metastasize to distant sites.

1.4.2 Hic-5: a stroma-associated receptor cofactor

Numerous regulators at the transcriptional level modulate stromal response to TGF-β and the ensuing reactive-stroma phenotype. One such important cofactor is Hic-5, which is typically localized exclusively to the prostate stroma under normal and malignant conditions (193). Hic-5 is derived from Hydrogen peroxide-Inducible Clone-5, referring to one stimulus that induces

upregulation of the protein (194). Additionally, Hic-5 is upregulated by TGF-β signaling, which indicates its expression in reactive stroma (76, 193-195).

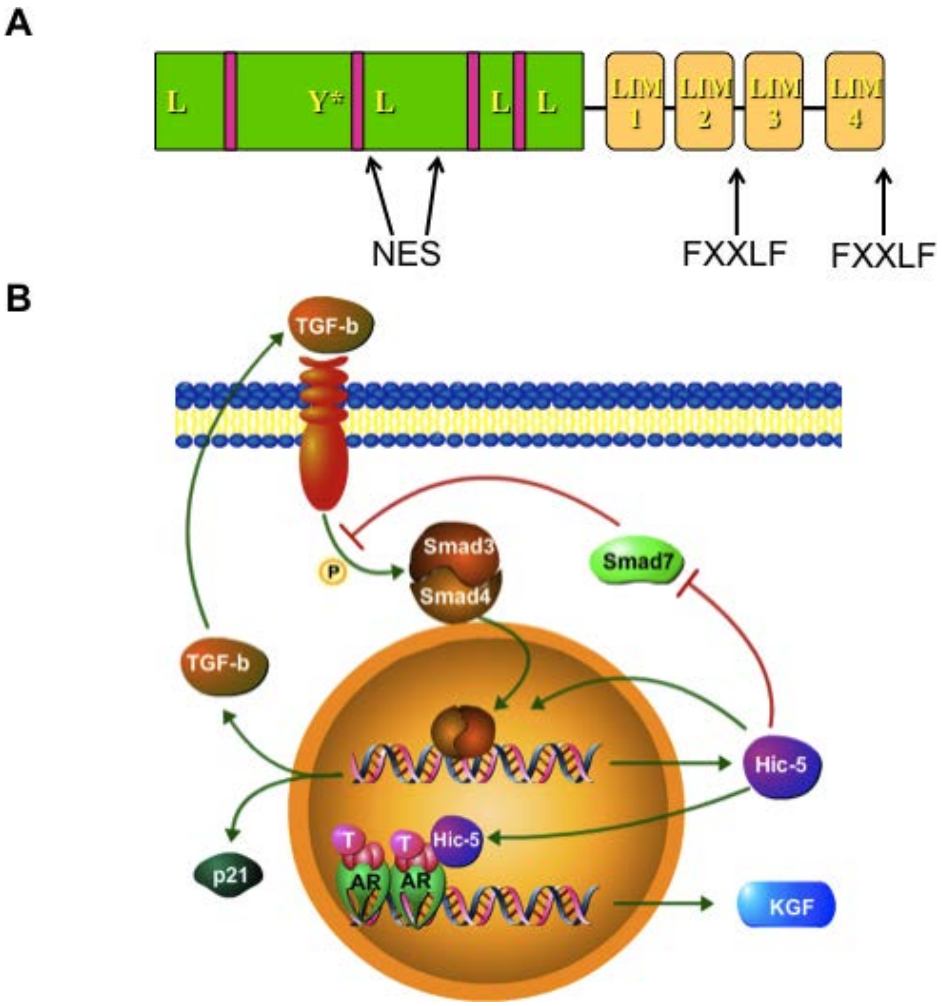

Figure 6: Hic-5 structure and pathway.

A. Hic-5 contains four N-terminal LD domains and four C-terminal LIM domains. B. Hic-5 transcription is induced by TGF-β-activated Smad signaling. Hic-5 then feeds back on the TGF-β pathway, inhibiting the inhibitory Smad7 and acting as a co-regulator for Smad2 and Smad3. Additionally, Hic-5 can act as a co-activator for nuclear receptors such as AR and GR.

Hic-5 belongs to the paxillin family of group III LIM domain-containing proteins, which also includes paxillin and leupaxin (196). The paxillin family of proteins shares a similar structure, with amino-terminal (N-terminal) leucine-rich (LD) motifs that vary in number and a conserved carboxy-terminal (C-terminal) set for four LIM domains, which are cysteine-rich regions composed of two zinc fingers (196-198). The most common splice variant of Hic-5 contains four LD domains (Figure 6A) (199). The family is also characterized by dual localizations within the nucleus and at focal adhesions in the cytoplasm (200). Within focal adhesions, Hic-5 functions as an adapter protein, binding to the focal adhesions through its LIM domains and inhibiting tyrosine phosphorylation of paxillin by binding to focal adhesion kinase (FAK) and protein tyrosine phosphatase-PEST (PTP-PEST) (198, 201, 202). The net effect of this inhibition is modulation of paxillin-mediated transduction of integrin signals, thus inhibiting behaviors such as cell spreading (203, 204). Hic-5 is also a key mediator in TGF-β-induced EMT in mouse kidney proximal epithelial tubule cells, mediating RhoA/ROCK-dependent stress-fiber formation, which further induces its own expression (205). Interestingly, Hic-5 is required for adhesion formation in three-dimensional ECMs and, with paxillin, for metastasis of breast cancer cells (204).

Under oxidative conditions, the cysteine residues at amino acids 64 and 91 within Hic-5 are oxidized, decreasing affinity for FAK and PTP-PEST (206). This leads to an inhibition of a potent nuclear export signal (NES) located between residues 64 and 98, thereby enhancing nuclear retention of Hic-5 (207). Within the nucleus, Hic-5 acts as a steroid receptor co-activator, where it has been implicated in co-activating GR, progesterone receptor (PR), and AR (208-210). It was independently cloned as Androgen Receptor-Associated protein 55 (ARA55) as interacting with AR to enhance transcriptional activity (210, 211). Hic-5 has no intrinsic

methyltransferase or histone acetyltransferase activity on its own, but rather acts as a scaffolding protein to recruit other cofactors through its FXXLF motifs (212). In the context of a mammary carcinoma cell line, Hic-5 recruits TIF-2 and CBP/p300 to glucocorticoid-responsive genes, such as c-*fos* and p21 (213). In prostate stromal cells, Hic-5 is necessary for full transactivation of the AR target gene KGF (Figure 6B) (193). Alternatively, in the absence of ligand, Hic-5 recruits the NCoR complex, repressing transcription at these sites (213, 214).

In addition to binding to nuclear receptors, Hic-5 also binds to other transcription factors. Hic-5 binds to Sp1 and recruits p300 through its LIM4 domain, enhancing p21 promoter transactivation (49). Additionally, it feeds back onto TGF-β signaling through interaction with Smad3. Interestingly, though, this interaction yields conflicting effects. In mouse myoblastic cells, the Sp1/Hic-5 complex is also bound to Smad3 in p21 promoter transactivation (49). However, within rat prostate and LNCaP cells, interaction of the Hic-5 C-terminus with the MH2 domain of Smad3 results in transcriptional inhibition of Smad3 targets, such as PAI-1 (215). A key protein that may account for the differing effects of Hic-5/Smad3 interaction is Smad7, a Smad3 inhibitor. In PC3 and WPMY-1 cells, Hic-5 inhibits Smad7-mediated inhibition through its LIM3 domain, permitting TGF-β-induced phosphorylation of Smad2 and non-Smad TGF-β responses (Figure 6B) (216).

The role of Hic-5 in disease is complex. In one clinical study, Hic-5 expression was higher in some patients with CRPC, correlating with cell-line studies that suggested that Hic-5 is upregulated in androgen-hypersensitive cells (217). Similarly, higher expression of Hic-5 in hypertrophic scarring fibroblasts inhibits proliferation but does not induce apoptosis, perpetuating fibrosis in hypertrophic scars (218, 219). However, other clinical studies in prostate

cancer demonstrated reduced expression of Hic-5 in stroma that also lost AR expression, a phenotype associated with an increased risk of biochemical relapse (220, 221).

Histological studies have previously shown Hic-5 expression to be predominantly stromal, even in advanced prostate cancer (193, 222). However, new evidence has developed of an epithelial role for Hic-5 in the prostate. Castration of mice induces epithelial expression of Hic-5 in normal prostate epithelium (223). Xenografts of benign and cancerous human prostate epithelium in mice also exhibit this induction upon castration (223). Overexpression of Hic-5 in LNCaP (LNCaP/Hic-5) cells reduced tumor growth and invasion and restored castrate responsiveness to mixed xenografts containing stroma with a TGF-β receptor 2 (Tgfbr2) knockout (223). Thus, Hic-5 may have an anti-proliferative, anti-tumorigenic role within the carcinoma epithelium itself. However, this is in contrast to expression of Hic-5 in the established PC3 cell line (193). As the PC3 line is also known to be androgen-insensitive, it may also be that the patient from which the line was derived was previously treated with castration or ADT and thus not reflective of treatment-naïve tumors (224).

1.5 GOALS OF THIS DISSERTATION

Previous research into effects of $1,25D_3$ on prostate stroma has been limited, and there is no information regarding the identity or potential biological impact of stromal cell-specific nuclear receptor co-regulators (e.g. Hic-5). Interestingly, the available data indicate that VDR expression is reduced in cancer-associated stroma (225). However, the research does not consider the effect of Hic-5, a cofactor of steroid hormone receptors. Although VDR is homologous to other steroid hormone receptors, the effect of Hic-5 on VDR target

transactivation has not been examined. The goals of this project are directed toward understanding this potential relation between Hic-5 and VDR and its effect on treatment in prostate cancer lines. In the scope of this dissertation, I reached two goals:

1. To determine the effect of Hic-5 expression on stromal expression and activity of VDR through molecular interactions
2. To determine the effect of ectopic Hic-5 expression on proliferation and viability of a $1,25D_3$-treated prostate cancer cell line.

The complex role of Hic-5 in previous research contributes to our current understanding of CRPC. ***This project outlines a novel association between VDR and Hic-5 that affects $1,25D_3$ action in both prostate cancer cells and stromal cells that comprise the tumor microenvironment. Therefore, any future consideration of $1,25D_3$ treatment in prostate cancer will need to consider how co-regulators such as Hic-5 could exert compartment-specific effects to either enhance the effectiveness of $1,25D_3$ therapy or limit its action.***

2.0 MATERIALS AND METHODS

2.1 CHEMICALS AND REAGENTS

Recombinant TGF-β1 was purchased from R&D Systems (Minneapolis, MN) and reconstituted in 4.0 mM HCl, according to the manufacturer's protocol. $1,25D_3$ was purchased from Cayman Chemical (Ann Arbor, MI) and reconstituted to 20 μM in cell culture-grade DMSO. Specific inhibitor of Smad3 (SIS3) was purchased from Sigma (St. Louis, MO) and reconstituted according to the manufacturer's protocol. A mouse monoclonal anti-Hic-5 antibody (clone 34/Hic-5) was purchased from BD Biosciences (San Jose, CA). A mouse monoclonal anti-VDR antibody (clone D-6), mouse monoclonal anti-SMAA antibody (clone 1A4), and rabbit polyclonal anti-α-tubulin antibody (clone H-300) were purchased from Santa Cruz Biotechnology (Santa Cruz, CA). Rabbit polyclonal antibodies directed against phospho-Erk1/2 (clone D13.14.4E) and Erk1/2 (clone 137F5) were purchased from Cell Signaling Technology (Beverly, MA). A mouse monoclonal antibody against GAPDH (clone 71.1) and secondary HRP-conjugated antibodies were purchased from Sigma.

2.2 CELL CULTURE

WPMY-1 and PS30 cells are commercially available and were purchased from American Type Culture Collection (Rockville, MD). Scr and shHic-5 cells were generated as described below. LNCaP cells transfected with control lentivirus (WT LNCaP) and lentivirus containing murine Hic-5 (LNCaP/Hic-5) were obtained as a gift from the laboratory of Neil Bhowmick (Cedars-Sinai Medical Center, Los Angeles, CA) (223). Cells were maintained in monolayer in RPMI-1640 medium containing 5% fetal bovine serum (FBS) (for WPMY-1 cells) or 10% FBS (for PS30, WT LNCaP, and LNCaP/Hic-5 cells) and 1% penicillin/streptomycin at 37˚C and 5% CO_2. Cells were passaged at ~90% confluence.

2.3 GENERATION OF STABLE KNOCKDOWN CELLS

Short-hairpin RNA (shRNA) sequences were designed against Hic-5 (SH1-4) or as a scrambled (Scr) control (Table 1). The oligonucleotides were annealed to form dsDNA and inserted into the pHR CMV PURO Wsin18 plasmid after enzymatic digestion by *Spe*I and *Pst*I. The plasmids were packaged into lentiviral vectors. WPMY-1 cells were seeded on 6-well cell culture dishes at a density of 2.5 x 10^5 per well for 24 hr before infection. Lentivirus infection media containing polybrene (8 μg/ml) was used to infect the cells for 24 h. The next day, the media was changed, and the cells were cultured for an additional 48 h, trypsinized, and passed to new tissue culture dishes. Cells were then treated with medium containing puromycin (1 μg/ml) for 3 days. The resulting pooled colonies were selected, transferred to 96-well dishes, and maintained

in puromycin selection medium. Pooled colonies were expanded in 30 mm dishes. The line generating the most efficient knockdown (SH2) was renamed shHic-5.

Table 1: Sequences of shRNA generated against Hic-5

Construct name	shRNA Sequence
Scr	5'-AAGGGTAGGTTCGACTAGCAGGACTCT-3'
SH1	5'-GGTTGCTTCATGAACTTAGTGCCAC-3'
SH2 (shHic-5)	5'-GGAACTTAATTCCACTCAATTCAAC-3'
SH3	5'-GATCGGTTGCGTCAGGAAATTAATG-3'
SH4	5'-GAGGACCAGTATGAAGATCAGAAAA-3'

2.4 RNA MICROARRAY

Scr and shHic-5 cells were plated at a density of 2.5 x 10^5 cells per well in a 6-well plate and cultured overnight. The cells were then cultured in serum-free medium for 24 hrs. The following day, they were treated with TGF-β (0, 2.0 ng/mL) and incubated at 37˚C for 10 hrs. The medium was then removed, and cells were lysed in 500 µL cold TRIzol (Life Technologies, Grand Island, NY). RNA was extracted using the RNeasy Mini kit (Qiagen, Valencia, CA). 300 ng of total RNA extracted from each of 5 replicate treatments were analyzed using Affymetrix Human Gene 1.0 ST Arrays (Santa Clara, CA). Bioinformatics were performed in R Statistical Software using Bioconductor and the Limma package. Briefly, array data was normalized using RMA, filtered by mapped probes and an arbitrary minimum expression threshold, and genes different between groups called by Benjamini-Hochberg adjusted p-values determined from Bayesian linear regression modeling.

2.5 WESTERN BLOT

$5.0*10^5$ WPMY-1 (Scr and shHic-5) or PS30 cells were plated on 65-mm plates and grown overnight. The following day, they were cultured in serum-free medium for ~2 hrs prior to the indicated treatment. At the conclusion of the indicated treatment, whole-cell lysates were obtained by lysing WPMY-1 (Scr and shHic-5) and PS30 cells in RIPA buffer (140 mM NaCl, 0.1% sodium deoxycholate, 10 mM Tris buffered to pH 8.0, 1 mM EDTA, 0.5 mM EGTA, 1% Triton-X, 0.1% SDS, 1 mM NaF, 1 mM PMSF, 100 μM sodium orthovanadate, protease inhibitor cocktail (Sigma)) and were quantified by the Lowry assay. 15-20 μg of total protein were electrophoresed in a 10% acrylamide gel and transferred to a PVDF membrane (Millipore, Billerica, MA) using a Transblot SD Semi-Dry Transfer Cell (Bio-Rad, Hercules, CA). Membranes were blocked in 5% dry milk dissolved in phosphate-buffered saline (PBS) containing 0.1% Tween-20 (PBS-T) for 30-60 minutes at room temperature on a rotator. The indicated antibody was added to a solution of PBS-T containing 2.5% dry milk at a concentration of 1:1000 and incubated on the blot overnight at 4˚C on a rocker. Membranes were washed three times for 5 minutes each in PBS-T, then incubated for 1-2 hrs in a solution of HRP-conjugated secondary antibody diluted 1:3000 in PBS-T containing 2.5% dry milk. Membranes were washed an additional three times for 5 minutes each in PBS-T, then incubated with Western Lightining ECL chemiluminescent reagent (Perkin-Elmer, Waltham, MA) to detect the HRP signal on chemiluminescent film. Densitometry was analyzed using ImageJ (NIH). Blots were stripped in Re-Blot Plus Strong solution following the manufacturer's instructions (Millipore) and re-probed for GAPDH, α-tubulin, or Erk1/2 expression as loading controls or additional proteins.

2.6 RNA ISOLATION AND REVERSE TRANSCRIPTION-QUANTITATIVE PCR

Scr and shHic-5 cells were plated in 6-well plates at a density of 1.75 x 10^5 cells per well and were grown overnight. The next day, they were cultured in serum-free medium for ~2 hr. TGF-β1 (0, 3.5 ng/mL) and 1,25D_3 (0, 100 nM) were added to fresh serum-free medium to add to the cells. The cells were incubated at 37˚C for 6 hrs. RNA extraction was performed as described, with the resulting RNA quantified using the NanoDrop ND-1000 spectrophotometer (Wilmington, DE). Complementary DNA (cDNA) was generated using the High Capacity RNA-to-cDNA kit (Applied Biosciences, Carlsbad, CA) according to the kit protocol. The resulting samples were then diluted to 100 µL with nuclease-free water. Reverse transcription-quantitative PCR (RT-qPCR) was then performed on the samples with the iTaq Sybr Green Supermix with ROX (Bio-Rad) on the Stratagene Mx3000P thermocycler (Cedar Creek, TX) with primers directed toward GAPDH, VDR, CYP24A1, and human Hic-5 (Table 1). Relative expression was quantified using the comparative Ct (ddCt) method.

In a similar experiment, LNCaP and LNCaP/Hic-5 cells were seeded on a 6-well plate at a density of 3.0 x 10^5 cells per well and cultured overnight. The next day, the cells were treated with 1,25D_3 (0, 100 nM) for 6 hrs. RNA extraction and cDNA synthesis were performed as described. RT-qPCR was performed with primers directed toward GAPDH, CYP24A1, and murine Hic-5 (Table 2).

Table 2: Primer sequences for RT-qPCR

Primer set	Sequences
GAPDH	Forward: 5'-ATCGTCCACCGCAAATGCTTCTA-3' Reverse: 5'-TGTTAGCCATGCCAATCTCATCT-3'
VDR	Forward: 5'-CTGACCCTGGAGACTTTGAC-3' Reverse: 5'-TTCCTCTGCACTTCCTCATC-3'
CYP24A1	Forward: 5'-ACCCAGGTGTTGGGATCCAGTGA-3' Reverse: 5'-AGCTCTGCTAATCGGCGACCA-3'
Hic-5 (human)	Forward: 5'-TCAGGAGAGCAGAAGGAGGA-3' Reverse: 5'-GGCTGGAAGATGGTTTTGAA-3'
Hic-5 (murine)	Forward: 5'- AGGATGCCCATCTCCACCAGGACA-3' Reverse: 5'- AGCACTCGGGGCAAAAGGGAG-3'

2.7 METABOLISM ASSAY

Scr and shHic-5 cells were plated at a density of 5.0 x 10^5 cells per 65-mm dish and were grown overnight. The next day, the cells were cultured in serum-free medium for ~2 hrs. Cells were treated in duplicate with 1,25D_3 (0, 100 nM) for 0 or 24 hrs at 37˚C. Reference treatments in cell-free dishes were included to account for spontaneous degradation of 1,25D_3. Cells were scraped into medium at each time-point, flash-frozen in liquid nitrogen, and stored at -80˚C prior to analysis by LC-MS/MS at the UPCI Clinical Pharmacologicy Analytical Facility. LC-MS/MS was performed as previously described (226).

2.8 LUCIFERASE EXPRESSION ASSAY

Plasmid pCYP24-537 was obtained from the laboratory of Pamela Hershberger (Roswell Park Cancer Institute), and plasmids p392, p451, p470, and p496 were obtained from the laboratory of David Callen (University of Adelaide) (227). Scr and shHic-5 cells were plated at a density of 7.5 x 10^4 cells per well in a 12-well plate and were grown overnight in antibiotic-free medium containing 5% FBS. The following day, the indicated plasmid containing a firefly luciferase reporter (0.5 μg/well) (Table 3), a *Renilla* luciferase plasmid containing a CMV reporter (0.1 μg/well), and X-tremeGENE lipophilic transfection reagent (5.0 μL/well) (Roche Applied Science, Indianapolis, IN) were incubated in OPTIMEM (100 μL/well) for 1 hr. Cells were then transfected with 100 μL of the mixture and incubated overnight. The following day, the transfection medium was removed, and the cells were cultured in serum-free medium for ~2 hrs. They were then treated in triplicate with TGF-β1 (0, 3.5 ng/mL) and 1,25D_3 (0, 100 nM) and incubated for 6 hr at 37˚C. Cells were lysed and freeze-fractured overnight in the passive lysis buffer contained in the Dual-Luciferase Reporter Assay system (Promega, Madison, WI). Lysates were analyzed in the Veritas Microplate Luminometer (Promega) using the Dual-Luciferase kit to record firefly and *Renilla* readings in relative luminescence units (RLU). Firefly values were normalized to *Renilla* values.

Table 3: List of luciferase reporter plasmids and their sequence spans

Plasmid	Sequence span
pCYP24-537	-537 to -5
p392-luc	-392 to +36
p451-luc	-451 to +36
p470-luc	-470 to +36
p496-luc	-496 to +36

2.9 *IN SILICO* ANALYSIS OF TRANSCRIPTION FACTORS

The sequence of the human CYP24A1 promoter from region −496 to -392 bp was obtained from RefSeqGene (accession number NG_008334.1) and a search for putative transcription factors was performed using the Transcription Element Search System (TESS) (228). Unique sites were analyzed in the literature for previously reported interactions of the target transcription factor with Hic-5.

2.10 PROLIFERATION ASSAY

LNCaP and LNCaP/Hic-5 cells were plated at 2.5 x 10^3 cells per well in a 96-well plate for at least 18 hr. The cells were carefully treated in triplicate with $1,25D_3$ (0, 10, 100 nM) in RPMI 1640 containing 10% FBS for 0 and 72 hr at 37˚C. At each time-point, the plate was aspirated and frozen overnight at -80˚C. The next day, the plate was thawed to room temperature. The CyQuant Cell Proliferation Assay kit (Invitrogen) was used to measure nuclear staining. Each well was incubated with the prepared dye mixture (100 µL/well) in the dark for 10 minutes.

Fluorescence was read at excitation wavelength of 480 nm and an emission wavelength of 520 nm on a SpectraMax Gemini EM plate reader (Molecular Devices, Sunnyvale, CA). Data at 72 hr was normalized to baseline at 0 hr.

2.11 CO-CULTURE PROLIFERATION ASSAY

25-mm circular coverslips were made suitable for co-culture using nail polish to create pedestals. Four drops of nail polish were added to each coverslip and then allowed to dry under an ultraviolet lamp for additional sterilization for 1 hr. The coverslips were then placed in 6-well dishes and incubated in poly-D-lysine (10 μg/mL) for either 2 hrs at 37˚C or overnight at 4˚C. The coverslips were then washed twice in water. LNCaP and LNCaP/Hic-5 cells were plated at 1.5 x 10^5 cells per well and grown overnight. Simultaneously, Scr and shHic-5 cells were plated at 2.0 x 10^5 cells per well in two other 6-well plates and grown overnight. The next day, the coverslips were moved to the 6-well plates containing the stromal cultures (Figure 7). Cells from two untreated coverslips from each epithelial line were washed in PBS and fixed to the coverslips immediately in 4% paraformaldehyde (PFA) at 0 hr to establish a baseline. The co-cultures were then treated with $1,25D_3$ (0, 100 nM) in RPMI 1640 medium containing 10% FBS for 72 hrs. The cells were washed once in PBS and then fixed to the coverslips in 4% PFA. The cells were then permeabilized in PBS containing 0.1% Triton-X. The cells were washed twice in PBS and then incubated with DAPI (1.0 mg/mL) at room temperature. The cells were washed twice in PBS, and the coverslips were mounted on slides using Vectashield medium (Vector Laboratories, Burlingame, CA). The slides were visualized and photographed under epifluorescence at 200X using the Olympus IX-81 microscope (Center Valley, PA). Counts

were averaged from 6 fields per coverslip and normalized to the 0-hr time-point for each respective epithelial line.

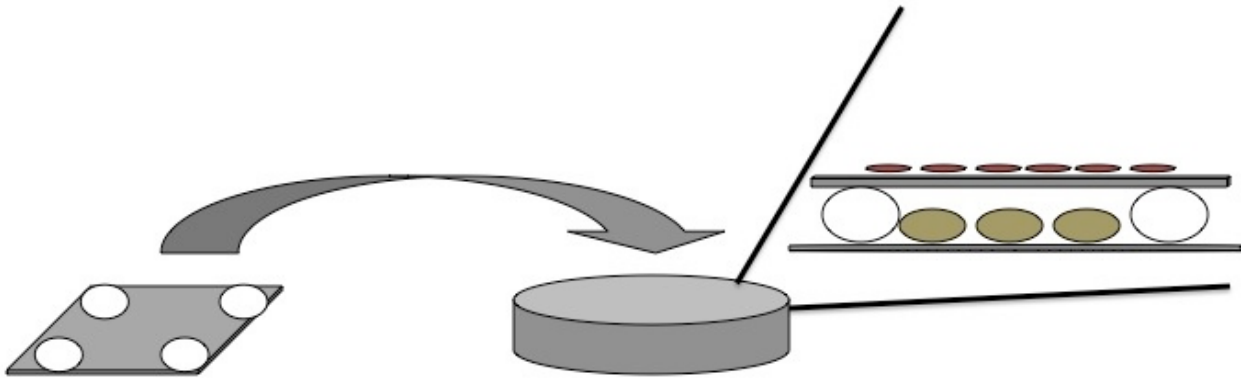

Figure 7: Schematic of co-culture assay.

Nail polish was placed at four points on the coverslip and dried. After treatment with poly-D-lysine, WT LNCaP and LNCaP/Hic-5 cells were plated on the coverslips and grown overnight. The next day, the coverslips were overlaid on the stromal layers. The nail-polish pedestals prevent extreme crushing of the stromal layer and permit exchange of paracrine factors into the greater medium.

2.12 CO-CULTURE VIABILITY ASSAY

18 mm x 18 mm coverslips were prepared as above. LNCaP/Hic-5, Scr, and shHic-5 cells were plated and grown as above. The co-cultures were treated with $1,25D_3$ (0, 10 nM) in RPMI-1640 medium supplemented with 10% FBS and incubated at 37˚C for 72 hrs. At the end of the incubation, the coverslips were moved to another 6-well plate and trypsinized in 1.0 mL trypsin for ~1 hr at 37˚C. The supernatants from the co-cultures were collected in 2.0-mL microcentrifuge tubes and centrifuged at 1.0×10^3 g for 10 minutes. The trypsinized

LNCaP/Hic-5 cells were added to their respective supernatant pellets and centrifuged again at 1.0 x 10^3 g and 4˚C for 10 minutes. The pellets were resuspended in 100 μL of medium and stored on ice until counting. Each sample was diluted with 100 μL of Trypan blue (Gibco, Grand Island, NY). 10 μL of the sample were loaded into both sides of a hemocytometer. Dead cells were counted in both sides of the hemocytometer under a light microscope by blue stain, whereas live cells were counted by dye exclusion. Three counts of the sample were taken and added together. Viability was determined by dividing the total number of live cells by the total number of cells counted.

2.13 STATISTICAL ANALYSIS

The UPCI Biostatistics Facility provided assistance with statistical analysis. Multiple comparisons were performed with the two-way or three-way mixed-models ANOVA with Satterthwaite approximation, followed by cell-means post-hoc test in SAS (229). Interval data and Western blot data that contained results below detectable levels were left untransformed, while ratio data that did not skew close to 0 were log-transformed, and proportion data was logit-transformed (230). RT-qPCR analysis was performed on the cycles scale, and confidence intervals were transformed to the concentration scale as estimates.

3.0 RESULTS

3.1 REGULATION OF VDR EXPRESSION BY TGF-β AND HIC-5 IN WPMY-1 PROSTATE STROMAL CELLS

Hic-5 functions as a co-activator of androgen receptor in WPMY-1 prostate stromal myofibroblast cells and is an established component of the TGF-β signaling pathway (49, 193, 215, 216, 219). To evaluate the impact of Hic-5 on the TGF-β response of WPMY-1 cells, a stable knockdown of Hic-5 using a specific, lentivirally encoded shRNA (shHic-5) was developed previously in the laboratory by Marjet Heitzer. Specifically, WPMY-1 cells were stably infected with lentivirus encoding either scrambled shRNA (Scr) or shHic-5. The response of generated Scr and shHic-5 lines to TGF-β was assessed by gene expression microarray 10 hours after treatment with 2.0 ng/mL TGF-β1 with assistance from Melanie Grubisha and Grant Buchanan. Of particular relevance here and shown in Figure 8, VDR was identified in the microarray as a TGF-β target whose mRNA expression was reduced upon Hic-5 knockdown. Basal expression of VDR was reduced upon Hic-5 knockdown in the microarray, although induction by TGF-β1 was retained. Detailed analysis of Hic-5 dependence of the TGF-β1-regulated transcriptome in WPMY-1 cells will be reported elsewhere.

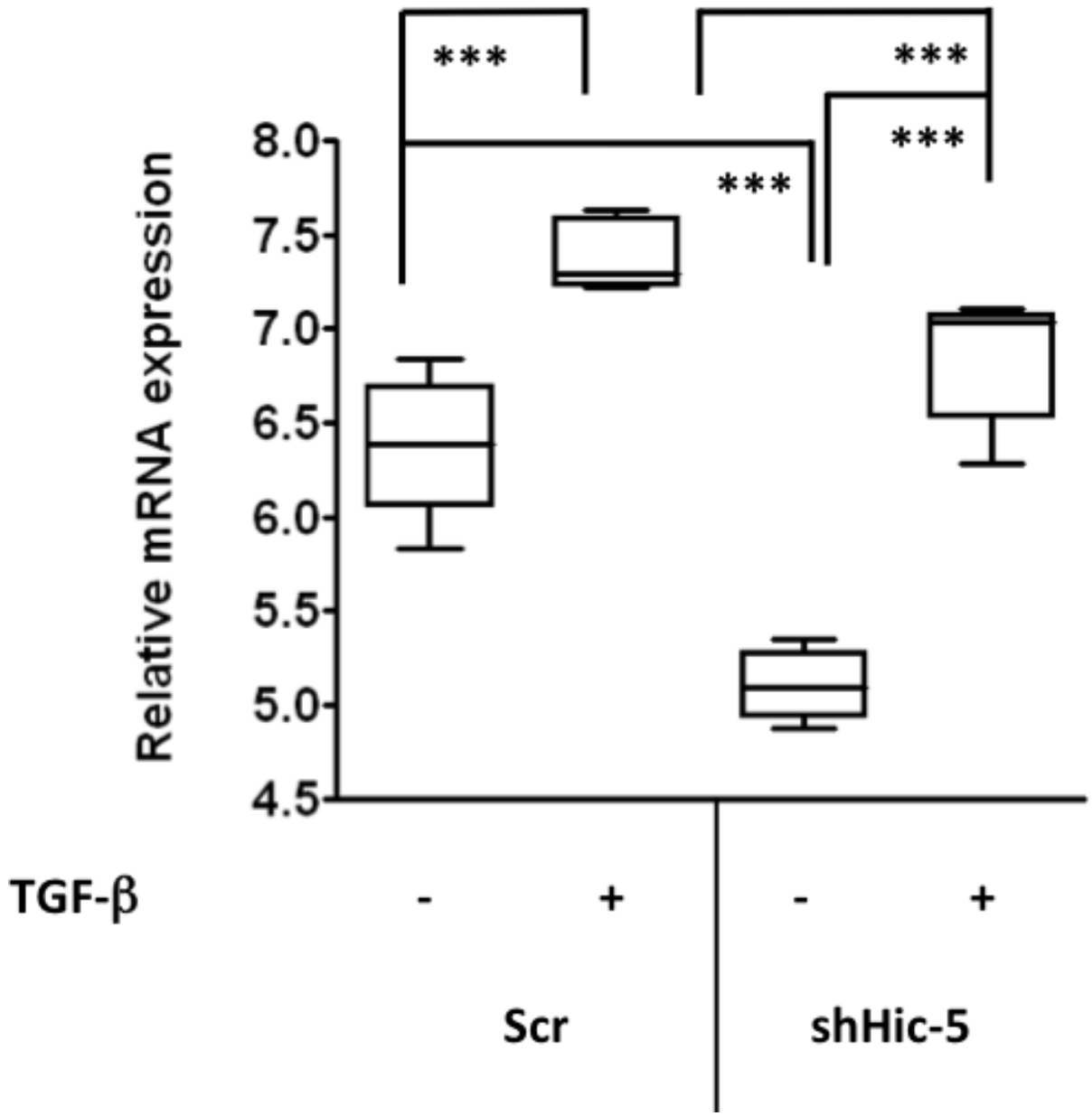

Figure 8: Basal and TGF-β1 induced VDR mRNA expression is reduced upon Hic-5 knockdown in WPMY-1 cells.

Scr and shHic-5 cells were treated with TGF-β□(0, 2.0 ng/mL) for 10 hrs and, and isolated RNA was hybridized to an Affymetrix Human Gene 1.0 ST microarray, which contained 14,267 human unique cDNA probes. Boxplots represent quartiles fromfive independent experiments. Two-sample t-tests were performed. *** $p < .001$.

In order to validate the microarray data, TGF-β1 and Hic-5 effects on *VDR* mRNA and protein expression were analyzed respectively using reverse transcription-quantitative PCR (RT-qPCR) and Western blotting in independent biological samples from Scr and shHic-5 cells. Figure 9A and Figure 10A show that expression of Hic-5 mRNA was indeed significantly reduced in shHic-5 cells. The use of 3.5 ng/mL TGF-β1 was optimal for my reagent preparation. While treatment of Scr cells with 3.5 ng/mL TGF-β1 induced expression of *VDR* mRNA 4-fold within 6 hours, this induction was inhibited by knockdown of Hic-5. Likewise, basal expression of *VDR* mRNA was reduced (Figure 9B, Figure 10B). Immunoblot analyses of Scr and shHic-5 cells 24h after treatment with or without 10 ng/mL TGF-β1 confirmed the effect of Hic-5 knockdown on basal and induced levels of VDR protein (Figure 9C-D). Therefore, Hic-5 regulates basal and TGF-β1-induced expression of VDR at the mRNA and protein level, supporting its role as a novel regulator of $1,25D_3$ and TGF-β1 signaling in prostate stromal cells.

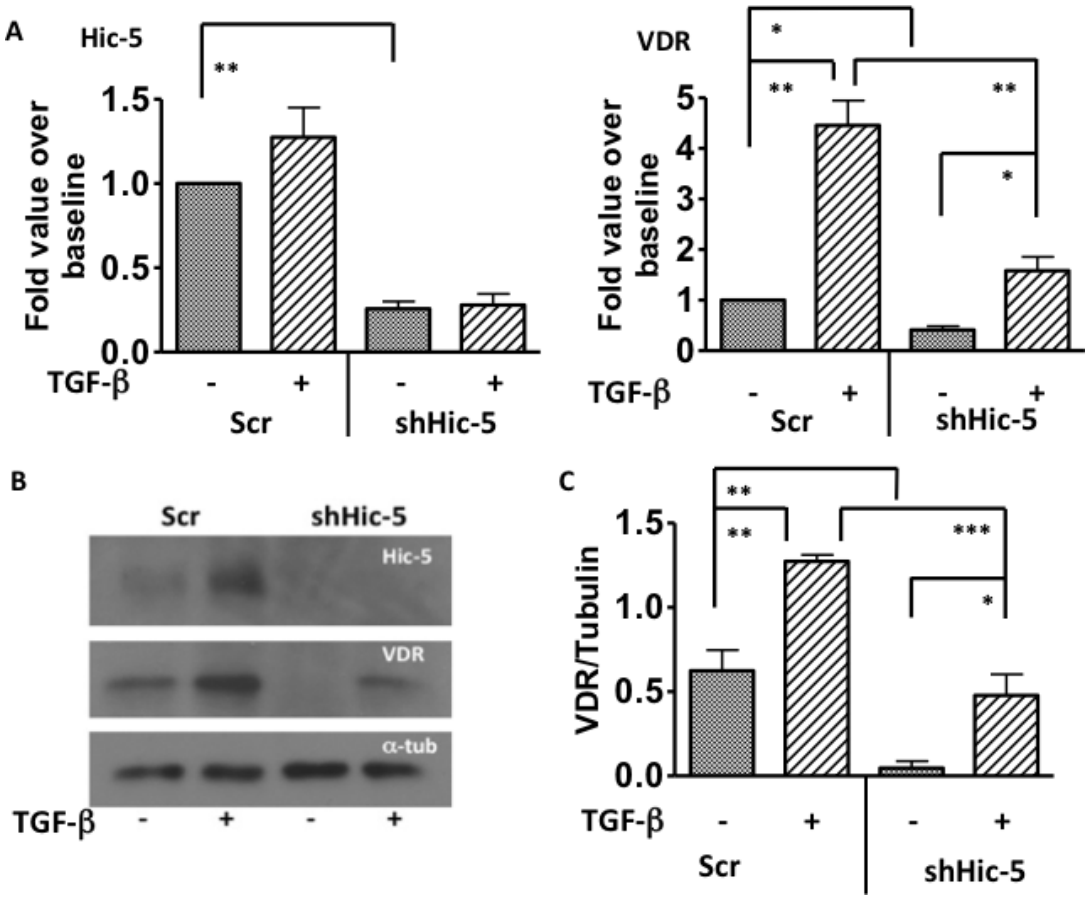

Figure 9: Hic-5 knockdown reduces basal and TGF-β-induced VDR mRNA and protein expression.

A, B. Scr and shHic-5 cells were serum-starved for 2 hr, then treated for 6 hr with TGF-β1 (0, 3.5 ng/mL). mRNA was extracted for cDNA synthesis and RT-qPCR probing for *Hic-5* (A), *VDR* (B), and *GAPDH* expression. Comparisons were made using the comparative Ct (ddCt) method. TGF-β1 induced VDR transcription in both Scr and shHic-5 cells. Data were analyzed with two-way ANOVA with mixed models with cell-means post-test. Bars represent mean±SEM of six independent experiments normalized to basal expression in Scr cells. * $p < 0.05$, ** $p < 0.01$. C. Scr and shHic-5 cells were serum-starved for 2 hr, then treated for 24 hr with TGF-β1 (0, 10 ng/mL). Blot is representative of three independent experiments. D. Western blot results were analyzed by densitometry in ImageJ. TGF-β1 induced VDR

expression in both Scr and shHic-5 cells. Basal expression of VDR in shHic-5 was below detectable levels, so the data was not transformed. Two-way mixed-models ANOVA followed by cell-means post-test were performed. Bars represent mean±SEM of three independent experiments. * $p < 0.05$, ** $p < 0.01$, *** $p < 0.001$.

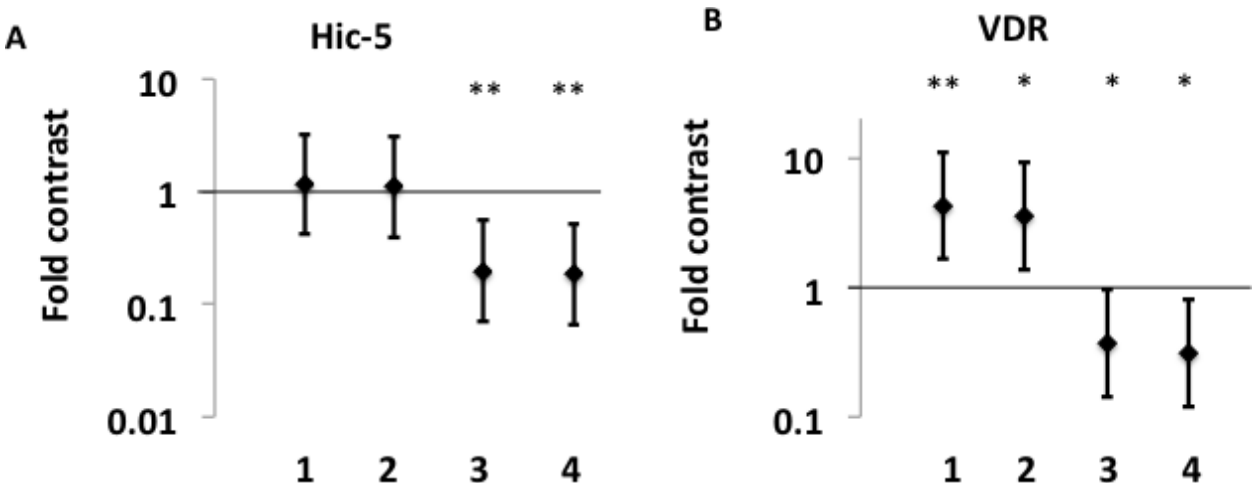

Figure 10: 95% confidence intervals of TGF-β1-induced *Hic-5* and *VDR* transcription contrasts in WPMY-1 cells.

Data for expression of (A) Hic-5 and (B) VDR were analyzed with two-way ANOVA with mixed models and are represented as 95% confidence intervals. Contrasts are representative of six independent experiments. 1, contrast between treated and untreated Scr. 2, contrast between treated and untreated shHic-5. 3, contrast between untreated treated Scr and shHic-5. 4, contrast between treated Scr and shHic-5. * $p < 0.05$, ** $p < 0.05$.

3.2 CROSS-TALK BETWEEN VDR AND TGF-β PATHWAY

The main effectors of the TGF-β signaling pathway are Smad2 and Smad3, which dimerize with Smad4 and translocate to the nucleus, where they act as transcription factors.(231) Smad3 has previously been implicated in potentiation of $1,25D_3$-induced transcription of VDR targets.(137) To investigate whether this specific pathway is necessary for VDR induction, Scr cells were treated with SIS3, as specific inhibitor of Smad3 phosphorylation, along with TGF-β. A 10 μM pre-incubation of SIS3 inhibited TGF-β-induced phosphorylation of Smad3 the greatest. (Figure 11A) Preliminary results indicate that while Smad3 inhibition by SIS3 was able to inhibit induction of smooth muscle alpha actin (SMAA), a Smad3 target, it was unable to inhibit VDR expression (Figure 11B-C).(232) Pending confirmation, this would suggest that induction of VDR expression by TGF-β is Smad-independent. Further repeats are necessary to confirm this result.

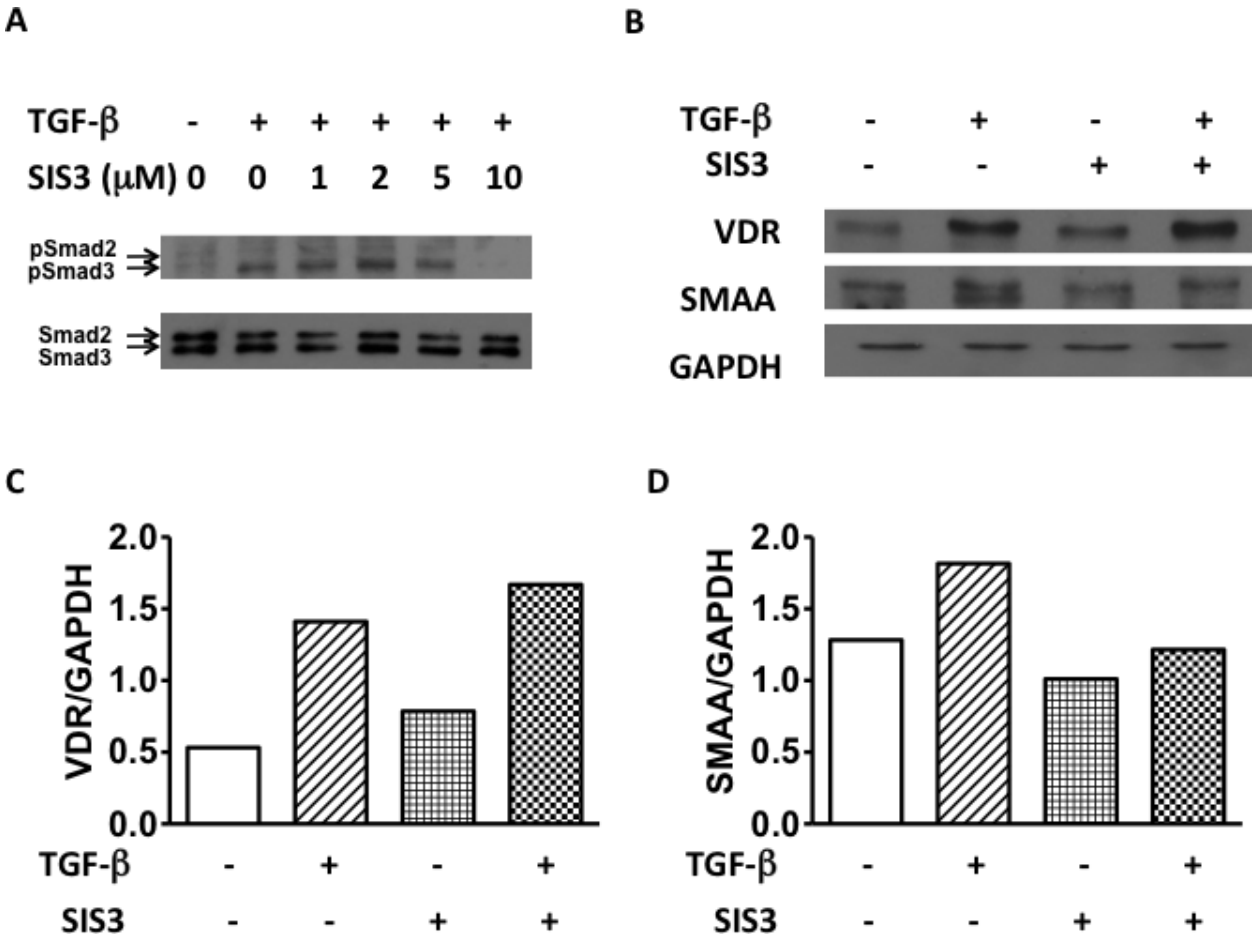

Figure 11: Inhibition of Smad3 phosphorylation does not repress TGF-β-mediated induction of VDR.

A. Scr cells were pre-incubated with the specific Smad3 inhibitor SIS3 (0, 1, 2, 5, 10 μM) for 1 hr and treated with 3.75 ng/mL TGF-β for 1 hr prior to harvest of protein. Analysis of pSmad2/3 staining indicated that the 10 μM treatment of SIS3 inhibited Smad3 phosphorylation the best. B. Scr cells were serum-starved for 2 hr, pre-incubated with SIS3 (0, 10 μM) for 1 hr, then treated with 3.75 ng/mL TGF-β for 24 hr. Cells were lysed in RIPA buffer and subject to Western blot for analysis of VDR, smooth muscle alpha-actin (SMAA), and GAPDH expression. C and D. Blots were analyzed by densitometry. Results are shown from one experiment.

$1,25D_3$ treatment in lung fibroblasts and epithelial cells demonstrated an anti-fibrotic effect, inhibiting expression of TGF-β-induced SMAA.(233) I sought to examine whether $1,25D_3$ exerted a similar anti-fibrotic effect on prostate stromal cells that were naïve to TGF-β exposure. WPMY-1 cells, which have a myofibroblastic phenotype, constitutively express SMAA (234). Therefore, I used the PS30 stromal line, an immortalized fibroblastic cell line derived from normal prostate stroma (235). TGF-β (3.5 ng/mL) induced SMAA 24 hrs after treatment in PS30 cells. However, supplementation of 100 nM $1,25D_3$ with TGF-β stimulation blunted SMAA expression (Figure 12A-B). This indicates that VDR and the TGF-β effector Smad3 interact at the transcriptional level in prostate stromal cells. In this context, liganded VDR inhibited Smad3 transduction.

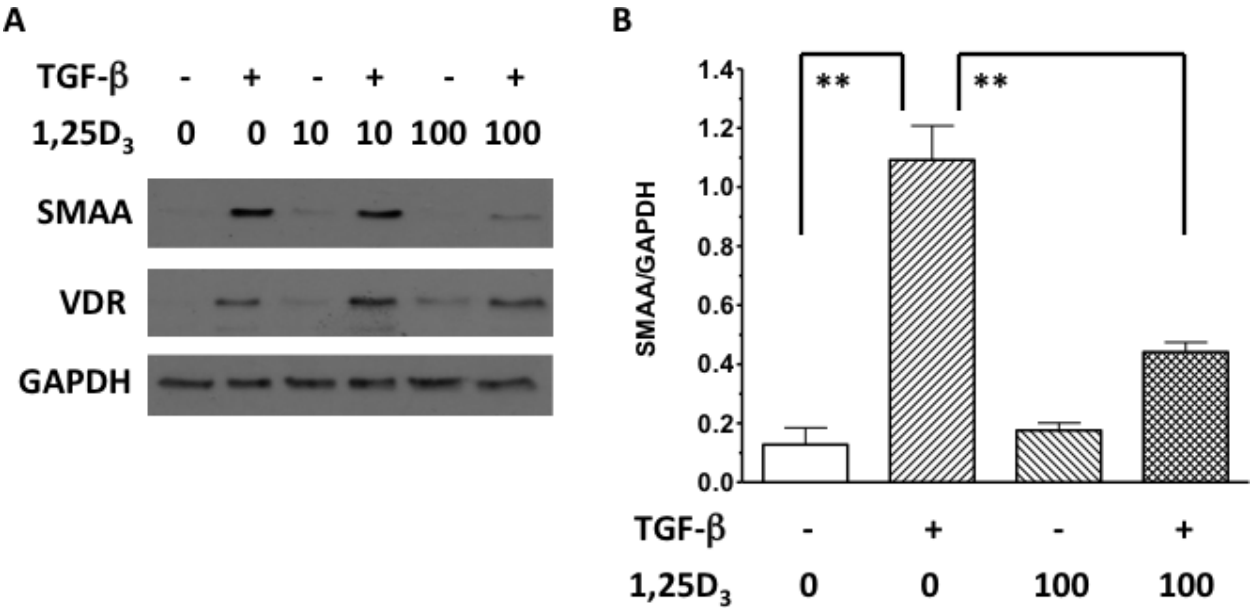

Figure 12: 1,25D$_3$ treatment of PS30 prostate stroma fibroblasts inhibited TGF-β-induced expression of SMAA.

PS30 cells were serum-starved for 2 hr and treated with TGF-β1 (0, 3.5 ng/mL) and 1,25D$_3$ (0, 10, 100 nM) for 24 hr. Cells were lysed in RIPA buffer and subject to Western blot analysis for expression of SMAA, VDR, and GAPDH. Blots were analyzed for densitometry. Bars represent mean±SEM of two independent experiments. Preliminary statistical analysis was performed using two-way ANOVA with mixed models followed by cell-means post-test. ** $p < 0.01$.

3.3 HIC-5 REGULATES 1,25D_3- AND TGF-β1-INDUCED EXPRESSION OF *CYP24A1* IN PROSTATE STROMAL CELLS

In osteoblasts and resting-zone chondrocytes, TGF-β regulates the activity of CYP24A1, a target of VDR that metabolizes active 1,25D_3 to its inactive form (236, 237). *CYP24A1* expression is a major barrier to effective 1,25D_3 treatment in prostate cancer, metabolizing 1,25D_3 to the inactive form 1,24,25D_3. This metabolite is further metabolized to calcitroic acid, which is then excreted in urine (122). However, the contribution of stromal cells to 1,25D_3 metabolism is not currently known, nor have compartment-specific regulators of *CYP24A1* expression been identified. To discern the effect of TGF-β on *CYP24A1* gene expression, Scr cells were co-treated with 3.5 ng/mL TGF-β and 100 nM 1,25D_3 and mRNA expression analyzed by RT-qPCR. Whereas treating with TGF-β1 alone minimally induced expression of *CYP24A1*, co-treatment with 1,25D_3 enhanced *CYP24A1* expression 300-fold above baseline and 10-fold above treatment with 1,25D_3 alone (Figure 13B, Figure 14B). One source of this enhanced gene expression may be the increased induction of VDR itself upon TGF-β treatment.

Analysis of mRNA expression in shHic-5 cells, which were demonstrated to have reduced Hic-5 expression that was not influenced by TGF-β or 1,25D_3 treatment (Figure 13A, Figure 14A), revealed similar dynamics, with minimal induction of *CYP24A1* upon TGF-β1 treatment, greater induction upon 1,25D_3 treatment, and enhanced expression upon co-treatment of TGF-β1 and 1,25D_3 (Figure 13B, Figure 14B). Direct comparison of the magnitude of these effects between Scr and shHic-5 cells identified a significant reduction in *CYP24A1* basal expression and a reduced 1,25D_3-induced response alone or in combination with TGF-β1.

Together, these results indicate that Hic-5 is required for maximal induction of *CYP24A1* by 1,25D_3 alone or in combination with TGF-β1.

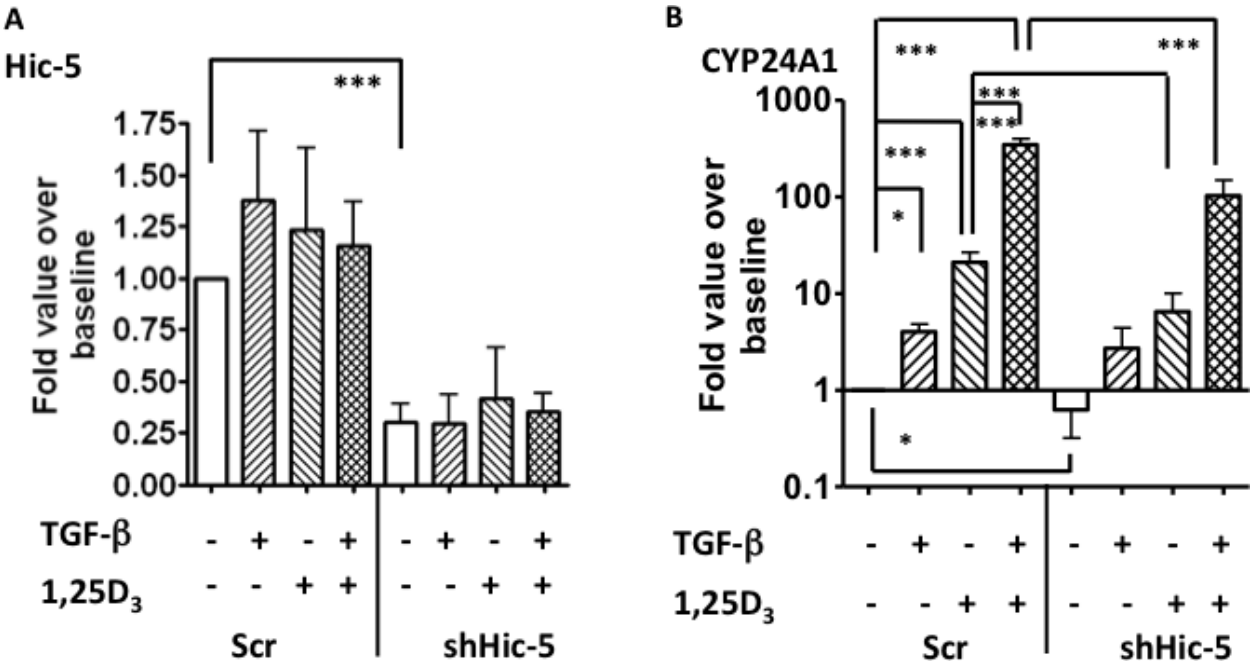

Figure 13: Hic-5 knockdown in WPMY-1 cells reduced TGF-ß-mediated enhancement of 1,25D$_3$-induced *CYP24A1* expression.

Scr and shHic-5 cells were serum-starved for 2 hr prior to a 6-hr treatment with TGF-β1 (0, 3.5 ng/mL) and 1,25D$_3$ (0, 100 nM). mRNA was extracted for cDNA synthesis and RT-qPCR analysis for expression of Hic-5 (A), CYP24A1 (B), and GAPDH. Comparisons were made using the ddCt method. Results were analyzed with three-way mixed-models ANOVA and cell-means post-test. Bars represent mean±SEM of three independent experiments normalized to the basal condition in Scr cells. * $p < 0.05$, *** $p < 0.001$.

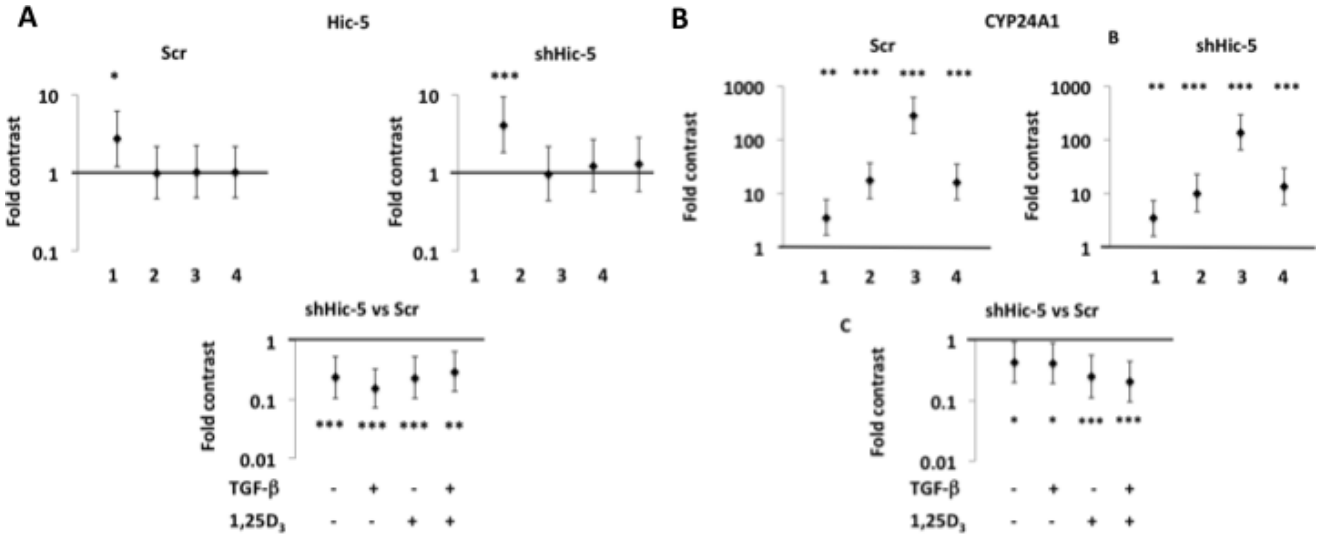

Figure 14: 95% confidence intervals of *Hic-5* and *CYP24A1* transcription contrasts in $1,25D_3$/TGF-β1 co-treatment in WPMY-1 cells.

Data for expression of (A) *Hic-5* and (B) *VDR* were analyzed with three-way ANOVA with mixed models and are represented as 95% confidence intervals. Contrasts are representative of three independent experiments. 1, contrast between TGF-β1 treatment and no treatment. 2, contrast between $1,25D_3$ treatment and no treatment. 3, contrast between TGF-β1/$1,25D_3$ co-treatment and no treatment. 4, contrast between TGF-β1/$1,25D_3$ co-treatment and $1,25D_3$ treatment alone. * $p < 0.05$, ** $p < 0.01$, *** $p < 0.001$.

Reduced *CYP24A1* mRNA expression upon Hic-5 knockdown may limit the auto-inhibitory effects of $1,25D_3$ on its own accumulation. Jan Beumer and Robert Parise from the Clinical Pharmacology Analytical Facility assisted with liquid chromatography-tandem mass spectrometry (LC-MS/MS) to analyze $1,25D_3$ concentration using medium and cellular content from Scr and shHic-5 cultures. Upon 24 hours of treatment, the $1,25D_3$ concentration in Scr cells and medium was reduced by 50% (Figure 15). In contrast, the $1,25D_3$ concentration in shHic-5 cells and medium was only reduced by about 15%. No spontaneous degradation occurred within the cell-free control medium, so the reduction of $1,25D_3$ in the Scr-associated medium was due solely to CYP24A1 activity. It thus appears that Hic-5 is necessary for optimal induction of a negative feedback loop on VDR activity through CYP24A1-mediated metabolism of $1,25D_3$.

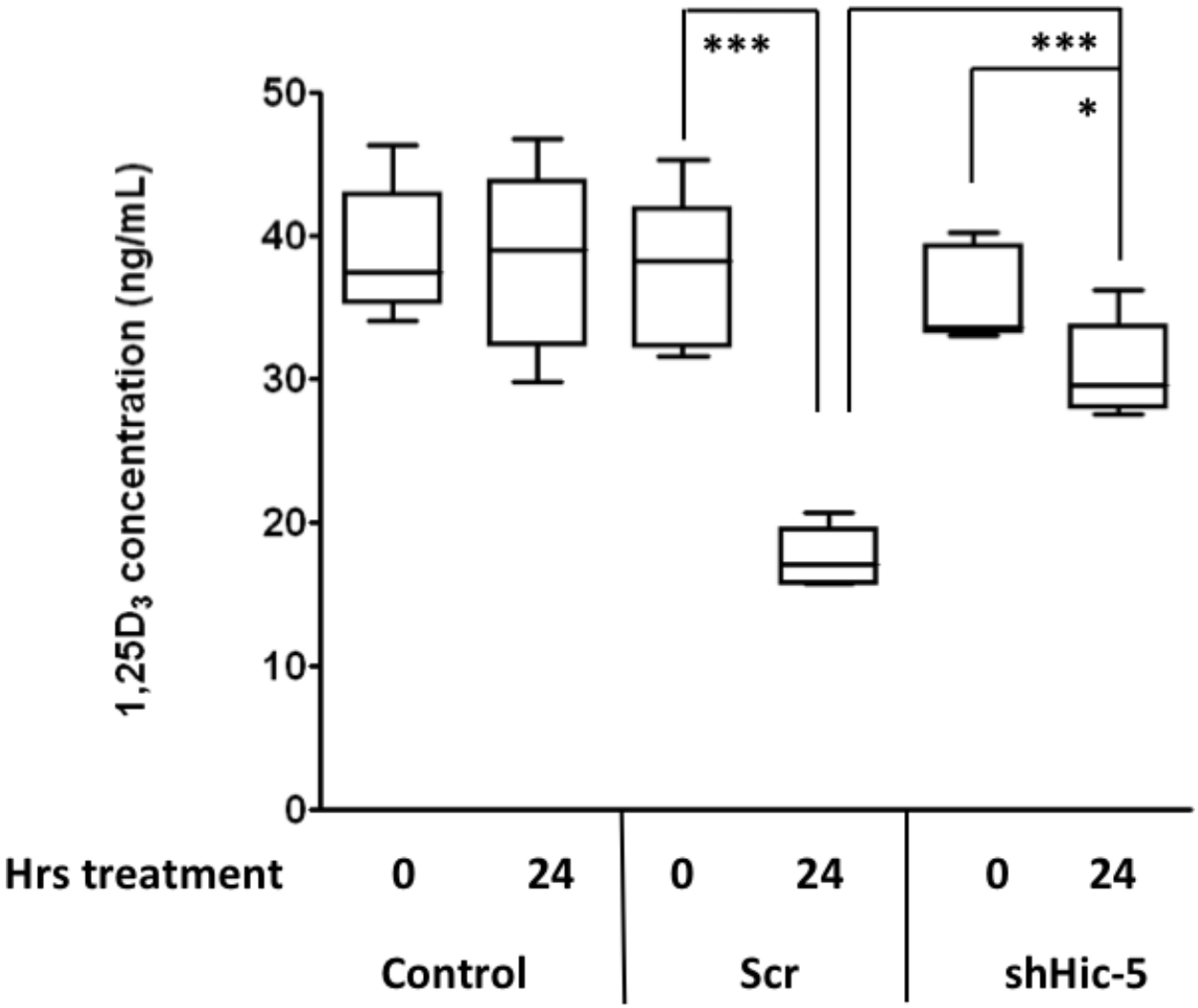

Figure 15: Hic-5 knockdown reduced CYP24A1 activity in shHic-5 cells.

Cells were serum-starved for 2 hr prior to treatment with 100 nM 1,25D3 and were harvested at 0 and 24 hr. Two cell-free control plates were set up to control for spontaneous degradation. Cells were scraped into their respective medium and flash-frozen in liquid nitrogen prior to mass spectrometry analysis. Boxplots represent data from three independent experiments. Data was analyzed by two-way mixed-models ANOVA followed by cell-means post-tests. * $p < 0.05$, *** $p < 0.001$.

3.4 IDENTIFICATION OF A HIC-5-RESPONSIVE ELEMENT WITHIN THE *CYP24A1* PROMOTER

Transfection experiments using luciferase reporter constructs were used to determine whether Hic-5 affects transcriptional activation from the proximal promoter of *CYP24A1*. A luciferase reporter construct (pCYP24-537) containing a 532-bp promoter sequence between 537 and 5 bp upstream of the transcription start site (TSS) included two known Vitamin D response elements (VDREs) located 293 bp and 172 bp upstream of the TSS (238). pCYP24-537 was transfected into Scr and shHic-5 cells and luciferase reporter activity measured upon induction by $1,25D_3$ alone or in combination with TGF-β1. As expected, $1,25D_3$ induced *CYP24A1* promoter-driven luciferase reporter activity in Scr cells, while treatment with TGF-β1 alone did not induce activity (Figure 16). However, co-treatment of $1,25D_3$ and TGF-β in Scr cells enhanced luciferase activity above that seen with $1,25D_3$ treatment alone, revealing a permissive effect when TGF-β1 is combined with $1,25D_3$. However, in shHic-5 cells transfected with pCYP24-537, treatment with $1,25D_3$ failed to induce luciferase expression above the baseline, and co-treatment with TGF-β only triggered a small induction that was significantly lower than for Scr cells. Hic-5 expression is therefore required for efficient VDR-mediated transcription induction from the proximal promoter region of *CYP24A1*.

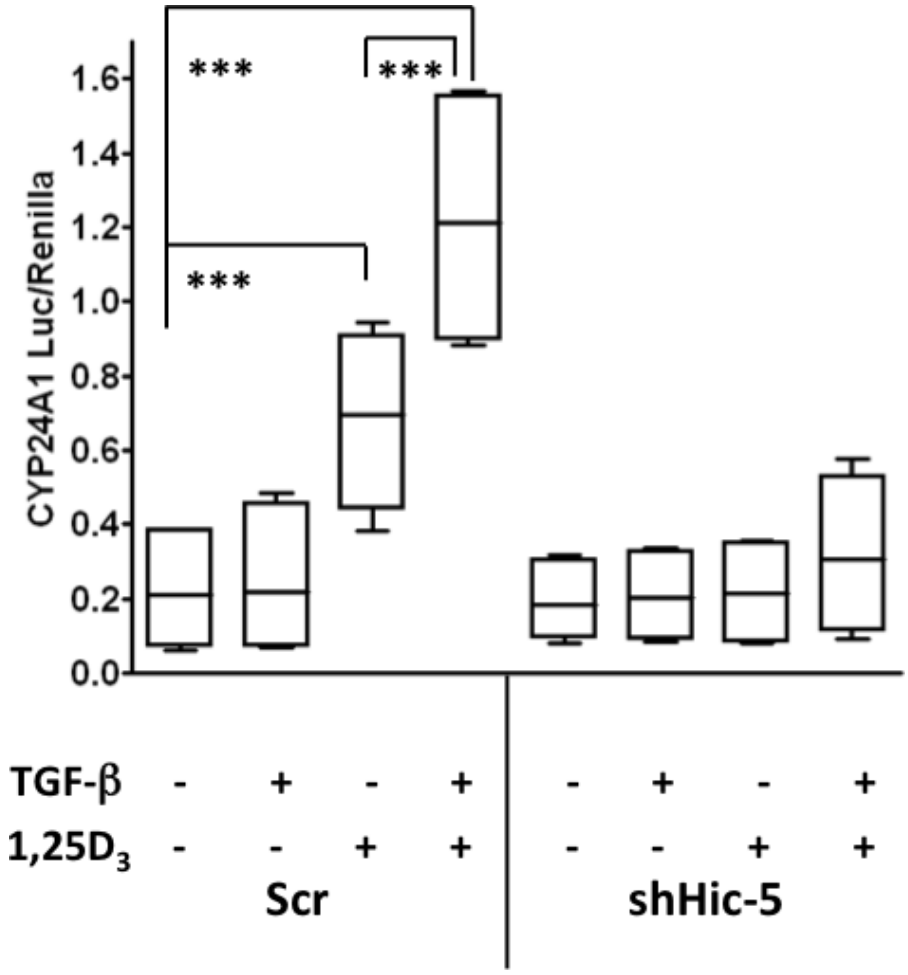

Figure 16: Hic-5 knockdown inhibits 1,25D$_3$-induced and TGF-β-enhanced luciferase expression from pCYP24-537-luc.

Scr and shHic-5 cells were transfected with pCYP24-537-luc overnight, serum-starved for 2 hr, and treated with TGF-β1 (0, 3.5 ng/mL) and/or 1,25D$_3$ (0, 100 nM) for 6 hr. Cells were lysed in Passive Lysis Buffer and freeze-fractured at -20˚C overnight. Samples from lysates were analyzed for luciferase activity. Boxplots represent data from two independent experiments performed in triplicate. Data was analyzed using three-way ANOVA with cell-means posttest. *** $p < 0.001$.

Recent research at the Callen laboratory demonstrated that 1,25-D_3-induced expression of a luciferase reporter containing portions of the *CYP24A1* promoter is dependent on a sequence 392 bp to 470 bp upstream of the TSS (227). Several deletion luciferase constructs that include the proximal promoter regions from 496 bp (p496-luc), 470 bp (p470-luc), 451 bp (p451-luc), and 392 bp (p392-luc) upstream of the TSS were examined to identify potential sites required for Hic-5 co-activation. Luciferase expression from p496-luc in Scr cells demonstrated enhanced expression upon co-treatment of TGF-β and 1,25D_3, supporting results obtained from the pCYP24-VDRE-luc construct (Figure 17). However, treatment of 1,25D_3 alone or together with TGF-β failed to induce minimal luciferase expression above baseline from p392-luc above baseline. The ability to both induce luciferase upon 1,25D_3 treatment above minimal levels and enhance its expression upon TGF-β co-treatment was restored in p451-luc, which demonstrated significant increases in expression above levels seen in p392-luc ($p = 0.0002$ for contrast of 1,25D_3 treatment alone, $p < 0.0001$ for contrast of 1,25D_3/TGF-β1 co-treatment). Therefore, a Hic-5-responsive sequence was identified at 392-451 bp upstream of the TSS.

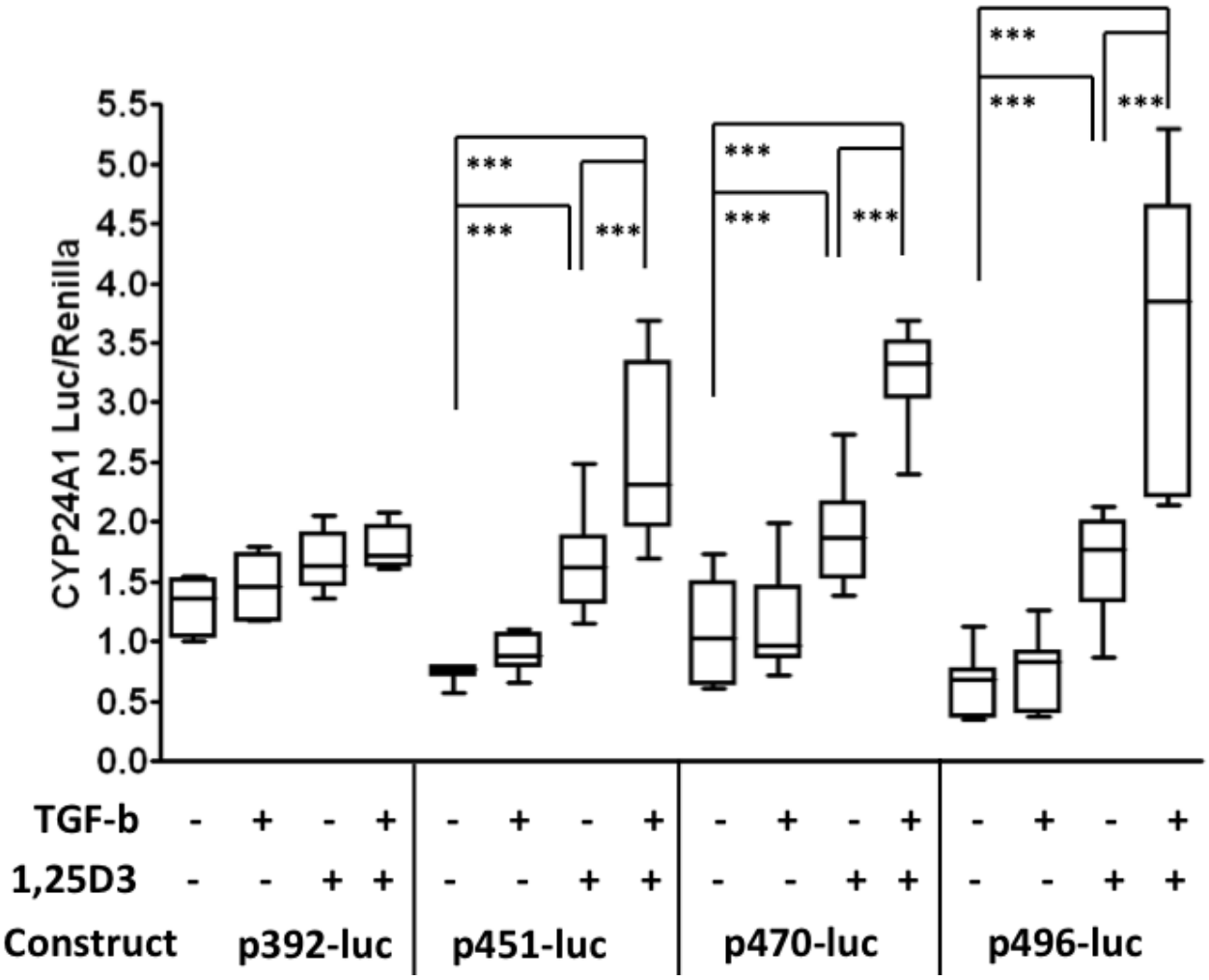

Figure 17: Mapping of *CYP24A1* promoter proximal region required for Hic-5 coactivation.

Transfections and treatments were performed as above with p392-luc, p451-luc, p470-luc, and p496-luc in Scr cells. Boxes represent two (p392-luc) or three (p451-luc, p470-luc, p496-luc) independent experiments performed in triplicate. Three-way ANOVA followed by cell-means post-tests were performed, *** $p<0.001$.

The identified Hic-5-responsive element within the *CYP24A1* promoter may involve previously unknown interactions with transcription factors other than Smad3 and VDR. The promoter sequence was analyzed *in silico* using TESS, an online software program developed at the University of Pennsylvania as a front-end for the TRANSFAC matrix (228). Two unique sites within the sequence 392-451 bp upstream of the TSS were identified (Figure 18). They correspond to consensus sequences for binding of transcription factors Sp1 and TCF4, which have previously been demonstrated to interact with Hic-5 (49, 239). However, the *in silico* analysis did not detect a consensus Smad-binding element or VDRE, indicating that VDR/Hic-5 interaction at the *CYP24A1* promoter may require binding of additional transcription factors to facilitate transactivation of the promoter.

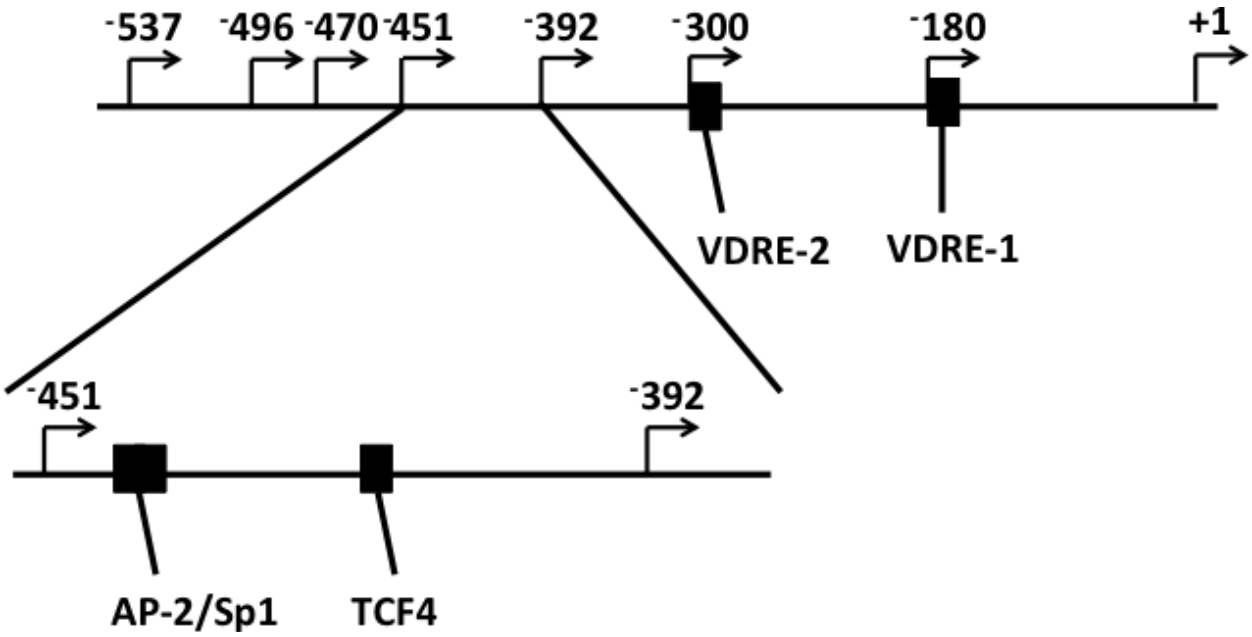

Figure 18: Proposed promoter map for CYP24A1.

Sequence was analyzed *in silico* using TESS (228).

3.5 OVEREXPRESSION OF HIC-5 SENSITIZES EPITHELIAL LNCAP CELLS TO THE ANTI-PROLIFERATIVE EFFECTS OF $1,25D_3$

Recent studies by the laboratory of Neil Bhowmick have revealed a previously unknown function of Hic-5 in prostate epithelial cells. Within 7 days of castration, Hic-5 expression was de-repressed in both endogenous mouse prostate epithelium and tumor xenografts derived from prostate cancer patients. Furthermore, aggressive tumor growth of mixed xenografts generated with *Tgfbr2* knockout of prostate stroma mixed with LNCaP cells was inhibited upon overexpression of murine Hic-5 in LNCaP cells (223). Thus, ectopic expression of Hic-5 in prostate epithelium was associated with reduced tumor growth and was uncovered following short-term castration.

Given my demonstration of Hic-5-mediated enhancement of VDR activity in WPMY-1 cells, I sought to determine whether overexpression of Hic-5 would sensitize LNCaP cells to $1,25D_3$-induced growth inhibition. I therefore examined the effects of $1,25D_3$ treatment on proliferation of LNCaP and LNCaP/Hic-5 cells using the CyQuant nuclear dye assay. LNCaP and LNCaP/Hic-5 cells were treated with 0, 10, and 100 nM $1,25D_3$ for 72 hours. As shown in Figure 19, growth of LNCaP cells was significant reduced in response to 100 nM $1,25D_3$, but only minimally at 10 nM. In contrast, LNCaP/Hic-5 cells experienced significantly greater growth inhibition in the presence of 10 nM $1,25D_3$ than in LNCaP cells. Furthermore, treatment at 100 nM also significantly inhibited growth in LNCaP/Hic-5 cells to a greater extent than in LNCaP cells. Thus, Hic-5 overexpression sensitized LNCaP cells to $1,25D_3$-induced growth inhibition at a lower concentration.

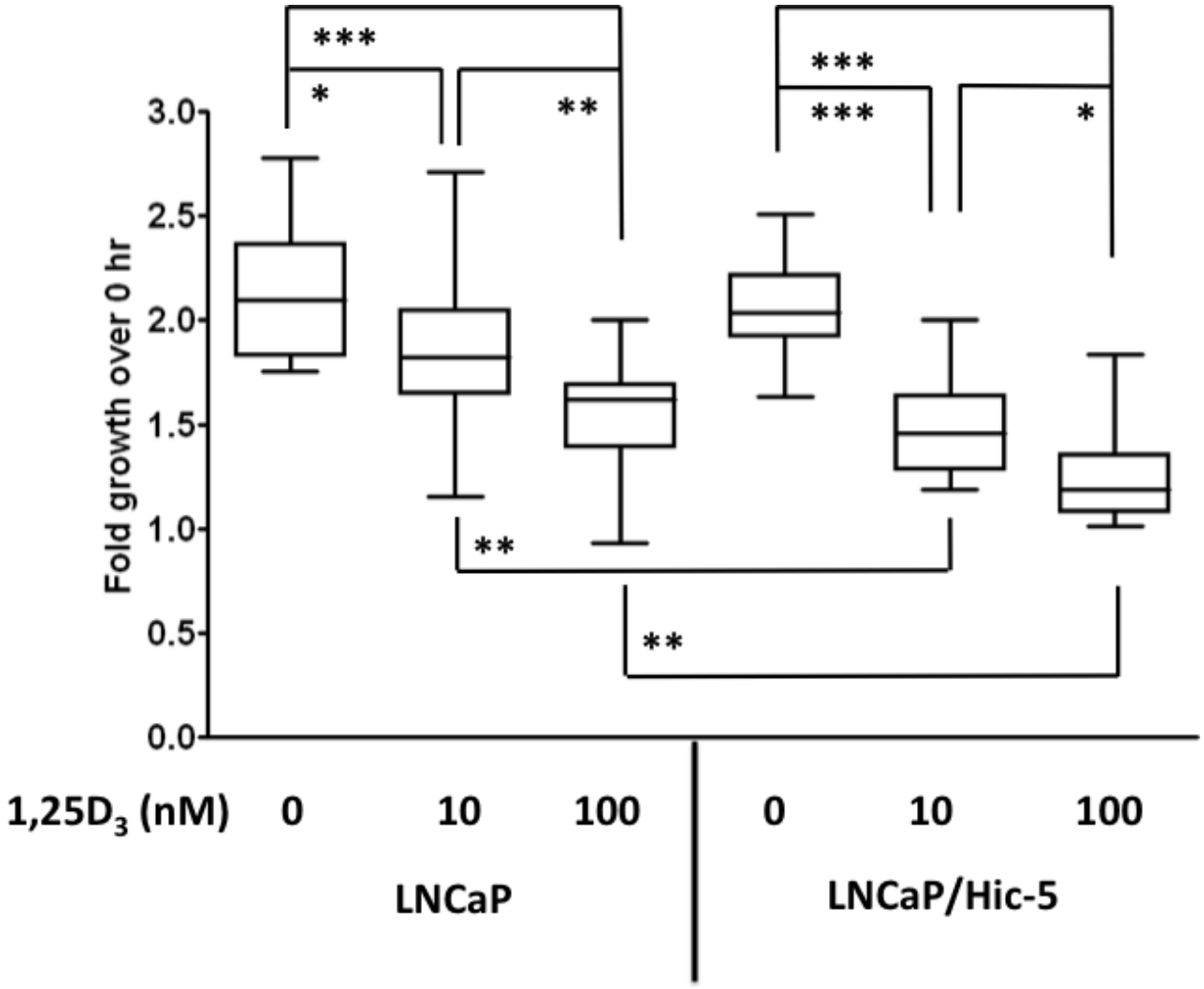

Figure 19: Overexpression of Hic-5 sensitizes LNCaP cells to 1,25D$_3$.

LNCaP and LNCap/Hic-5 cells were treated in triplicate in 96-well plates with 0, 10, and 100 nM 1,25D$_3$ at 0 and 72 hr. Upon removal of medium, the plates were frozen overnight at -80˚C. Upon thawing, cells were lysed and stained in CyQuant assay buffer and read on a fluorimeter. Boxes represent results of five independent experiments performed in triplicate. Two-way ANOVA with mixed models followed by cell-means post-tests were performed on the log-transformed data. * $p < 0.05$, *** $p < 0.001$.

CYP24A1 expression is correlated with cellular resistance to $1,25D_3$ treatment (122). Given my observation that Hic-5 is required for efficient $1,25D_3$-induced transcription of *CYP24A1* in WPMY-1 cells, I expected ectopic Hic-5 expression in LNCaP cells to exhibit more potent induction of *CYP24A1*. mRNA extracted from LNCaP and LNCaP/Hic-5 cells treated with 100 nM $1,25D_3$ was analyzed by RT-qPCR to test whether the sensitization of LNCaP/Hic-5 cells to $1,25D_3$ –induced growth inhibition is attributed to a reduction in *CYP24A1* expression. 100 nM $1,25D_3$ induced expression of *CYP24A1* in LNCaP and LNCaP/Hic-5 cells, but there was no significant difference between the two (Figure 20, Figure 21). Therefore, overexpression of Hic-5 in LNCaP cells does not alter the extent of *CYP24A1* expression. The sensitization of LNCaP/Hic-5 cells to the anti-proliferative effect of $1,25D_3$ treatment therefore appears to be independent of *CYP24A1* activity.

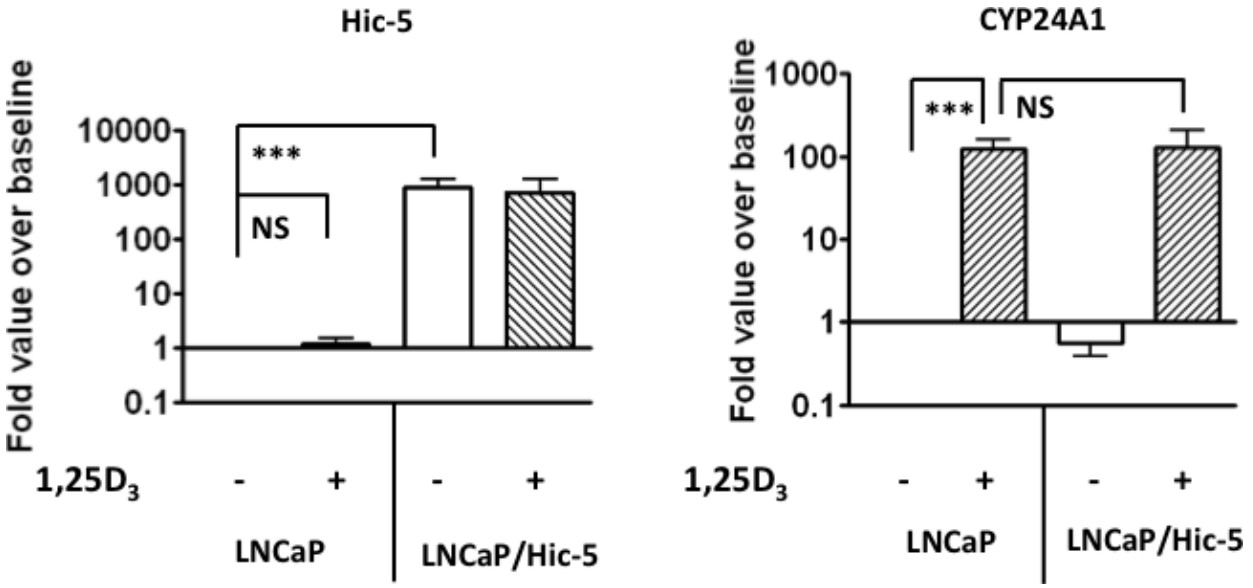

Figure 20: Hic-5 overexpression did not affect 1,25D$_3$-induced expression of *CYP24A1* in LNCaP cells.

LNCaP or LNCaP/Hic-5 cells were treated with 1,25D$_3$ (0, 100 nM) for 6 hr. mRNA was extracted for cDNA synthesis and RT-qPCR. Comparisons were made using the ddCt method. Data were analyzed with two-way mixed-models ANOVA and cell-means post-test. Bars represent mean±SEM from four independent experiments normalized to basal expression in WT LNCaP cells. NS = not significant, *** $p < 0.001$.

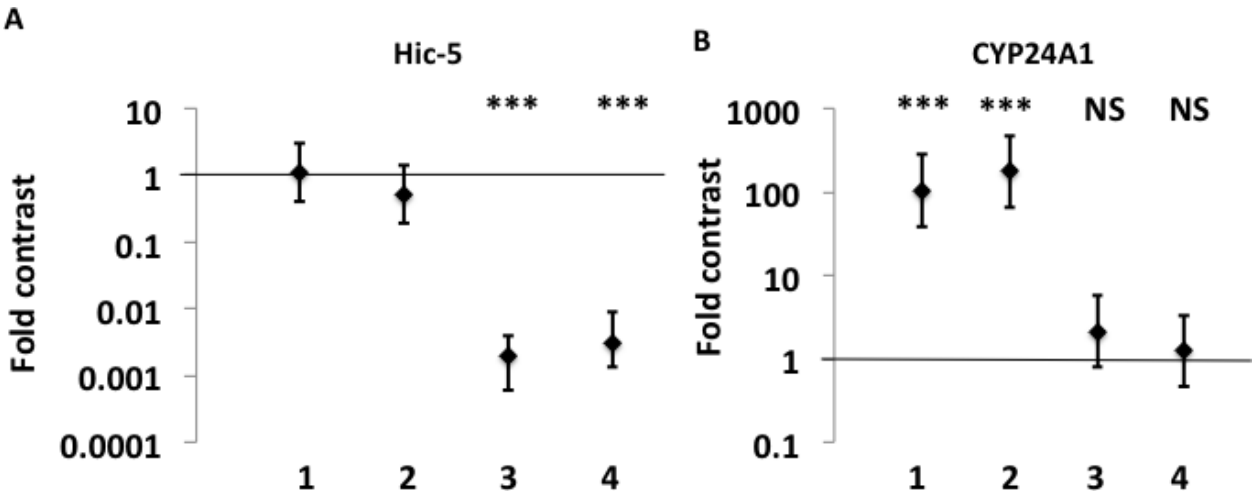

Figure 21: 95% confidence interals of *Hic-5* and *CYP24A1* transcription contrasts in 1,25D3-treated LNCaP and LNCaP/Hic-5 cells.

Data for expression of (A) *Hic-5* and (B) *CYP24A1* were analyzed with two-way ANOVA with mixed models and are represented as 95% confidence intervals. Contrasts are representative of four independent experiments. 1, contrast between treated and untreated LNCaP cells. 2, contrast between treated and untreated LNCaP/Hic-5 cells. 3, contrast between untreated LNCaP and LNCaP/Hic-5 cells. 4, contrast between treated LNCaP and LNCaP/Hic-5 cells. NS = not significant, *** $p < 0.001$.

3.6 COMPARTMENT-SPECIFIC EFFECTS OF HIC-5 ENHANCE GROWTH-INHIBITORY EFFECTS OF 1,25D$_3$ TREATMENT ON LNCAP CELLS

As shown above, ectopic Hic-5 expression sensitizes LNCaP cells to enhanced 1,25D$_3$-induced growth inhibition by a mechanism apparently independent of CYP24A1 activity. However, knockdown of Hic-5 in WPMY-1 cells reduced the 1,25D$_3$-induced activity of VDR, thus reducing *CYP24A1* expression and metabolism of 1,25D$_3$. These findings suggest that reduced stromal Hic-5 expression in a two-compartment model system would limit inactivating metabolic activity of CYP24A1, further enhancing growth-inhibitory effects of 1,25D$_3$ on LNCaP/Hic-5 cells (Figure 22A-B). An *in vitro* co-culture experiment was therefore designed to test how expression of Hic-5 in stromal and/or epithelial cells affected 1,25D$_3$ inhibition of the LNCaP and LNCaP/Hic-5 tumor lines. As shown in Figure 23, proliferation of LNCaP cells was not significantly affected by a 72-hr treatment of 100 nM 1,25D$_3$ in co-culture with Scr stromal cells. However, when co-cultured with shHic-5 cells, 1,25D$_3$-induced growth inhibition of LNCaP cells was enhanced compared to co-culture with Scr cells. In contrast, LNCaP/Hic-5 cells were sensitive to the growth-inhibitory effects of 1,25D$_3$ in co-culture with Scr and shHic-5 stromal cells, but the inhibition was significantly amplified in co-culture with shHic-5 cells (Figure 24). More importantly, after treatment there were fewer viable LNCaP/Hic-5 cells in co-culture with shHic-5 stromal cells than were present at 0 hr.

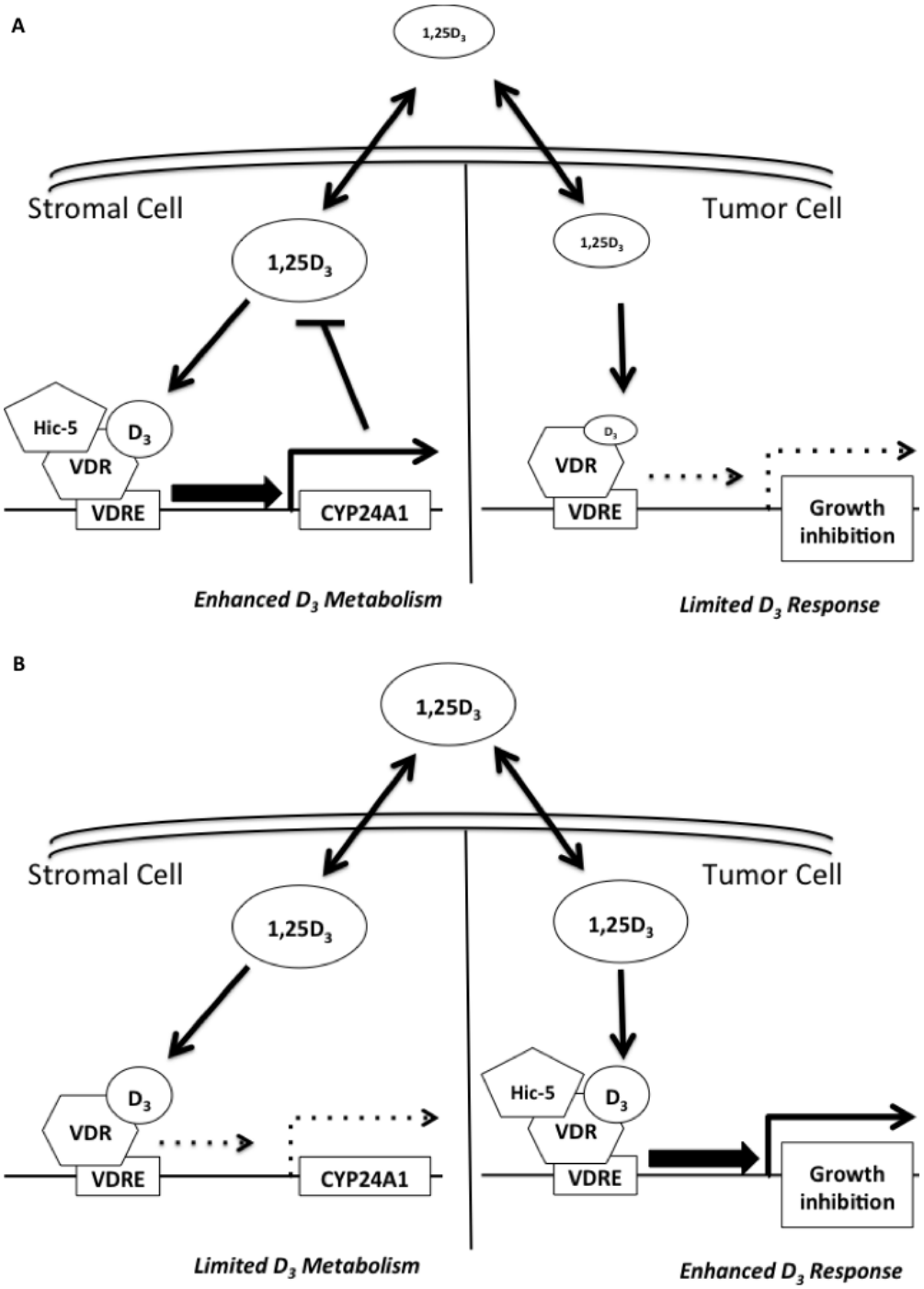

Figure 22: Proposed model of Hic-5 impact on VDR action in the tumor microenvironment.

$1,25D_3$-induced expression of CYP24A1 in Hic-5-expressing stromal cells (A) metabolizes $1,25D_3$ to an inactive form, inhibiting its anti-proliferative effects on the tumor. If Hic-5 is depleted in the stromal layer (B), CYP24A1 expression is inhibited, and more active $1,25D_3$ is available to the tumor to induce growth inhibition.

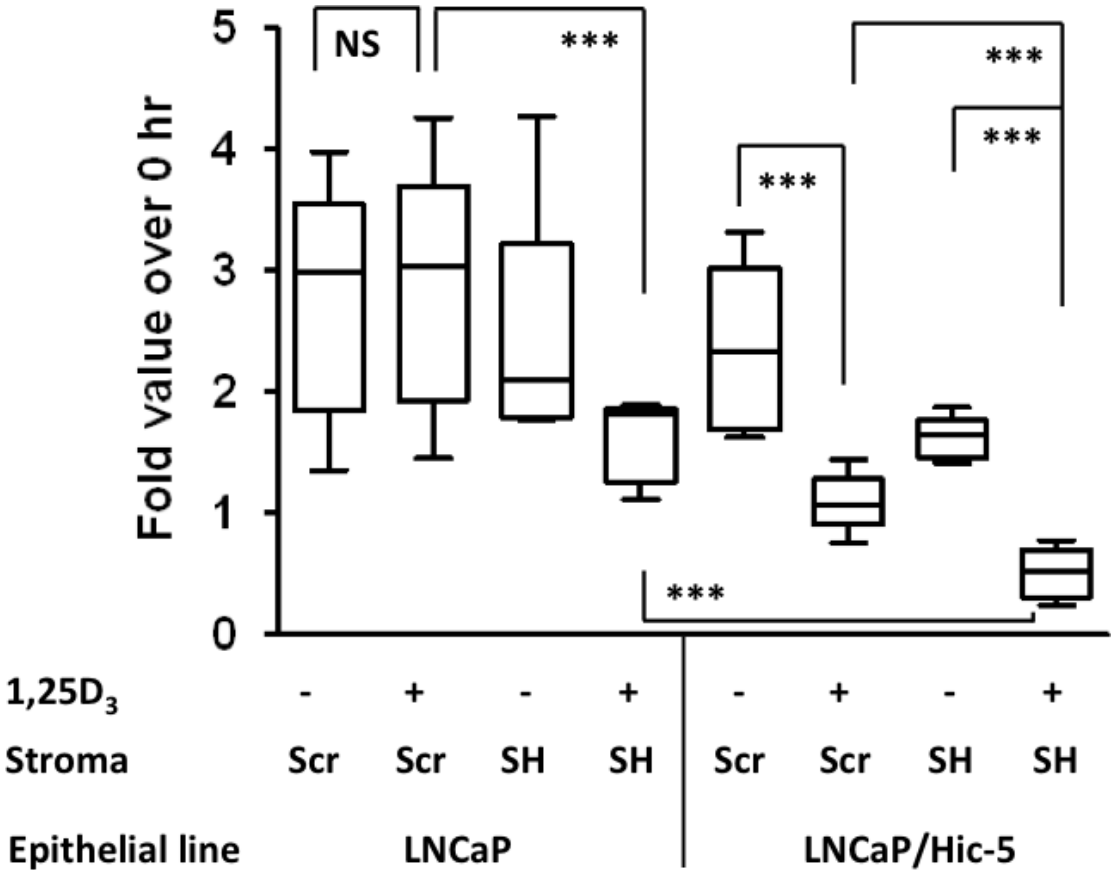

Figure 23: Knockdown of Hic-5 in WPMY-1 cells sensitizes LNCaP and LNCaP/Hic-5 cells to 1,25D$_3$-induced inhibition in co-cultures.

LNCaP and LNCaP/Hic-5 cells were cultured on coverslips separately from Scr (Scr) and shHic-5 (SH) cells, then co-cultured in the absence (-) or presence (+) of 1,25D$_3$ (100 nM) for 72 hr, fixed to the coverslip, and stained with DAPI. Cells were counted at six random fields per coverslip, averaged, and compared against cell numbers obtained at 0 hr.. Boxplots represent data from five independent experiments. A three-way ANOVA followed by cell-means post-tests were performed on the log-transformed data. NS = not significant, * $p < 0.05$, ** $p < 0.01$, *** $p < 0.001$.

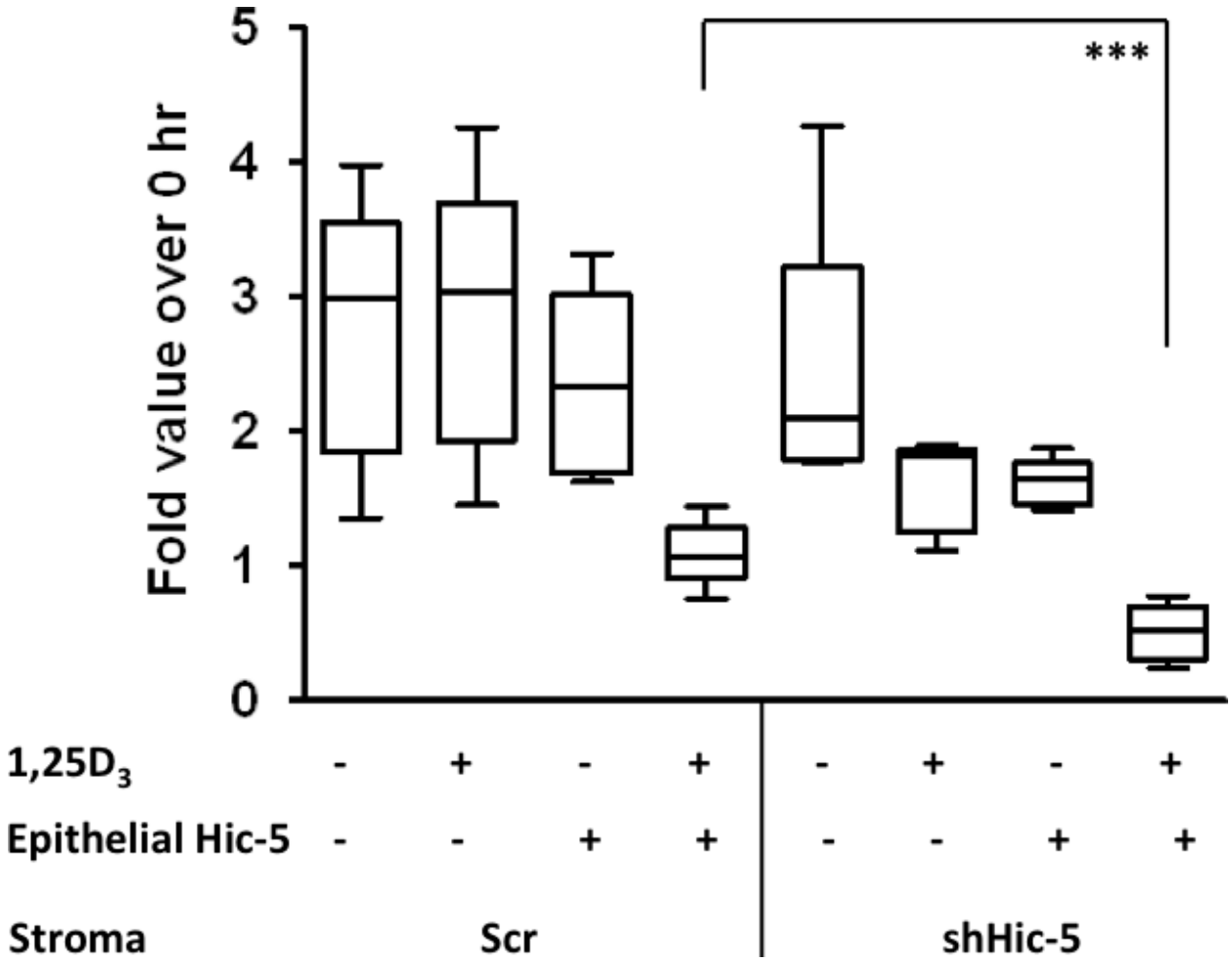

Figure 24: Knockdown of Hic-5 in WPMY-1 cells sensitizes LNCaP/Hic-5 cells to enhanced $1,25D_3$-induced inhibition in co-cultures.

The data from Figure 23 were rearranged to disentangle comparisons in the chart.

The decrease below baseline of LNCaP/Hic-5 cells treated with 1,25D_3 in co-culture with shHic-5 cells suggested a cytotoxic effect within this co-culture. To examine this possibility, I utilized an alternative approach. Specifically, LNCaP/Hic-5 cells co-cultured with Scr or shHic-5 cells were treated with the minimal 10 nM 1,25D_3 dose, and instead of being fixed to the coverslip, LNCaP/Hic-5 cells were trypsinized and combined with a pellet derived from the surrounding co-culture medium. The cells were then stained with Trypan blue to measure viable (Trypan blue-negative) cells. Consistent between the methods, the results in Figure 25 show that even lower doses reduced viability of LNCaP/Hic-5 cells co-cultured with Scr cells, and this was enhanced when co-cultured with shHic-5 cells. This demonstrated that the enhanced sensitization of LNCaP/Hic-5 cells co-cultured with shHic-5 cells to 1,25D_3 treatment resulted in significantly reduced viability of the prostate cancer cell line.

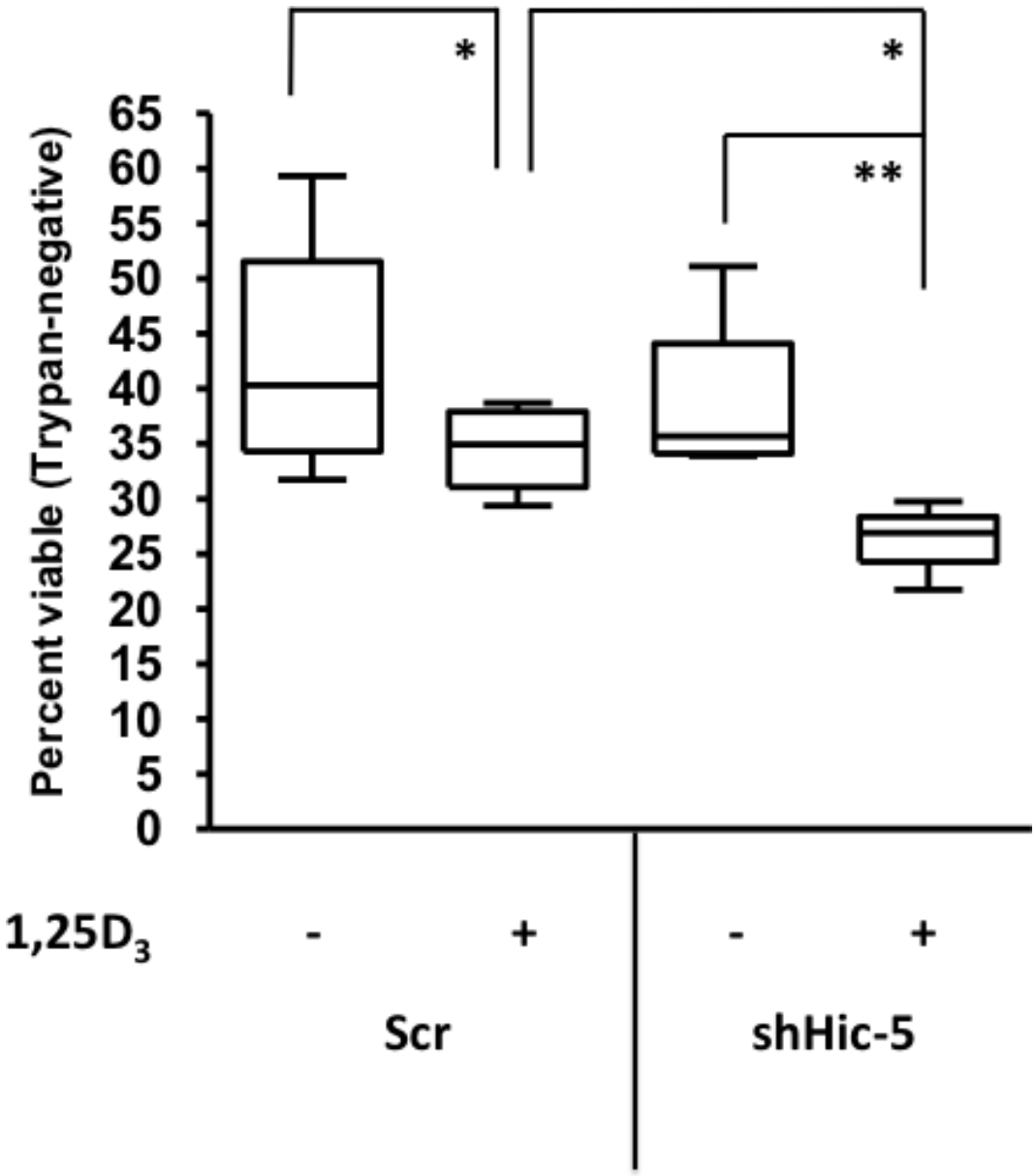

Figure 25: Knockdown of Hic-5 in WPMY-1 cells sensitizes LNCaP/Hic-5 cells to 1,25D$_3$-induced cell death in co-culture.

Co-cultures were set up and treated as previously. Cell pellets from trypsinized coverslips were combined with floating cells in the medium, resuspended, and stained with Trypan blue to assess viability. Boxplots represent four independent experiments. A two way ANOVA with mixed models followed by cell-means post-test were performed on the logit-transformed data. * < 0.05, ** < 0.01.

4.0 DISCUSSION

4.1 SUMMARY OF FINDINGS

The work presented here demonstrates the role of Hic-5, a nuclear receptor co-regulator, in VDR expression and activity in the prostate tumor microenvironment. TGF-β, an upstream regulator of Hic-5, induces expression of VDR and enhances $1,25D_3$-induced expression of CYP24A1, a VDR target gene and negative regulator of $1,25D_3$ in WPMY-1 prostate stromal cells. Preliminary work indicates that VDR induction does not depend on Smad3 signaling, suggesting the importance of Smad-independent pathways in VDR action. However, $1,25D_3$ treatment reduced SMAA expression in TGF-β-treated PS30 prostate stroma cell line, which models a normal prostate stroma naïve to TGF-β. Thus, VDR activity within the stromal microenvironment affects TGF-β-induced Smad-dependent pathways and may be enhanced by Smad-dependent and –independent pathways.

Hic-5, which is localized to the prostate stroma, is required for basal VDR expression in WPMY-1 cells. Knockdown of Hic-5 inhibited $1,25D_3$-induced transcription of *CYP24A1*, allowing $1,25D_3$ to accumulate in the culture medium without being metabolized. From deletion analysis of the *CYP24A1* promoter, I identified a Hic-5-responsive sequence at 392-451 bp upstream of the TSS. *In silico* analysis found two putative binding sites for AP-2/Sp1 and TCF4, two transcription factors known to interact with Hic-5.

Ectopic Hic-5 expression in the LNCaP prostate tumor line sensitized 1,25D_3-induced growth inhibition at lower concentrations independent of CYP24A1 activity. From the above data, I was able to design a model in which stromal expression of Hic-5 metabolizes 1,25D_3 to levels that cannot induce growth inhibition in prostate tumor cell line. However, epithelial expression of Hic-5 sensitizes the tumor line to the lower 1,25D_3 concentration and enhanced growth inhibition upon ablation of stromal Hic-5 (Figure 22). The model was supported by results from my *in vitro* co-culture proliferation assay. Furthermore, 1,25D_3 not only reduced proliferation, but also reduced viability of LNCaP/Hic-5 cells in co-culture with WPMY-1 cells ablated of Hic-5. Therefore, Hic-5 expression differentially regulates VDR effects between the epithelial and stromal compartments in prostate cancer.

4.2 EFFECTS OF TGF-β ON VDR EXPRESSION AND ACTIVITY IN THE MICROENVIRONMENT

Previous studies examining VDR expression in prostate stromal cells had focused on comparing normal stroma-associated fibroblasts with cancer-associated fibroblasts (CAFs). Those studies had concluded that VDR expression was comparable in CAFs and normal stroma-associated fibroblasts (225). However, examination of dendritic-cell differentiation to Langerhans cells demonstrated that treatment of myeloid cells with TGF-β induced VDR expression.(240) This presented a dichotomy, as prostate cancer cells typically express high levels of TGF-β, which in turn induces stromal fibroblasts to undergo transdifferentiation to myofibroblasts, a characteristic of reactive stroma (179). I found that TGF-β treatment of the WPMY-1 stromal cell line induced VDR expression.

An interesting consequence of TGF-β treatment on WPMY-1 cells is a permissive enhancement of 1,25D_3-induced *CYP24A1* transcription. TGF-β was previously found to induce *CYP24A1* expression in resting-zone chondrocytes and osteoblast-like cell lines, but its effect on enhancement on 1,25D_3-induced transcription was only observed upon pre-incubation of TGF-β (236, 237). An increase in CYP24A1 expression in the tumor microenvironment would increase metabolism of 1,25D_3 and therefore decrease its availability to the tumor (160). Therefore, high tumor and stromal expression of TGF-β may negatively impact 1,25D_3 therapy. The consequences of stromal VDR expression, especially under the influence of TGF-β, have not been previously examined in conjunction with clinical trials, and it may be a contributing factor influencing the outcomes of clinical trials, such as ASCENT, which yielded mixed results in Phase II and III trials (159).

4.3 HIC-5 AS A STROMAL REGULATOR OF VDR EXPRESSION AND ACTIVITY

Despite playing an active role in mediating transactivation of nuclear receptor targets, the co-regulator Hic-5 has not yet been found to regulate nuclear receptor expression. My study provides the first evidence of Hic-5 as a co-regulator of VDR expression as well as its activity. Hic-5 knockdown reduced basal and TGF-β-induced VDR expression. The mechanisms responsible for Hic-5-mediated VDR expression, both basal and TGF-β mediated, have yet to be defined, but may utilize Smad transcription factors, which have been previously shown to interact with Hic-5 (49, 215). However, my preliminary research from suggests that TGF-β-induced expression of VDR is not dependent on Smad3 signaling. Moreover, treatment of

osteoblasts with 1,25D_3 actually decreased expression of Smad2 in osteoblasts.(241) Further studies may therefore be focused on potential Smad-independent TGF-β signaling pathways which may impact on Hic-5 regulation of VDR expression.

In addition to affecting VDR expression, Hic-5 also impacts 1,25D_3-induced transactivation of the *CYP24A1* promoter, with reduced *CYP24A1* expression upon Hic-5 silencing. This extends the range of Hic-5 targets within the nuclear receptor superfamily beyond AR, GR, and PR (193, 209, 213). In the WPMY-1 prostate stromal cell line, Hic-5 acts as an AR co-activator that influences expression of paracrine factors, such as KGF, which in turn affect the neighboring tumor (193). The consequence of decreased 1,25D_3-induced *CYP24A1* expression upon Hic-5 knockdown is increased accumulation of unmetabolized 1,25D_3 in the culture medium. If this mechanism were applied to a clinical condition, reduced stromal Hic-5 expression may enhance therapeutic benefit of 1,25D_3 for patients with prostate cancer by prolonging its bioavailability (220, 221). Although Hic-5 knockdown completely inhibited VDR transactivation of the proximal *CYP24A1* promoter in transiently transfected cells, induction of endogenous *CYP24A1* was significantly reduced, but not completely inhibited upon Hic-5 knockdown upon TGF-β co-treatment with 1,25D_3. Nonetheless, the reduction of *CYP24A1* expression was functionally significant, as 1,25D_3 metabolism was dramatically reduced in shHic-5 cells.

Hic-5 does not interact directly with DNA, but it may bind to multiple transcription factors in complex, thus acting as a bridge between transcription factors binding at multiple sites throughout the promoter. Deletion analysis revealed a region of importance at 392-451 bp upstream from the transcription start site. Despite the presence of confirmed VDREs in p392, these sequences were not sufficient to induce transcription. *In silico* analysis of the -392 to -451

bp region of the *CYP24A1* promoter using TESS did not reveal a traditional VDRE, but instead indicated two potential Hic-5 targets (Figure 17) (227, 238). One proposed site at 445 to 452 bp upstream of the TSS showed high homology with the AP-2/Sp1 binding sequence. Sp1 knockdown is associated with reduction in $1,25D_3$-induced *CYP24A1* expression, and Hic-5 itself is a co-activator of Sp1 (49, 242). Additionally, a putative Sp1 site has been previously reported (243). Another site identified at 420 to 424 bp upstream of the TSS shares high homology with the TCF/LEF consensus binding sequence. Hic-5 has previously been demonstrated to interact with TCF4, but in this case it functions to repress TCF4 transcriptional activation (223, 239). Thus, the cytosolic function of Hic-5 as a scaffolding protein may extend to its nuclear receptor co-factor function, bridging VDR binding within target genes to other transcription factors.

4.4 DIFFERENTIAL HIC-5 EFFECTS IN TUMOR EPITHELIUM AND SENSITIZATION TO THERAPY

Although Hic-5 expression is mainly confined to the stromal compartment in the prostate, it is de-repressed upon short-term castration in mouse prostate epithelium and human prostate xenografts in mice (193, 223). Furthermore, as shown here, ectopic Hic-5 expression also enhances VDR activity in the LNCaP human prostate cancer cell line, leading to enhanced sensitivity to $1,25D_3$-induced growth inhibition. This enhanced sensitivity may also be influenced by the lack of Hic-5 effects on *CYP24A1* expression in LNCaP cells, highlighting the cell-specific effects of Hic-5 as a VDR co-activator. Genome-wide analysis comparing the VDR cistrome and transcriptome in prostate cancer and stromal cells with altered Hic-5 expression

will enhance my understanding of the seemingly paradoxical cell-specific transcriptional co-activation of VDR targets by Hic-5.

The distinct consequences of Hic-5 co-activation of VDR in prostate cancer (reduced proliferation) versus stromal (increased $1,25D_3$ metabolism) cells provide the context for examining cancer cell/stromal cell co-cultures as an *in vitro* mimic of the tumor microenvironment. As I demonstrated above, the most potent anti-proliferative effects of $1,25D_3$ on LNCaP cells occurs when they ectopically express Hic-5 and are co-cultured with stromal cells ablated of Hic-5. I predict that this is due to the reduced stroma-mediated CYP24A1 activity, reducing metabolism of $1,25D_3$, coupled with enhanced VDR regulation of anti-proliferation genes upon co-activation by ectopic Hic-5 expression. Regulation of Bax and Bcl-2, two target genes associated with apoptosis, may account for the enhanced $1,25\text{-}D_3$-induced cytotoxic activity observed in LNCaP cells ectopically expressing Hic-5 and co-cultured with stromal cells ablated of Hic-5 (67, 120).

4.5 LIMITATIONS OF RESEARCH

My results demonstrated a role for the nuclear receptor co-regulator Hic-5 in regulating VDR expression and activity in WPMY-1 prostate stromal cells and sensitization to $1,25D_3$-induced growth inhibition in LNCaP cells. However, VDR expression is not solely dependent upon Hic-5, as silencing of Hic-5 within WPMY-1 cells did not affect TGF-β induction of VDR expression or its synergistic activation with $1,25D_3$ of CYP24A1 gene expression. This correlates with a preliminary observation that upregulation of VDR is not dependent on Smad3 signaling. Given the role of Hic-5 in the Smad-dependent response to TGF-β treatment, I hypothesize that TGF-β

contributes to VDR induction by Smad-independent pathways, such as through ERK, JNK, and p38, in the Hic-5-silenced cells (49, 215, 244). Further experiments investigating $1,25D_3$ metabolism upon TGF-β treatment will clarify the biological effects of the Smad-independent pathways on $1,25D_3$ action.

I also found that co-culturing Hic-5-silenced WPMY-1 cells sensitized Hic-5-overexpressing LNCaP cells to enhanced cell death, as measured by the Trypan blue exclusion assay. However, this result does not tell us what cell-death pathway is being activated. Experiments to analyze induction of the intrinsic apoptosis pathway through caspase-3 cleavage were unsuccessful. However, expression of Bcl-2, an upstream mitochondrial target whose overexpression blocks $1,25D_3$-mediated growth inhibition, should be investigated (119, 120). Additionally, I cannot rule out the action of other pro-apoptotic proteins, such as caspase-8, Bid, and AIF (122).

The greatest limitation of my studies relates to the fact that the experiments were performed in specific cell lines, which maintain specific characteristics. For example, the LNCaP cell line is AR-positive, is dependent on androgens for survival, and does not express 5α-reductase (245, 246). One sub-line of LNCaP, C4-2, is androgen-insensitive and expresses low levels of p53 (247). Ectopic expression of Hic-5 in this cell line will be necessary to investigate whether a functional AR is important to $1,25D_3$ response, activation of VDR and its associated co-factors, or upregulation of CYP24A1. Additionally, mouse xenografts with LNCaP tend to develop small tumors, so that growth of stromal cells mixed with them may outpace growth of the tumor cell line, preventing formation of a palpable tumor.(223) Neil Bhowmick, my collaborator at UCLA, noticed this in his studies. The RWPE-2 line, an androgen-sensitive prostate tumor line that is derived from the immortalized benign RWPE-1

line upon transformation with Ki-Ras, forms palpable tumors upon grafting into nude mice (248). Thus, the RWPE-2 line may prove useful in developing a palpable tumor that ectopically expresses Hic-5 and extends my research beyond the context of one cell line.

To extend my results into translational studies, use of primary cell cultures will be necessary. Data obtained from cell lines may not accurately model prostate cancer as observed in therapy-naïve patients, who may contain heterogeneous genotypes. Therefore, ectopic expression of Hic-5 within primary tumor cultures will be important for xenograft formation to model disease progression as observed in patients and potential treatment outcomes upon $1,25D_3$ therapy. This would not just apply to primary tumor cultures, but also to derivation of CAFs to model a stromal microenvironment developed *in vivo*. Previously, other members of the DeFranco laboratory have had difficulty expressing an shRNA construct directed against Hic-5 in primary stromal cells using lentiviral techniques. Recent studies, however, have demonstrated success in silencing Dkk-3 in primary prostate stromal cells (PrSCs) (249). The lentivirus technique used in this study may be useful for achieving the goal of developing a stable knockdown in primary stromal lines.

Overall, my work presented here demonstrates differential function of a co-regulator on $1,25D_3$ response in the tumor and stromal microenvironments of prostate cancer. This presents a new area of therapy that needs to be investigated further.

4.6 CLINICAL SIGNIFICANCE

One of the main themes of this project was to examine the relevance of the stromal microenvironment to $1,25D_3$ metabolism and VDR activity in prostate cancer cells. As

demonstrated from my results, expression of Hic-5 in prostate stromal cells is necessary for efficient 1,25D_3-induced transcription of *CYP24A1*, which in turn metabolizes the compound to an inactive form. One study demonstrated that high expression of Hic-5 was correlated with castration resistance and androgen hypersensitivity in late-stage prostate cancer (217). Intriguingly, the DU145 cell line, which was derived from a brain metastasis of CRPC, expresses high amounts of CYP24A1 and is intrinsically resistant to 1,25D_3 treatment (250). Although CYP24A1 expression in CRPC-associated stroma has not yet been researched, it is likely that castrate resistance may also influence CYP24A1 metabolism of 1,25D_3 and thus resistance to therapy. The inconsistent data of the ASCENT trials supports this hypothesis, indicating that adjuvant therapy with taxotere chemotherapy in CRPC may not be successful.

Instead, my data suggests that a more appropriate period to treat patients with 1,25D_3 is during ADT. Previous studies demonstrated that castration of mice de-repressed Hic-5 expression in the epithelium of endogenous prostate and xenografts from cancer patients (223). Furthermore, ectopic expression in LNCaP cells inhibited growth and invasion of a mixed epithelial-stromal xenograft (223). My data demonstrated that ectopic Hic-5 expression sensitized LNCaP cells to 1,25D_3-induced growth inhibition at lower concentrations. From this, I hypothesize that maximum therapeutic benefit of 1,25D_3 may be achieved during ADT, when epithelial Hic-5 de-repression may occur. Such a therapeutic regimen may require less 1,25D_3 in order to achieve benefit, thus reducing the risk of hypercalcemia. This assertion is supported by a study in which the anti-androgen Casodex failed to inhibit 1,25D_3-induced growth inhibition in an androgen-independent derivative of the LNCaP cell line (251). However, additional studies had found that Casodex did inhibit 1,25D_3-induced growth inhibition in the parental cell line (252). Furthermore, data on tumor expression of Hic-5 is inconsistent and do not distinguish

between epithelial and stromal expression of Hic-5 (Table 4) (217, 220, 221, 253, 254). Therefore, care must be taken to ensure that $1,25D_3$ adjuvant therapy to ADT confers maximal benefit in a preclinical *in vivo* model.

Table 4: List of clinical studies for Hic-5 expression in prostate cancer.

Author	Source	Treatment	State	Hic-5 expression	Citation
Mestayer (2003)	Tumor, benign	None	Naïve	Decreased in tumor	(253)
Fujimoto (2001)	Tumor	None	Naïve	Increased in higher-grade	(254)
Miyoshi (2003)	Tumor	None, ADT	Naïve, CRPC	Decreased in CRPC, but higher expression associated with shorter recurrence-free survival	(221)
Fujimoto (2007)	Tumor and stroma from longitudinal progression	None, ADT	Naïve, CRPC	Increased in tumors from 2 of 6 patients with CRPC	(217)
Wikstrom (2009)	Stroma from longitudinal progression	None, transurethral resection, orchiectomy	Naïve, CRPC	Decreased in stroma correlated with shorter period to CRPC state	(220)

4.7 FUTURE DIRECTIONS

The general theme demonstrated within this work relates to the novel function of a nuclear receptor co-regulator within the stromal microenvironment of prostate cancer. In addition to providing the tumor a source of growth factors and a fertile matrix for invasion, the tumor microenvironment has recently been shown to secrete growth factors in the presence of chemotherapeutic compounds, inducing the acquisition of drug resistance within the tumor (255). Hic-5 expression in the prostate stroma contributes to intratumoral $1,25D_3$ resistance by co-activating the *CYP24A1* autoinhibitory metabolic feedback loop. Expression within the tumor

itself, however, confers enhanced sensitization to $1,25D_3$-induced growth inhibition. Differences in expression of other co-regulators between the tumor and the stroma, such as an altered balance between p160-family co-activators and co-repressors, may contribute to the differing action of Hic-5 in the two compartments (256). Based on the work presented here, I hypothesize that Hic-5 recruits different co-regulators to its target nuclear receptor depending on the context of the promoter and cell type.

At the level of the *CYP24A1* promoter, a Hic-5 responsive element was identified at 392-451 bp upstream of the TSS and was associated via *in silico* analysis with motifs for AP-2/Sp1 and TCF4 binding. Sp1 and TCF4 have previously been associated with Hic-5 binding, although in opposing effects (49, 223, 239). To target these specific sites, I propose a mutation reporter assay in which the individual sites are mutated to a string of bases that do not resemble any consensus binding motifs for VDR, AP-2/Sp1, or TCF4. The result of this experiment would be not only identifying potential Hic-5 interacting partners at the locus, but also identifying other novel regulators of *CYP24A1* transcription. From this, I would investigate additional cross-talk pathways that may mediate metabolism of $1,25D_3$, which may eventually lead to further adjuvant therapy to reduce metabolism and prolong bioavailability.

Advanced technologies like ChIP-seq (chromatin immunoprecipitation with sequencing) have facilitated whole-genome identification of unique cis-acting DNA sequences that are bound by trans-acting transcription factors and co-regulators. The unique pattern of these sites, the cistrome, creates a signature by which cell-type effects may be identified. Different patterns of binding sites may indicate prognosis of disease (257). The VDR cistrome describing binding of co-activators and co-repressors has recently been described in a colon cancer line (258). However, no genome-wide study has yet been performed to identify the VDR cistrome in

prostate cancer cells loci of Hic-5-responsive elements. My data suggests that Hic-5 bridges different transcription factors to facilitate cross-talk, enhancing their effects. Utilizing ChIP-seq, I would seek to understand the specific interaction dynamics between Hic-5 and liganded VDR within prostate stromal and tumor cells. Specifically, I have had difficulty with traditional ChIP-PCR due to the high G/C content (76%) within the identified target sequence in the *CYP24A1* promoter at 392-451 bp upstream of the TSS. Whole-genome techniques such as ChIP-seq may improve processivity and fidelity at this site and identify other sites where VDR interacts with Hic-5. Additionally, I also propose identifying the effect of Hic-5 on binding stability of VDR at VDREs. However, it must be cautioned that VDR may bind to VDREs in a ligand-independent manner (259). Therefore, ChIP-seq analysis will also examine binding of RNA polymerase II and co-activator complexes with VDR to examine whether Hic-5 interaction is required for recruitment and maximal transactivation.

Hic-5 binding within the VDR cistrome may influence how VDR target genes are expressed throughout the genome. While my research demonstrates a requirement of Hic-5 expression for full VDR transactivation of *CYP24A1*, this may not be the case at other target sites. At the *MYC* promoter, which VDR negatively regulates, Hic-5 binds to TCF4, inhibiting *MYC* transcription (126, 223). Thus, the result may be enhanced VDR activity in both transcriptional activation and repression. Whole-genome microarray analysis of the VDR transcriptome in Hic-5-ablated cells may point to novel sites of interaction and enhancement as well as downstream effects. Indeed, it may also be possible that Hic-5 expression may antagonize $1,25D_3$-induced transcription or repression of VDR target genes, depending on the context of the cell line. Thus, I propose that microarray analysis be performed in a cell line

ablated of Hic-5 expression (for example, comparing stromal Scr to shHic-5) and another line with ectopic Hic-5 expression (for example, comparing epithelial LNCaP to LNCaP/Hic-5).

While my results have demonstrated associations between Hic-5 and VDR, I have not yet been able to demonstrate physical interactions between Hic-5 and VDR. A major impediment in my attempts at co-immunoprecipitation (co-IP) in Scr cells was that the molecular weights of VDR and Hic-5 are approximately 55 kDa, similar to the molecular weight for the heavy chains of immunoglobulin G (IgG). This introduces a confounding effect on co-IP experiments on intact proteins. Instead, I propose two experiments. Ectopic expression of each protein with expression tags in a model mammalian cell line, such as HEK293, may allow for more specific co-IP than in systems that I am currently using. If the confounding effects of IgG are not reduced in this system, a mammalian two-hybrid reporter assay may provide quantitative analysis of VDR/Hic-5 binding, including efficiency of reporter transactivation (260). Within either system, I would be able to delete domains from each protein in order to determine which are necessary for interaction. Previously, the LIM4 domains of Hic-5 were shown to interact with the tau2 transactivation domain within GR (208). Given the structural similarities between members of the nuclear receptor superfamily, I would expect the LIM4 domain of Hic-5 to interact with the C-terminal AF-2 transactivation domain of VDR.

The differential effects of Hic-5 on VDR activity within epithelial and stromal compartments of prostate cancer presented an *in vitro* context by which $1,25D_3$-induced growth inhibition of LNCaP cells was further sensitized by ectopic expression of Hic-5 in the tumor line and knockdown of Hic-5 in the stromal WPMY-1 line. To translate this result to the clinic, it needs to be validated in an *in vivo* setting. I propose grafting LNCaP cells ectopically expressing Hic-5 mixed with primary CAFs containing control knockdown or Hic-5 knockdown into

immunocompromised mice. Upon formation of palpable tumors, I would castrate the mice, treat them intravenously with $1,25D_3$ and later measure tumor size, invasive capacity, and markers for stromal transdifferentiation. Based on the results presented here, I predict that $1,25D_3$ treatment of mice containing LNCaP/Hic-5 xenografts mixed with CAFs of Hic-5 would induce the least tumor growth, inhibit invasion the greatest, and reduce expression of myofibroblastic markers. Previously, Neil Bhowmick, my collaborator at UCLA, attempted to mix LNCaP and LNCaP/Hic-5 cells with Scr and shHic-5 WPMY-1 sublines, but WPMY-1 growth outpaced LNCaP growth and prevented tumor formation. The selection of primary CAFs, which were previously associated with tumors themselves, should improve the probability of forming palpable tumors in mice.

Differential effects of Hic-5 in epithelial and stromal compartments of prostate cancer have profound consequences on activation of the VDR pathway in prostate cancer. Much of the future work proposed here suggests critical work in understanding the interaction between VDR and Hic-5 and epithelial-stromal communication within the tumor microenvironment. Results from these studies may eventually lead to targeted treatment of prostate cancer through multiple signaling pathways interacting with $1,25D_3$ in the future, prolonging prognosis of patients undergoing ADT.

5.0 REFERENCES

1. Siegel R, Naishadham D, Jemal A. Cancer statistics, 2012. CA Cancer J Clin. 2012;62:10-29.

2. Etzioni R, Tsodikov A, Mariotto A, Szabo A, Falcon S, Wegelin J, et al. Quantifying the role of PSA screening in the US prostate cancer mortality decline. Cancer causes & control : CCC. 2008;19:175-81.

3. Brawley OW. Prostate cancer epidemiology in the United States. World J Urol. 2012;30:195-200.

4. Howlader N, Noone A, Krapcho M, Neyman N, Aminou R, Altekruse S, et al. SEER Cancer Statistics Review, 1975-2009 (Vintage 2009 Populations). 2012; Available from: http://seer.cancer.gov/csr/1975_2009_pops09/

5. Cooperberg MR, Carroll PR, Klotz L. Active surveillance for prostate cancer: progress and promise. Journal of clinical oncology : official journal of the American Society of Clinical Oncology. 2011;29:3669-76.

6. Carter HB, Albertsen PC, Barry MJ, Etzioni R, Freedland SJ, Greene KL, et al. Early detection of prostate cancer: AUA guideline. American Urological Association; 2013.

7. Ryan CJ, Smith MR, de Bono JS, Molina A, Logothetis CJ, de Souza P, et al. Abiraterone in metastatic prostate cancer without previous chemotherapy. The New England journal of medicine. 2013;368:138-48.

8. Petrylak DP. Docetaxel for the treatment of hormone-refractory prostate cancer. Reviews in urology. 2003;5 Suppl 2:S14-21.

9. Hannema SE, Hughes IA. Regulation of Wolffian duct development. Hormone research. 2007;67:142-51.

10. Prins GS, Putz O. Molecular signaling pathways that regulate prostate gland development. Differentiation. 2008;76:641-59.

11. Marker PC, Donjacour AA, Dahiya R, Cunha GR. Hormonal, cellular, and molecular control of prostatic development. Dev Biol. 2003;253:165-74.

12. Hayward SW, Baskin LS, Haughney PC, Foster BA, Cunha AR, Dahiya R, et al. Stromal development in the ventral prostate, anterior prostate and seminal vesicle of the rat. Acta Anat (Basel). 1996;155:94-103.

13. Hayward SW, Baskin LS, Haughney PC, Cunha AR, Foster BA, Dahiya R, et al. Epithelial development in the rat ventral prostate, anterior prostate and seminal vesicle. Acta Anat (Basel). 1996;155:81-93.

14. Kyprianou N, Isaacs JT. Activation of programmed cell death in the rat ventral prostate after castration. Endocrinology. 1988;122:552-62.

15. McNeal JE. Normal histology of the prostate. The American journal of surgical pathology. 1988;12:619-33.

16. Selman SH. The McNeal prostate: a review. Urology. 2011;78:1224-8.

17. Feldman BJ, Feldman D. The development of androgen-independent prostate cancer. Nature reviews Cancer. 2001;1:34-45.

18. Woenckhaus J, Fenic I. Proliferative inflammatory atrophy: a background lesion of prostate cancer? Andrologia. 2008;40:134-7.

19. Putzi MJ, De Marzo AM. Morphologic transitions between proliferative inflammatory atrophy and high-grade prostatic intraepithelial neoplasia. Urology. 2000;56:828-32.

20. Bostwick DG, Qian J. High-grade prostatic intraepithelial neoplasia. Modern Pathol. 2004;17:360-79.

21. Abd TT, Goodman M, Hall J, Ritenour CW, Petros JA, Marshall FF, et al. Comparison of 12-core versus 8-core prostate biopsy: multivariate analysis of large series of US veterans. Urology. 2011;77:541-7.

22. Egevad L, Mazzucchelli R, Montironi R. Implications of the International Society of Urological Pathology modified Gleason grading system. Archives of pathology & laboratory medicine. 2012;136:426-34.

23. Tosoian JJ, Trock BJ, Landis P, Feng Z, Epstein JI, Partin AW, et al. Active surveillance program for prostate cancer: an update of the Johns Hopkins experience. Journal of clinical oncology : official journal of the American Society of Clinical Oncology. 2011;29:2185-90.

24. Moul JW. Treatment of metastatic prostate cancer. Braz J Urol. 2000;26:132-45.

25. Yang W, Levine AC. Androgens and prostate cancer bone metastases: effects on both the seed and the soil. Endocrinol Metab Clin North Am. 2011;40:643-53, x.

26. Logothetis CJ, Lin SH. Osteoblasts in prostate cancer metastasis to bone. Nature reviews Cancer. 2005;5:21-8.

27. Droz J-P, Fléchon A, Terret C. Prostate cancer: management of advanced disease. Annals of oncology : official journal of the European Society for Medical Oncology / ESMO. 2002;13:89-94.

28. Robinson-Rechavi M, Carpentier AS, Duffraisse M, Laudet V. How many nuclear hormone receptors are there in the human genome? Trends in genetics : TIG. 2001;17:554-6.

29. Tenbaum S, Baniahmad A. Nuclear receptors: structure, function and involvement in disease. The international journal of biochemistry & cell biology. 1997;29:1325-41.

30. Kuiper GG, Brinkmann AO. Steroid hormone receptor phosphorylation: is there a physiological role? Molecular and cellular endocrinology. 1994;100:103-7.

31. Fuller PJ. The steroid receptor superfamily: mechanisms of diversity. FASEB journal : official publication of the Federation of American Societies for Experimental Biology. 1991;5:3092-9.

32. Luisi BF, Xu WX, Otwinowski Z, Freedman LP, Yamamoto KR, Sigler PB. Crystallographic analysis of the interaction of the glucocorticoid receptor with DNA. Nature. 1991;352:497-505.

33. Miyamoto T, Kakizawa T, Ichikawa K, Nishio S, Takeda T, Suzuki S, et al. The role of hinge domain in heterodimerization and specific DNA recognition by nuclear receptors. Molecular and cellular endocrinology. 2001;181:229-38.

34. Arriagada G, Paredes R, Olate J, van Wijnen A, Lian JB, Stein GS, et al. Phosphorylation at serine 208 of the 1alpha,25-dihydroxy Vitamin D3 receptor modulates the interaction with transcriptional coactivators. The Journal of steroid biochemistry and molecular biology. 2007;103:425-9.

35. Aranda A, Pascual A. Nuclear hormone receptors and gene expression. Physiological reviews. 2001;81:1269-304.

36. Scherrer LC, Picard D, Massa E, Harmon JM, Simons SS, Jr., Yamamoto KR, et al. Evidence that the hormone binding domain of steroid receptors confers hormonal control on chimeric proteins by determining their hormone-regulated binding to heat-shock protein 90. Biochemistry. 1993;32:5381-6.

37. Pratt WB, Toft DO. Steroid receptor interactions with heat shock protein and immunophilin chaperones. Endocrine reviews. 1997;18:306-60.

38. Echeverria PC, Mazaira G, Erlejman A, Gomez-Sanchez C, Piwien Pilipuk G, Galigniana MD. Nuclear import of the glucocorticoid receptor-hsp90 complex through the nuclear pore complex is mediated by its interaction with Nup62 and importin beta. Molecular and cellular biology. 2009;29:4788-97.

39. Pratt WB, Silverstein AM, Galigniana MD. A model for the cytoplasmic trafficking of signalling proteins involving the hsp90-binding immunophilins and p50cdc37. Cellular signalling. 1999;11:839-51.

40. Maruvada P, Baumann CT, Hager GL, Yen PM. Dynamic shuttling and intranuclear mobility of nuclear hormone receptors. The Journal of biological chemistry. 2003;278:12425-32.

41. Yang J, DeFranco DB. Assessment of glucocorticoid receptor-heat shock protein 90 interactions in vivo during nucleocytoplasmic trafficking. Mol Endocrinol. 1996;10:3-13.

42. White DM, Takeda T, DeGroot LJ, Stefansson K, Arnason BG. Beta-trace gene expression is regulated by a core promoter and a distal thyroid hormone response element. The Journal of biological chemistry. 1997;272:14387-93.

43. Chandran UR, DeFranco DB. Regulation of gonadotropin-releasing hormone gene transcription. Behavioural brain research. 1999;105:29-36.

44. Jansa P, Forejt J. A novel type of retinoic acid response element in the second intron of the mouse H2Kb gene is activated by the RAR/RXR heterodimer. Nucleic acids research. 1996;24:694-701.

45. Naar AM, Boutin JM, Lipkin SM, Yu VC, Holloway JM, Glass CK, et al. The orientation and spacing of core DNA-binding motifs dictate selective transcriptional responses to three nuclear receptors. Cell. 1991;65:1267-79.

46. Mangelsdorf DJ, Thummel C, Beato M, Herrlich P, Schutz G, Umesono K, et al. The nuclear receptor superfamily: the second decade. Cell. 1995;83:835-9.

47. Khan SH, Awasthi S, Guo C, Goswami D, Ling J, Griffin PR, et al. Binding of the N-terminal region of coactivator TIF2 to the intrinsically disordered AF1 domain of the glucocorticoid receptor is accompanied by conformational reorganizations. The Journal of biological chemistry. 2012;287:44546-60.

48. McKenna NJ, O'Malley BW. Minireview: nuclear receptor coactivators--an update. Endocrinology. 2002;143:2461-5.

49. Shibanuma M, Kim-Kaneyama JR, Sato S, Nose K. A LIM protein, Hic-5, functions as a potential coactivator for Sp1. Journal of cellular biochemistry. 2004;91:633-45.

50. Coquelin A, Desjardins C. Luteinizing hormone and testosterone secretion in young and old male mice. The American journal of physiology. 1982;243:E257-63.

51. Grino PB, Griffin JE, Wilson JD. Testosterone at high concentrations interacts with the human androgen receptor similarly to dihydrotestosterone. Endocrinology. 1990;126:1165-72.

52. Prins GS, Birch L, Greene GL. Androgen receptor localization in different cell types of the adult rat prostate. Endocrinology. 1991;129:3187-99.

53. Berges RR, Vukanovic J, Epstein JI, CarMichel M, Cisek L, Johnson DE, et al. Implication of cell kinetic changes during the progression of human prostatic cancer. Clinical cancer research : an official journal of the American Association for Cancer Research. 1995;1:473-80.

54. Franck-Lissbrant I, Haggstrom S, Damber JE, Bergh A. Testosterone stimulates angiogenesis and vascular regrowth in the ventral prostate in castrated adult rats. Endocrinology. 1998;139:451-6.

55. English HF, Kyprianou N, Isaacs JT. Relationship between DNA fragmentation and apoptosis in the programmed cell death in the rat prostate following castration. The Prostate. 1989;15:233-50.

56. Tomlins SA, Rhodes DR, Perner S, Dhanasekaran SM, Mehra R, Sun XW, et al. Recurrent fusion of TMPRSS2 and ETS transcription factor genes in prostate cancer. Science. 2005;310:644-8.

57. Byrne RL, Leung H, Neal DE. Peptide growth factors in the prostate as mediators of stromal epithelial interaction. British journal of urology. 1996;77:627-33.

58. McMenamin ME, Soung P, Perera S, Kaplan I, Loda M, Sellers WR. Loss of PTEN expression in paraffin-embedded primary prostate cancer correlates with high Gleason score and advanced stage. Cancer research. 1999;59:4291-6.

59. Han G, Buchanan G, Ittmann M, Harris JM, Yu X, Demayo FJ, et al. Mutation of the androgen receptor causes oncogenic transformation of the prostate. Proceedings of the National Academy of Sciences of the United States of America. 2005;102:1151-6.

60. Immediate versus deferred treatment for advanced prostatic cancer: initial results of the Medical Research Council Trial. The Medical Research Council Prostate Cancer Working Party Investigators Group. British journal of urology. 1997;79:235-46.

61. Pagliarulo V, Bracarda S, Eisenberger MA, Mottet N, Schroder FH, Sternberg CN, et al. Contemporary role of androgen deprivation therapy for prostate cancer. European urology. 2012;61:11-25.

62. Schellhammer PF, Sharifi R, Block NL, Soloway MS, Venner PM, Patterson AL, et al. Clinical benefits of bicalutamide compared with flutamide in combined androgen blockade for patients with advanced prostatic carcinoma: final report of a double-blind, randomized, multicenter trial. Casodex Combination Study Group. Urology. 1997;50:330-6.

63. Labrie F, Cusan L, Seguin C, Belanger A, Pelletier G, Reeves J, et al. Antifertility effects of LHRH agonists in the male rat and inhibition of testicular steroidogenesis in man. International journal of fertility. 1980;25:157-70.

64. Redding TW, Schally AV. Inhibition of prostate tumor growth in two rat models by chronic administration of D-Trp6 analogue of luteinizing hormone-releasing hormone. Proceedings of the National Academy of Sciences of the United States of America. 1981;78:6509-12.

65. Nicholson RI, Walker KJ, Maynard PV. Anti-tumour potential of a new luteinizing hormone releasing hormone analogue, ICI 118630. European journal of cancer. 1980;Suppl 1:295-9.

66. Agarwal DK, Costello AJ, Peters J, Sikaris K, Crowe H. Differential response of prostate specific antigen to testosterone surge after luteinizing hormone-releasing hormone analogue in prostate cancer and benign prostatic hyperplasia. BJU international. 2000;85:690-5.

67. Perlman H, Zhang X, Chen MW, Walsh K, Buttyan R. An elevated bax/bcl-2 ratio corresponds with the onset of prostate epithelial cell apoptosis. Cell death and differentiation. 1999;6:48-54.

68. Van Antwerp DJ, Martin SJ, Kafri T, Green DR, Verma IM. Suppression of TNF-alpha-induced apoptosis by NF-kappaB. Science. 1996;274:787-9.

69. Keller ET, Chang C, Ershler WB. Inhibition of NFkappaB activity through maintenance of IkappaBalpha levels contributes to dihydrotestosterone-mediated repression of the interleukin-6 promoter. The Journal of biological chemistry. 1996;271:26267-75.

70. Nelius T, Filleur S, Yemelyanov A, Budunova I, Shroff E, Mirochnik Y, et al. Androgen receptor targets NFkappaB and TSP1 to suppress prostate tumor growth in vivo. International journal of cancer Journal international du cancer. 2007;121:999-1008.

71. Morgentaler A, Traish AM. Shifting the paradigm of testosterone and prostate cancer: the saturation model and the limits of androgen-dependent growth. European urology. 2009;55:310-20.

72. McDonnell TJ, Troncoso P, Brisbay SM, Logothetis C, Chung LW, Hsieh JT, et al. Expression of the protooncogene bcl-2 in the prostate and its association with emergence of androgen-independent prostate cancer. Cancer research. 1992;52:6940-4.

73. Colombel M, Symmans F, Gil S, O'Toole KM, Chopin D, Benson M, et al. Detection of the apoptosis-suppressing oncoprotein bc1-2 in hormone-refractory human prostate cancers. The American journal of pathology. 1993;143:390-400.

74. Koivisto P, Kononen J, Palmberg C, Tammela T, Hyytinen E, Isola J, et al. Androgen receptor gene amplification: a possible molecular mechanism for androgen deprivation therapy failure in prostate cancer. Cancer research. 1997;57:314-9.

75. Taplin ME, Balk SP. Androgen receptor: a key molecule in the progression of prostate cancer to hormone independence. Journal of cellular biochemistry. 2004;91:483-90.

76. Li P, Yu X, Ge K, Melamed J, Roeder RG, Wang Z. Heterogeneous expression and functions of androgen receptor co-factors in primary prostate cancer. The American journal of pathology. 2002;161:1467-74.

77. Craft N, Shostak Y, Carey M, Sawyers CL. A mechanism for hormone-independent prostate cancer through modulation of androgen receptor signaling by the HER-2/neu tyrosine kinase. Nature medicine. 1999;5:280-5.

78. Sharifi N, Dahut WL, Steinberg SM, Figg WD, Tarassoff C, Arlen P, et al. A retrospective study of the time to clinical endpoints for advanced prostate cancer. BJU international. 2005;96:985-9.

79. Berthold DR, Pond GR, Roessner M, de Wit R, Eisenberger M, Tannock AI. Treatment of hormone-refractory prostate cancer with docetaxel or mitoxantrone: relationships between prostate-specific antigen, pain, and quality of life response and survival in the TAX-327 study. Clinical cancer research : an official journal of the American Association for Cancer Research. 2008;14:2763-7.

80. Harrington JA, Jones RJ. Management of metastatic castration-resistant prostate cancer after first-line docetaxel. European journal of cancer. 2011;47:2133-42.

81. Huldschinsky K. Heilung von Rachitis durch Kunstliche Hohensonne. [Rickets Cured by Ultraviolet Irradiation.]. Dtsch Med Wochenschr. 1919;45:712-3.

82. Rajakumar K, Greenspan SL, Thomas SB, Holick MF. SOLAR ultraviolet radiation and vitamin D: a historical perspective. American journal of public health. 2007;97:1746-54.

83. Holick MF, MacLaughlin JA, Clark MB, Holick SA, Potts JT, Jr., Anderson RR, et al. Photosynthesis of previtamin D3 in human skin and the physiologic consequences. Science. 1980;210:203-5.

84. Holick MF, MacLaughlin JA, Doppelt SH. Regulation of cutaneous previtamin D3 photosynthesis in man: skin pigment is not an essential regulator. Science. 1981;211:590-3.

85. Saarem K, Bergseth S, Oftebro H, Pedersen JI. Subcellular localization of vitamin D3 25-hydroxylase in human liver. The Journal of biological chemistry. 1984;259:10936-40.

86. Axen E, Bergman T, Wikvall K. Purification and characterization of a vitamin D3 25-hydroxylase from pig liver microsomes. The Biochemical journal. 1992;287 (Pt 3):725-31.

87. Gascon-Barre M, Demers C, Ghrab O, Theodoropoulos C, Lapointe R, Jones G, et al. Expression of CYP27A, a gene encoding a vitamin D-25 hydroxylase in human liver and kidney. Clinical endocrinology. 2001;54:107-15.

88. Hollis BW. Circulating 25-hydroxyvitamin D levels indicative of vitamin D sufficiency: implications for establishing a new effective dietary intake recommendation for vitamin D. The Journal of nutrition. 2005;135:317-22.

89. Takeyama K, Kitanaka S, Sato T, Kobori M, Yanagisawa J, Kato S. 25-Hydroxyvitamin D3 1alpha-hydroxylase and vitamin D synthesis. Science. 1997;277:1827-30.

90. Zehnder D, Bland R, Williams MC, McNinch RW, Howie AJ, Stewart PM, et al. Extrarenal expression of 25-hydroxyvitamin d(3)-1 alpha-hydroxylase. The Journal of clinical endocrinology and metabolism. 2001;86:888-94.

91. Chen TC, Wang L, Whitlatch LW, Flanagan JN, Holick MF. Prostatic 25-hydroxyvitamin D-1alpha-hydroxylase and its implication in prostate cancer. Journal of cellular biochemistry. 2003;88:315-22.

92. Laudet V. Evolution of the nuclear receptor superfamily: early diversification from an ancestral orphan receptor. Journal of molecular endocrinology. 1997;19:207-26.

93. A unified nomenclature system for the nuclear receptor superfamily. Cell. 1999;97:161-3.

94. Yasmin R, Williams RM, Xu M, Noy N. Nuclear import of the retinoid X receptor, the vitamin D receptor, and their mutual heterodimer. The Journal of biological chemistry. 2005;280:40152-60.

95. Rotkiewicz P, Sicinska W, Kolinski A, DeLuca HF. Model of three-dimensional structure of vitamin D receptor and its binding mechanism with 1alpha,25-dihydroxyvitamin D(3). Proteins. 2001;44:188-99.

96. Rochel N, Wurtz JM, Mitschler A, Klaholz B, Moras D. The crystal structure of the nuclear receptor for vitamin D bound to its natural ligand. Molecular cell. 2000;5:173-9.

97. Zhang J, Chalmers MJ, Stayrook KR, Burris LL, Wang Y, Busby SA, et al. DNA binding alters coactivator interaction surfaces of the intact VDR-RXR complex. Nature structural & molecular biology. 2011;18:556-63.

98. Bettoun DJ, Burris TP, Houck KA, Buck DW, 2nd, Stayrook KR, Khalifa B, et al. Retinoid X receptor is a nonsilent major contributor to vitamin D receptor-mediated transcriptional activation. Mol Endocrinol. 2003;17:2320-8.

99. Kim JY, Son YL, Lee YC. Involvement of SMRT corepressor in transcriptional repression by the vitamin D receptor. Mol Endocrinol. 2009;23:251-64.

100. Malloy PJ, Pike JW, Feldman D. The vitamin D receptor and the syndrome of hereditary 1,25-dihydroxyvitamin D-resistant rickets. Endocrine reviews. 1999;20:156-88.

101. Kim S, Shevde NK, Pike JW. 1,25-Dihydroxyvitamin D3 stimulates cyclic vitamin D receptor/retinoid X receptor DNA-binding, co-activator recruitment, and histone

acetylation in intact osteoblasts. Journal of bone and mineral research : the official journal of the American Society for Bone and Mineral Research. 2005;20:305-17.

102. Pike JW, Pathrose P, Barmina O, Chang CY, McDonnell DP, Yamamoto H, et al. Synthetic LXXLL peptide antagonize 1,25-dihydroxyvitamin D3-dependent transcription. Journal of cellular biochemistry. 2003;88:252-8.

103. Zhang C, Baudino TA, Dowd DR, Tokumaru H, Wang W, MacDonald PN. Ternary complexes and cooperative interplay between NCoA-62/Ski-interacting protein and steroid receptor coactivators in vitamin D receptor-mediated transcription. The Journal of biological chemistry. 2001;276:40614-20.

104. Rachez C, Lemon BD, Suldan Z, Bromleigh V, Gamble M, Naar AM, et al. Ligand-dependent transcription activation by nuclear receptors requires the DRIP complex. Nature. 1999;398:824-8.

105. Sanchez-Martinez R, Zambrano A, Castillo AI, Aranda A. Vitamin D-dependent recruitment of corepressors to vitamin D/retinoid X receptor heterodimers. Molecular and cellular biology. 2008;28:3817-29.

106. Guenther MG, Barak O, Lazar MA. The SMRT and N-CoR corepressors are activating cofactors for histone deacetylase 3. Molecular and cellular biology. 2001;21:6091-101.

107. Sakaki T, Sawada N, Nonaka Y, Ohyama Y, Inouye K. Metabolic studies using recombinant escherichia coli cells producing rat mitochondrial CYP24 CYP24 can convert 1alpha,25-dihydroxyvitamin D3 to calcitroic acid. European journal of biochemistry / FEBS. 1999;262:43-8.

108. Getzenberg RH, Light BW, Lapco PE, Konety BR, Nangia AK, Acierno JS, et al. Vitamin D inhibition of prostate adenocarcinoma growth and metastasis in the Dunning rat prostate model system. Urology. 1997;50:999-1006.

109. Kovalenko PL, Zhang Z, Yu JG, Li Y, Clinton SK, Fleet JC. Dietary vitamin D and vitamin D receptor level modulate epithelial cell proliferation and apoptosis in the prostate. Cancer Prev Res (Phila). 2011;4:1617-25.

110. Wagner D, Trudel D, Van der Kwast T, Nonn L, Giangreco AA, Li D, et al. Randomized clinical trial of vitamin d3 doses on prostatic vitamin d metabolite levels and ki67 labeling in prostate cancer patients. The Journal of clinical endocrinology and metabolism. 2013;98:1498-507.

111. Washington MN, Kim JS, Weigel NL. 1alpha,25-dihydroxyvitamin D3 inhibits C4-2 prostate cancer cell growth via a retinoblastoma protein (Rb)-independent G1 arrest. The Prostate. 2011;71:98-110.

112. Flores O, Wang Z, Knudsen KE, Burnstein KL. Nuclear targeting of cyclin-dependent kinase 2 reveals essential roles of cyclin-dependent kinase 2 localization and cyclin E in vitamin D-mediated growth inhibition. Endocrinology. 2010;151:896-908.

113. Thorne JL, Maguire O, Doig CL, Battaglia S, Fehr L, Sucheston LE, et al. Epigenetic control of a VDR-governed feed-forward loop that regulates p21(waf1/cip1) expression and function in non-malignant prostate cells. Nucleic acids research. 2011;39:2045-56.

114. Yang ES, Burnstein KL. Vitamin D inhibits G1 to S progression in LNCaP prostate cancer cells through p27Kip1 stabilization and Cdk2 mislocalization to the cytoplasm. The Journal of biological chemistry. 2003;278:46862-8.

115. Uhmann A, Niemann H, Lammering B, Henkel C, Hess I, Nitzki F, et al. Antitumoral effects of calcitriol in basal cell carcinomas involve inhibition of hedgehog signaling and induction of vitamin D receptor signaling and differentiation. Molecular cancer therapeutics. 2011;10:2179-88.

116. Ayers KL, Therond PP. Evaluating Smoothened as a G-protein-coupled receptor for Hedgehog signalling. Trends in cell biology. 2010;20:287-98.

117. Peehl DM, Shinghal R, Nonn L, Seto E, Krishnan AV, Brooks JD, et al. Molecular activity of 1,25-dihydroxyvitamin D3 in primary cultures of human prostatic epithelial cells revealed by cDNA microarray analysis. The Journal of steroid biochemistry and molecular biology. 2004;92:131-41.

118. McGaffin KR, Chrysogelos SA. Identification and characterization of a response element in the EGFR promoter that mediates transcriptional repression by 1,25-dihydroxyvitamin D3 in breast cancer cells. Journal of molecular endocrinology. 2005;35:117-33.

119. Blutt SE, McDonnell TJ, Polek TC, Weigel NL. Calcitriol-induced apoptosis in LNCaP cells is blocked by overexpression of Bcl-2. Endocrinology. 2000;141:10-7.

120. Kizildag S, Ates H, Kizildag S. Treatment of K562 cells with 1,25-dihydroxyvitamin D3 induces distinct alterations in the expression of apoptosis-related genes BCL2, BAX, BCLXL, and p21. Annals of hematology. 2010;89:1-7.

121. Guzey M, Kitada S, Reed JC. Apoptosis induction by 1alpha,25-dihydroxyvitamin D3 in prostate cancer. Molecular cancer therapeutics. 2002;1:667-77.

122. Muindi JR, Yu WD, Ma Y, Engler KL, Kong RX, Trump DL, et al. CYP24A1 inhibition enhances the antitumor activity of calcitriol. Endocrinology. 2010;151:4301-12.

123. Ye H, Cande C, Stephanou NC, Jiang S, Gurbuxani S, Larochette N, et al. DNA binding is required for the apoptogenic action of apoptosis inducing factor. Nature structural biology. 2002;9:680-4.

124. Cande C, Cohen I, Daugas E, Ravagnan L, Larochette N, Zamzami N, et al. Apoptosis-inducing factor (AIF): a novel caspase-independent death effector released from mitochondria. Biochimie. 2002;84:215-22.

125. Konety BR, Schwartz GG, Acierno JS, Jr., Becich MJ, Getzenberg RH. The role of vitamin D in normal prostate growth and differentiation. Cell growth & differentiation :

the molecular biology journal of the American Association for Cancer Research. 1996;7:1563-70.

126. Palmer HG, Gonzalez-Sancho JM, Espada J, Berciano MT, Puig I, Baulida J, et al. Vitamin D(3) promotes the differentiation of colon carcinoma cells by the induction of E-cadherin and the inhibition of beta-catenin signaling. The Journal of cell biology. 2001;154:369-87.

127. Ordonez-Moran P, Larriba MJ, Palmer HG, Valero RA, Barbachano A, Dunach M, et al. RhoA-ROCK and p38MAPK-MSK1 mediate vitamin D effects on gene expression, phenotype, and Wnt pathway in colon cancer cells. The Journal of cell biology. 2008;183:697-710.

128. Krishnan AV, Shinghal R, Raghavachari N, Brooks JD, Peehl DM, Feldman D. Analysis of vitamin D-regulated gene expression in LNCaP human prostate cancer cells using cDNA microarrays. The Prostate. 2004;59:243-51.

129. Peng L, Malloy PJ, Feldman D. Identification of a functional vitamin D response element in the human insulin-like growth factor binding protein-3 promoter. Mol Endocrinol. 2004;18:1109-19.

130. Liu B, Lee KW, Anzo M, Zhang B, Zi X, Tao Y, et al. Insulin-like growth factor-binding protein-3 inhibition of prostate cancer growth involves suppression of angiogenesis. Oncogene. 2007;26:1811-9.

131. Boyle BJ, Zhao XY, Cohen P, Feldman D. Insulin-like growth factor binding protein-3 mediates 1 alpha,25-dihydroxyvitamin d(3) growth inhibition in the LNCaP prostate cancer cell line through p21/WAF1. The Journal of urology. 2001;165:1319-24.

132. Hampel OZ, Kattan MW, Yang G, Haidacher SJ, Saleh GY, Thompson TC, et al. Quantitative immunohistochemical analysis of insulin-like growth factor binding protein-3 in human prostatic adenocarcinoma: a prognostic study. The Journal of urology. 1998;159:2220-5.

133. Perry AS, Loftus B, Moroose R, Lynch TH, Hollywood D, Watson RW, et al. In silico mining identifies IGFBP3 as a novel target of methylation in prostate cancer. British journal of cancer. 2007;96:1587-94.

134. Maund SL, Barclay WW, Hover LD, Axanova LS, Sui G, Hipp JD, et al. Interleukin-1alpha mediates the antiproliferative effects of 1,25-dihydroxyvitamin D3 in prostate progenitor/stem cells. Cancer research. 2011;71:5276-86.

135. Ding N, Yu RT, Subramaniam N, Sherman MH, Wilson C, Rao R, et al. A Vitamin D Receptor/SMAD Genomic Circuit Gates Hepatic Fibrotic Response. Cell. 2013;153:601-13.

136. Luderer HF, Nazarian RM, Zhu ED, Demay MB. Ligand-dependent actions of the vitamin D receptor are required for activation of TGF-beta signaling during the inflammatory response to cutaneous injury. Endocrinology. 2013;154:16-24.

137. Yanagi Y, Suzawa M, Kawabata M, Miyazono K, Yanagisawa J, Kato S. Positive and negative modulation of vitamin D receptor function by transforming growth factor-beta signaling through smad proteins. The Journal of biological chemistry. 1999;274:12971-4.

138. Subramaniam N, Leong GM, Cock TA, Flanagan JL, Fong C, Eisman JA, et al. Cross-talk between 1,25-dihydroxyvitamin D3 and transforming growth factor-beta signaling requires binding of VDR and Smad3 proteins to their cognate DNA recognition elements. The Journal of biological chemistry. 2001;276:15741-6.

139. Penna G, Fibbi B, Amuchastegui S, Corsiero E, Laverny G, Silvestrini E, et al. The vitamin D receptor agonist elocalcitol inhibits IL-8-dependent benign prostatic hyperplasia stromal cell proliferation and inflammatory response by targeting the RhoA/Rho kinase and NF-kappaB pathways. The Prostate. 2009;69:480-93.

140. Segain JP, Raingeard de la Bletiere D, Sauzeau V, Bourreille A, Hilaret G, Cario-Toumaniantz C, et al. Rho kinase blockade prevents inflammation via nuclear factor kappa B inhibition: evidence in Crohn's disease and experimental colitis. Gastroenterology. 2003;124:1180-7.

141. Harant H, Andrew PJ, Reddy GS, Foglar E, Lindley IJ. 1alpha,25-dihydroxyvitamin D3 and a variety of its natural metabolites transcriptionally repress nuclear-factor-kappaB-mediated interleukin-8 gene expression. European journal of biochemistry / FEBS. 1997;250:63-71.

142. Inoue K, Slaton JW, Eve BY, Kim SJ, Perrotte P, Balbay MD, et al. Interleukin 8 expression regulates tumorigenicity and metastases in androgen-independent prostate cancer. Clinical cancer research : an official journal of the American Association for Cancer Research. 2000;6:2104-19.

143. Belt AR, Baldassare JJ, Molnar M, Romero R, Hertelendy F. The nuclear transcription factor NF-kappaB mediates interleukin-1beta-induced expression of cyclooxygenase-2 in human myometrial cells. American journal of obstetrics and gynecology. 1999;181:359-66.

144. Moreno J, Krishnan AV, Feldman D. Molecular mechanisms mediating the anti-proliferative effects of Vitamin D in prostate cancer. The Journal of steroid biochemistry and molecular biology. 2005;97:31-6.

145. Moreno J, Krishnan AV, Swami S, Nonn L, Peehl DM, Feldman D. Regulation of prostaglandin metabolism by calcitriol attenuates growth stimulation in prostate cancer cells. Cancer research. 2005;65:7917-25.

146. Vo BT, Morton D, Jr., Komaragiri S, Millena AC, Leath C, Khan SA. TGF-beta effects on prostate cancer cell migration and invasion are mediated by PGE2 through activation of PI3K/AKT/mTOR pathway. Endocrinology. 2013;154:1768-79.

147. Schwartz GG, Hanchette CL. UV, latitude, and spatial trends in prostate cancer mortality: all sunlight is not the same (United States). Cancer causes & control : CCC. 2006;17:1091-101.

148. Matsuoka LY, Wortsman J, Haddad JG, Hollis BW. In vivo threshold for cutaneous synthesis of vitamin D3. The Journal of laboratory and clinical medicine. 1989;114:301-5.

149. de Vries E, Soerjomataram I, Houterman S, Louwman MW, Coebergh JW. Decreased risk of prostate cancer after skin cancer diagnosis: a protective role of ultraviolet radiation? American journal of epidemiology. 2007;165:966-72.

150. Nair-Shalliker V, Smith DP, Egger S, Hughes AM, Kaldor JM, Clements M, et al. Sun exposure may increase risk of prostate cancer in the high UV environment of New South Wales, Australia: a case-control study. International journal of cancer Journal international du cancer. 2012;131:E726-32.

151. Ahn J, Peters U, Albanes D, Purdue MP, Abnet CC, Chatterjee N, et al. Serum vitamin D concentration and prostate cancer risk: a nested case-control study. Journal of the National Cancer Institute. 2008;100:796-804.

152. Barnett CM, Nielson CM, Shannon J, Chan JM, Shikany JM, Bauer DC, et al. Serum 25-OH vitamin D levels and risk of developing prostate cancer in older men. Cancer causes & control : CCC. 2010;21:1297-303.

153. Fang F, Kasperzyk JL, Shui I, Hendrickson W, Hollis BW, Fall K, et al. Prediagnostic plasma vitamin D metabolites and mortality among patients with prostate cancer. PloS one. 2011;6:e18625.

154. Shui IM, Mucci LA, Kraft P, Tamimi RM, Lindstrom S, Penney KL, et al. Vitamin D-related genetic variation, plasma vitamin D, and risk of lethal prostate cancer: a prospective nested case-control study. Journal of the National Cancer Institute. 2012;104:690-9.

155. Gilbert R, Metcalfe C, Fraser WD, Donovan J, Hamdy F, Neal DE, et al. Associations of circulating 25-hydroxyvitamin D with prostate cancer diagnosis, stage and grade. International journal of cancer Journal international du cancer. 2012;131:1187-96.

156. Huang SP, Huang CY, Wu WJ, Pu YS, Chen J, Chen YY, et al. Association of vitamin D receptor FokI polymorphism with prostate cancer risk, clinicopathological features and recurrence of prostate specific antigen after radical prostatectomy. International journal of cancer Journal international du cancer. 2006;119:1902-7.

157. Henner WD, Beer TM. A New Formulation of Calcitriol (DN-101) for High-Dose Pulse Administration in Prostate Cancer Therapy. Reviews in urology. 2003;5 Suppl 3:S38-44.

158. Beer TM, Ryan CW, Venner PM, Petrylak DP, Chatta GS, Ruether JD, et al. Double-blinded randomized study of high-dose calcitriol plus docetaxel compared with placebo plus docetaxel in androgen-independent prostate cancer: a report from the ASCENT Investigators. Journal of clinical oncology : official journal of the American Society of Clinical Oncology. 2007;25:669-74.

159. Scher HI, Jia X, Chi K, de Wit R, Berry WR, Albers P, et al. Randomized, open-label phase III trial of docetaxel plus high-dose calcitriol versus docetaxel plus prednisone for patients with castration-resistant prostate cancer. Journal of clinical oncology : official journal of the American Society of Clinical Oncology. 2011;29:2191-8.

160. Miller GJ, Stapleton GE, Hedlund TE, Moffat KA. Vitamin D receptor expression, 24-hydroxylase activity, and inhibition of growth by 1alpha,25-dihydroxyvitamin D3 in seven human prostatic carcinoma cell lines. Clinical cancer research : an official journal of the American Association for Cancer Research. 1995;1:997-1003.

161. Mimori K, Tanaka Y, Yoshinaga K, Masuda T, Yamashita K, Okamoto M, et al. Clinical significance of the overexpression of the candidate oncogene CYP24 in esophageal cancer. Annals of oncology : official journal of the European Society for Medical Oncology / ESMO. 2004;15:236-41.

162. Chen G, Kim SH, King AN, Zhao L, Simpson RU, Christensen PJ, et al. CYP24A1 is an independent prognostic marker of survival in patients with lung adenocarcinoma. Clinical cancer research : an official journal of the American Association for Cancer Research. 2011;17:817-26.

163. Smith DC, Johnson CS, Freeman CC, Muindi J, Wilson JW, Trump DL. A Phase I trial of calcitriol (1,25-dihydroxycholecalciferol) in patients with advanced malignancy. Clinical cancer research : an official journal of the American Association for Cancer Research. 1999;5:1339-45.

164. Carroll MF, Schade DS. A practical approach to hypercalcemia. American family physician. 2003;67:1959-66.

165. Knudson AG. Two genetic hits (more or less) to cancer. Nature reviews Cancer. 2001;1:157-62.

166. Olumi AF, Grossfeld GD, Hayward SW, Carroll PR, Tlsty TD, Cunha GR. Carcinoma-associated fibroblasts direct tumor progression of initiated human prostatic epithelium. Cancer research. 1999;59:5002-11.

167. Gleave M, Hsieh JT, Gao CA, von Eschenbach AC, Chung LW. Acceleration of human prostate cancer growth in vivo by factors produced by prostate and bone fibroblasts. Cancer research. 1991;51:3753-61.

168. Zhau HE, Hong SJ, Chung LW. A fetal rat urogenital sinus mesenchymal cell line (rUGM): accelerated growth and conferral of androgen-induced growth responsiveness upon a human bladder cancer epithelial cell line in vivo. International journal of cancer Journal international du cancer. 1994;56:706-14.

169. Chung LW, Cunha GR. Stromal-epithelial interactions: II. Regulation of prostatic growth by embryonic urogenital sinus mesenchyme. The Prostate. 1983;4:503-11.

170. Cunha GR, Battle E, Young P, Brody J, Donjacour A, Hayashi N, et al. Role of epithelial-mesenchymal interactions in the differentiation and spatial organization of visceral smooth muscle. Epithelial cell biology. 1992;1:76-83.

171. Barron DA, Rowley DR. The reactive stroma microenvironment and prostate cancer progression. Endocrine-related cancer. 2012;19:R187-204.

172. Sugimura Y, Foster BA, Hom YK, Lipschutz JH, Rubin JS, Finch PW, et al. Keratinocyte growth factor (KGF) can replace testosterone in the ductal branching morphogenesis of the rat ventral prostate. The International journal of developmental biology. 1996;40:941-51.

173. Planz B, Wang Q, Kirley SD, Lin CW, McDougal WS. Androgen responsiveness of stromal cells of the human prostate: regulation of cell proliferation and keratinocyte growth factor by androgen. The Journal of urology. 1998;160:1850-5.

174. Hayward SW, Cunha GR, Dahiya R. Normal development and carcinogenesis of the prostate. A unifying hypothesis. Annals of the New York Academy of Sciences. 1996;784:50-62.

175. Grossfeld GD, Hayward SW, Tlsty TD, Cunha GR. The role of stroma in prostatic carcinogenesis. Endocrine-related cancer. 1998;5:253-70.

176. Thompson TC, Timme TL, Kadmon D, Park SH, Egawa S, Yoshida K. Genetic predisposition and mesenchymal-epithelial interactions in ras+myc-induced carcinogenesis in reconstituted mouse prostate. Molecular carcinogenesis. 1993;7:165-79.

177. Nemeth JA, Harb JF, Barroso U, Jr., He Z, Grignon DJ, Cher ML. Severe combined immunodeficient-hu model of human prostate cancer metastasis to human bone. Cancer research. 1999;59:1987-93.

178. Tuxhorn JA, Ayala GE, Smith MJ, Smith VC, Dang TD, Rowley DR. Reactive stroma in human prostate cancer: induction of myofibroblast phenotype and extracellular matrix remodeling. Clinical cancer research : an official journal of the American Association for Cancer Research. 2002;8:2912-23.

179. Peehl DM, Sellers RG. Induction of smooth muscle cell phenotype in cultured human prostatic stromal cells. Experimental cell research. 1997;232:208-15.

180. Basanta D, Strand DW, Lukner RB, Franco OE, Cliffel DE, Ayala GE, et al. The role of transforming growth factor-beta-mediated tumor-stroma interactions in prostate cancer progression: an integrative approach. Cancer research. 2009;69:7111-20.

181. Tuxhorn JA, Ayala GE, Rowley DR. Reactive stroma in prostate cancer progression. The Journal of urology. 2001;166:2472-83.

182. Wang J, Dodd C, Shankowsky HA, Scott PG, Tredget EE. Deep dermal fibroblasts contribute to hypertrophic scarring. Laboratory investigation; a journal of technical methods and pathology. 2008;88:1278-90.

183. Schafer M, Werner S. Cancer as an overhealing wound: an old hypothesis revisited. Nature reviews Molecular cell biology. 2008;9:628-38.

184. Gerber HP, Kowalski J, Sherman D, Eberhard DA, Ferrara N. Complete inhibition of rhabdomyosarcoma xenograft growth and neovascularization requires blockade of both tumor and host vascular endothelial growth factor. Cancer research. 2000;60:6253-8.

185. Kaminski A, Hahne JC, Haddouti el M, Florin A, Wellmann A, Wernert N. Tumour-stroma interactions between metastatic prostate cancer cells and fibroblasts. International journal of molecular medicine. 2006;18:941-50.

186. Royuela M, De Miguel MP, Bethencourt FR, Sanchez-Chapado M, Fraile B, Paniagua R. Transforming growth factor beta 1 and its receptor types I and II. Comparison in human normal prostate, benign prostatic hyperplasia, and prostatic carcinoma. Growth Factors. 1998;16:101-10.

187. Ao M, Williams K, Bhowmick NA, Hayward SW. Transforming growth factor-beta promotes invasion in tumorigenic but not in nontumorigenic human prostatic epithelial cells. Cancer research. 2006;66:8007-16.

188. Grubisha MJ, Cifuentes ME, Hammes SR, Defranco DB. A local paracrine and endocrine network involving TGFbeta, Cox-2, ROS, and estrogen receptor beta influences reactive stromal cell regulation of prostate cancer cell motility. Mol Endocrinol. 2012;26:940-54.

189. Wilson MJ, Sellers RG, Wiehr C, Melamud O, Pei D, Peehl DM. Expression of matrix metalloproteinase-2 and -9 and their inhibitors, tissue inhibitor of metalloproteinase-1 and -2, in primary cultures of human prostatic stromal and epithelial cells. Journal of cellular physiology. 2002;191:208-16.

190. Vollmer G, Michna H, Schneider MR, Knuppen R. Stromal expression of tenascin is inversely correlated to epithelial differentiation of hormone dependent tissues. The Journal of steroid biochemistry and molecular biology. 1994;48:487-94.

191. Ricciardelli C, Mayne K, Sykes PJ, Raymond WA, McCaul K, Marshall VR, et al. Elevated levels of versican but not decorin predict disease progression in early-stage prostate cancer. Clinical cancer research : an official journal of the American Association for Cancer Research. 1998;4:963-71.

192. Verona EV, Elkahloun AG, Yang J, Bandyopadhyay A, Yeh IT, Sun LZ. Transforming growth factor-beta signaling in prostate stromal cells supports prostate carcinoma growth by up-regulating stromal genes related to tissue remodeling. Cancer research. 2007;67:5737-46.

193. Heitzer MD, DeFranco DB. Hic-5/ARA55, a LIM domain-containing nuclear receptor coactivator expressed in prostate stromal cells. Cancer research. 2006;66:7326-33.

194. Shibanuma M, Mashimo J, Kuroki T, Nose K. Characterization of the TGF beta 1-inducible hic-5 gene that encodes a putative novel zinc finger protein and its possible involvement in cellular senescence. The Journal of biological chemistry. 1994;269:26767-74.

195. Shibanuma M, Mashimo J, Mita A, Kuroki T, Nose K. Cloning from a mouse osteoblastic cell line of a set of transforming-growth-factor-beta 1-regulated genes, one of which seems to encode a follistatin-related polypeptide. European journal of biochemistry / FEBS. 1993;217:13-9.

196. Deakin NO, Pignatelli J, Turner CE. Diverse roles for the paxillin family of proteins in cancer. Genes & cancer. 2012;3:362-70.

197. Hagmann J, Grob M, Welman A, van Willigen G, Burger MM. Recruitment of the LIM protein hic-5 to focal contacts of human platelets. Journal of cell science. 1998;111 (Pt 15):2181-8.

198. Thomas SM, Hagel M, Turner CE. Characterization of a focal adhesion protein, Hic-5, that shares extensive homology with paxillin. Journal of cell science. 1999;112 (Pt 2):181-90.

199. Gao Z, Schwartz LM. Identification and analysis of Hic-5/ARA55 isoforms: Implications for integrin signaling and steroid hormone action. FEBS letters. 2005;579:5651-7.

200. Dawid IB, Breen JJ, Toyama R. LIM domains: multiple roles as adapters and functional modifiers in protein interactions. Trends in genetics : TIG. 1998;14:156-62.

201. Fujita H, Kamiguchi K, Cho D, Shibanuma M, Morimoto C, Tachibana K. Interaction of Hic-5, A senescence-related protein, with focal adhesion kinase. The Journal of biological chemistry. 1998;273:26516-21.

202. Nishiya N, Iwabuchi Y, Shibanuma M, Cote JF, Tremblay ML, Nose K. Hic-5, a paxillin homologue, binds to the protein-tyrosine phosphatase PEST (PTP-PEST) through its LIM 3 domain. The Journal of biological chemistry. 1999;274:9847-53.

203. Nishiya N, Tachibana K, Shibanuma M, Mashimo JI, Nose K. Hic-5-reduced cell spreading on fibronectin: competitive effects between paxillin and Hic-5 through interaction with focal adhesion kinase. Molecular and cellular biology. 2001;21:5332-45.

204. Deakin NO, Turner CE. Distinct roles for paxillin and Hic-5 in regulating breast cancer cell morphology, invasion, and metastasis. Molecular biology of the cell. 2011;22:327-41.

205. Tumbarello DA, Turner CE. Hic-5 contributes to epithelial-mesenchymal transformation through a RhoA/ROCK-dependent pathway. Journal of cellular physiology. 2007;211:736-47.

206. Shibanuma M, Mori K, Kim-Kaneyama JR, Nose K. Involvement of FAK and PTP-PEST in the regulation of redox-sensitive nuclear-cytoplasmic shuttling of a LIM protein, Hic-5. Antioxidants & redox signaling. 2005;7:335-47.

207. Shibanuma M, Kim-Kaneyama JR, Ishino K, Sakamoto N, Hishiki T, Yamaguchi K, et al. Hic-5 communicates between focal adhesions and the nucleus through oxidant-sensitive nuclear export signal. Molecular biology of the cell. 2003;14:1158-71.

208. Guerrero-Santoro J, Yang L, Stallcup MR, DeFranco DB. Distinct LIM domains of Hic-5/ARA55 are required for nuclear matrix targeting and glucocorticoid receptor binding and coactivation. Journal of cellular biochemistry. 2004;92:810-9.

209. Aghajanova L, Velarde MC, Giudice LC. The progesterone receptor coactivator Hic-5 is involved in the pathophysiology of endometriosis. Endocrinology. 2009;150:3863-70.

210. Fujimoto N, Yeh S, Kang HY, Inui S, Chang HC, Mizokami A, et al. Cloning and characterization of androgen receptor coactivator, ARA55, in human prostate. The Journal of biological chemistry. 1999;274:8316-21.

211. Rahman MM, Miyamoto H, Lardy H, Chang C. Inactivation of androgen receptor coregulator ARA55 inhibits androgen receptor activity and agonist effect of antiandrogens in prostate cancer cells. Proceedings of the National Academy of Sciences of the United States of America. 2003;100:5124-9.

212. He B, Minges JT, Lee LW, Wilson EM. The FXXLF motif mediates androgen receptor-specific interactions with coregulators. The Journal of biological chemistry. 2002;277:10226-35.

213. Heitzer MD, DeFranco DB. Mechanism of action of Hic-5/androgen receptor activator 55, a LIM domain-containing nuclear receptor coactivator. Mol Endocrinol. 2006;20:56-64.

214. Xie S, Ni J, Lee YF, Liu S, Li G, Shyr CR, et al. Increased acetylation in the DNA-binding domain of TR4 nuclear receptor by the coregulator ARA55 leads to suppression of TR4 transactivation. The Journal of biological chemistry. 2011;286:21129-36.

215. Wang H, Song K, Sponseller TL, Danielpour D. Novel function of androgen receptor-associated protein 55/Hic-5 as a negative regulator of Smad3 signaling. The Journal of biological chemistry. 2005;280:5154-62.

216. Wang H, Song K, Krebs TL, Yang J, Danielpour D. Smad7 is inactivated through a direct physical interaction with the LIM protein Hic-5/ARA55. Oncogene. 2008;27:6791-805.

217. Fujimoto N, Miyamoto H, Mizokami A, Harada S, Nomura M, Ueta Y, et al. Prostate cancer cells increase androgen sensitivity by increase in nuclear androgen receptor and androgen receptor coactivators; a possible mechanism of hormone-resistance of prostate cancer cells. Cancer investigation. 2007;25:32-7.

218. Dabiri G, Tumbarello DA, Turner CE, Van de Water L. TGF-beta1 slows the growth of pathogenic myofibroblasts through a mechanism requiring the focal adhesion protein, Hic-5. The Journal of investigative dermatology. 2008;128:280-91.

219. Dabiri G, Tumbarello DA, Turner CE, Van de Water L. Hic-5 promotes the hypertrophic scar myofibroblast phenotype by regulating the TGF-beta1 autocrine loop. The Journal of investigative dermatology. 2008;128:2518-25.

220. Wikstrom P, Marusic J, Stattin P, Bergh A. Low stroma androgen receptor level in normal and tumor prostate tissue is related to poor outcome in prostate cancer patients. The Prostate. 2009;69:799-809.

221. Miyoshi Y, Ishiguro H, Uemura H, Fujinami K, Miyamoto H, Miyoshi Y, et al. Expression of AR associated protein 55 (ARA55) and androgen receptor in prostate cancer. The Prostate. 2003;56:280-6.

222. Heitzer MD, DeFranco DB. Hic-5/ARA55: a prostate stroma-specific AR coactivator. Steroids. 2007;72:218-20.

223. Li X, Martinez-Ferrer M, Botta V, Uwamariya C, Banerjee J, Bhowmick NA. Epithelial Hic-5/ARA55 expression contributes to prostate tumorigenesis and castrate responsiveness. Oncogene. 2011;30:167-77.

224. Kaighn ME, Narayan KS, Ohnuki Y, Lechner JF, Jones LW. Establishment and characterization of a human prostatic carcinoma cell line (PC-3). Investigative urology. 1979;17:16-23.

225. Hidalgo AA, Paredes R, Garcia VM, Flynn G, Johnson CS, Trump DL, et al. Altered VDR-mediated transcriptional activity in prostate cancer stroma. The Journal of steroid biochemistry and molecular biology. 2007;103:731-6.

226. Zhang Q, Kanterewicz B, Buch S, Petkovich M, Parise R, Beumer J, et al. CYP24 inhibition preserves 1alpha,25-dihydroxyvitamin D(3) anti-proliferative signaling in lung cancer cells. Molecular and cellular endocrinology. 2012;355:153-61.

227. Kumar R, Iachini DN, Neilsen PM, Kaplan J, Michalakas J, Anderson PH, et al. Systematic characterisation of the rat and human CYP24A1 promoter. Molecular and cellular endocrinology. 2010;325:46-53.

228. Schug J. Using TESS to predict transcription factor binding sites in DNA sequence. Current protocols in bioinformatics / editoral board, Andreas D Baxevanis [et al]. 2008;Chapter 2:Unit 2 6.

229. Searle SR. Linear models for unbalanced data: Wiley; 1987.

230. Keene ON. The log transformation is special. Statistics in medicine. 1995;14:811-9.

231. Moustakas A. Smad signalling network. Journal of cell science. 2002;115:3355-6.

232. Hu B, Wu Z, Phan SH. Smad3 mediates transforming growth factor-beta-induced alpha-smooth muscle actin expression. American journal of respiratory cell and molecular biology. 2003;29:397-404.

233. Ramirez AM, Wongtrakool C, Welch T, Steinmeyer A, Zugel U, Roman J. Vitamin D inhibition of pro-fibrotic effects of transforming growth factor beta1 in lung fibroblasts and epithelial cells. The Journal of steroid biochemistry and molecular biology. 2010;118:142-50.

234. Webber MM, Trakul N, Thraves PS, Bello-DeOcampo D, Chu WW, Storto PD, et al. A human prostatic stromal myofibroblast cell line WPMY-1: a model for stromal-epithelial interactions in prostatic neoplasia. Carcinogenesis. 1999;20:1185-92.

235. Diaw L, Roth M, Schwinn DA, d'Alelio ME, Green LJ, Tangrea JA. Characteristics of a human prostate stromal cell line related to its use in a stromal-epithelial coculture model for the study of cancer chemoprevention. In Vitro Cell Dev Biol Anim. 2005;41:142-8.

236. Staal A, van den Bemd GJ, Birkenhager JC, Pols HA, van Leeuwen JP. Consequences of vitamin D receptor regulation for the 1,25-dihydroxyvitamin D3-induced 24-hydroxylase activity in osteoblast-like cells: initiation of the C24-oxidation pathway. Bone. 1997;20:237-43.

237. Pedrozo HA, Boyan BD, Mazock J, Dean DD, Gomez R, Schwartz Z. TGFbeta1 regulates 25-hydroxyvitamin D3 1alpha- and 24-hydroxylase activity in cultured growth plate chondrocytes in a maturation-dependent manner. Calcified tissue international. 1999;64:50-6.

238. Chen KS, DeLuca HF. Cloning of the human 1 alpha,25-dihydroxyvitamin D-3 24-hydroxylase gene promoter and identification of two vitamin D-responsive elements. Biochimica et biophysica acta. 1995;1263:1-9.

239. Ghogomu SM, van Venrooy S, Ritthaler M, Wedlich D, Gradl D. HIC-5 is a novel repressor of lymphoid enhancer factor/T-cell factor-driven transcription. The Journal of biological chemistry. 2006;281:1755-64.

240. Gobel F, Taschner S, Jurkin J, Konradi S, Vaculik C, Richter S, et al. Reciprocal role of GATA-1 and vitamin D receptor in human myeloid dendritic cell differentiation. Blood. 2009;114:3813-21.

241. Chen J, Olivares-Navarrete R, Wang Y, Herman TR, Boyan BD, Schwartz Z. Protein-disulfide isomerase-associated 3 (Pdia3) mediates the membrane response to 1,25-dihydroxyvitamin D3 in osteoblasts. The Journal of biological chemistry. 2010;285:37041-50.

242. Jiang Y, Fleet JC. Phorbol esters enhance 1alpha,25-dihydroxyvitamin D3-regulated 25-hydroxyvitamin D-24-hydroxylase (CYP24A1) gene expression through ERK-mediated phosphorylation of specific protein 3 (Sp3) in Caco-2 cells. Molecular and cellular endocrinology. 2012;361:31-9.

243. Tashiro K, Ishii C, Ryoji M. Role of distal upstream sequence in vitamin D-induced expression of human CYP24 gene. Biochemical and biophysical research communications. 2007;358:259-65.

244. Qi X, Pramanik R, Wang J, Schultz RM, Maitra RK, Han J, et al. The p38 and JNK pathways cooperate to trans-activate vitamin D receptor via c-Jun/AP-1 and sensitize human breast cancer cells to vitamin D(3)-induced growth inhibition. The Journal of biological chemistry. 2002;277:25884-92.

245. Yang Q, Fung KM, Day WV, Kropp BP, Lin HK. Androgen receptor signaling is required for androgen-sensitive human prostate cancer cell proliferation and survival. Cancer cell international. 2005;5:8.

246. Horoszewicz JS, Leong SS, Chu TM, Wajsman ZL, Friedman M, Papsidero L, et al. The LNCaP cell line--a new model for studies on human prostatic carcinoma. Progress in clinical and biological research. 1980;37:115-32.

247. Thalmann GN, Anezinis PE, Chang SM, Zhau HE, Kim EE, Hopwood VL, et al. Androgen-independent cancer progression and bone metastasis in the LNCaP model of human prostate cancer. Cancer research. 1994;54:2577-81.

248. Bello D, Webber MM, Kleinman HK, Wartinger DD, Rhim JS. Androgen responsive adult human prostatic epithelial cell lines immortalized by human papillomavirus 18. Carcinogenesis. 1997;18:1215-23.

249. Zenzmaier C, Sampson N, Plas E, Berger P. Dickkopf-related protein 3 promotes pathogenic stromal remodeling in benign prostatic hyperplasia and prostate cancer. The Prostate. 2013.

250. Ly LH, Zhao XY, Holloway L, Feldman D. Liarozole acts synergistically with 1alpha,25-dihydroxyvitamin D3 to inhibit growth of DU 145 human prostate cancer cells by blocking 24-hydroxylase activity. Endocrinology. 1999;140:2071-6.

251. Yang ES, Maiorino CA, Roos BA, Knight SR, Burnstein KL. Vitamin D-mediated growth inhibition of an androgen-ablated LNCaP cell line model of human prostate cancer. Molecular and cellular endocrinology. 2002;186:69-79.

252. Murthy S, Agoulnik IU, Weigel NL. Androgen receptor signaling and vitamin D receptor action in prostate cancer cells. The Prostate. 2005;64:362-72.

253. Mestayer C, Blanchere M, Jaubert F, Dufour B, Mowszowicz I. Expression of androgen receptor coactivators in normal and cancer prostate tissues and cultured cell lines. The Prostate. 2003;56:192-200.

254. Fujimoto N, Mizokami A, Harada S, Matsumoto T. Different expression of androgen receptor coactivators in human prostate. Urology. 2001;58:289-94.

255. Sun Y, Campisi J, Higano C, Beer TM, Porter P, Coleman I, et al. Treatment-induced damage to the tumor microenvironment promotes prostate cancer therapy resistance through WNT16B. Nature medicine. 2012;18:1359-68.

256. Cano P, Godoy A, Escamilla R, Dhir R, Onate SA. Stromal-epithelial cell interactions and androgen receptor-coregulator recruitment is altered in the tissue microenvironment of prostate cancer. Cancer research. 2007;67:511-9.

257. Habashy HO, Powe DG, Rakha EA, Ball G, Paish C, Gee J, et al. Forkhead-box A1 (FOXA1) expression in breast cancer and its prognostic significance. European journal of cancer. 2008;44:1541-51.

258. Meyer MB, Pike JW. Corepressors (NCoR and SMRT) as well as coactivators are recruited to positively regulated 1alpha,25-dihydroxyvitamin D3-responsive genes. The Journal of steroid biochemistry and molecular biology. 2013;136:120-4.

259. Ting HJ, Messing J, Yasmin-Karim S, Lee YF. Identification of microRNA-98 as a therapeutic target inhibiting prostate cancer growth and a biomarker induced by vitamin D. The Journal of biological chemistry. 2013;288:1-9.

260. He R, Li X. Mammalian two-hybrid assay for detecting protein-protein interactions in vivo. Methods Mol Biol. 2008;439:327-37.